MEMBRANE MICRODOMAINS AND GLYCOSYLATION

OF ACTIVATING RECEPTORS

INFLUENCE NATURAL KILLER CELL REGULATION

DISSERTATION

submitted to the
Combined Faculties for the Natural Sciences
and for Mathematics
of the Ruperto-Carola University of Heidelberg, Germany
for the degree of
Doctor of Natural Sciences

presented by

Diplom-Biochemikerin Stefanie Margraf-Schönfeld

born in: Offenbach am Main

Oral-examination: _____

Referees: Prof. Dr. H.-G. Kräusslich

Prof. Dr. C. Watzl

Für einen ganz besonderen Menschen

- Ich werde für immer an Deiner Seite sein -

Wer an der Küste bleibt,
kann keine neuen Ozeane
entdecken.

Ferdinand Magellan

Acknowledgments

First of all I'd like to thank Prof. Dr. Carsten Watzl. Thank you for excellent supervision, for always taking the time for helpful discussions. Your optimism, your persistence and support extremely motivated me. Thanks for leaving your door always open.

Furthermore I highly appreciate that Prof. Dr. med. Hans-Georg Kräusslich agreed to represent this work in the Faculty of Natural Science of the University Heidelberg.

I would also like to thank all past and present members of the "Watzl lab", especially:

Maren – for all her time in the "quarantine lab", for her great support, for always having a sympathetic ear, for every conversion and every shared silence.

André – for Fasching, the glue under my chair and every humorous moment, bringing some light into serious lab work and severe moments.

Doris – for all her help concerning Western blotting, as well as for all her strange music and a great time during Dubrovnik and Vienna.

Stephan- special thanks goes to the captain of the lab. Your piraty behavior to keep every lab "treasure" always amuses me.

Sabine – for all your honey, your flowers and your enthusiasm.

Carolin – for being a great help during her bachelor thesis and for always being good-humored.

Petra – for all your confidence, every conversation and "bearded" moments.

Stephan– for always being the silent part of the lab.

Birgitta – for the experience that sassiness does not stop over age.

Mina – for all the presents of the garden and for exuding calm.

Christian–for all your laugh and for being the lab egg.

I'd also like to thank all former members, Kristine Kohl, Wolfgang Merkt, Franziska Stöcklin, Sabrina Hoffmann, Patrick Rämer and Rauf Bhat as well as all people in the Institute for Immunology of the University Heidelberg for their support and help.

Last but not least I want to thank the persons in my private life: my parents for always supporting and believing in me, my brother for all his optimism and support, my grandparents and all my friends for backing me up, even in hard times.

Finally I want to thank Kurt.
Thank you for everything you are and for everything you gave to me.
I'll never forget any moment with you.
You've showed me how valuable life can be!

SUMMARY

Natural killer (NK) cells represent the first lymphoid subpopulation in the defense against tumors and viral infection. The activity of NK cells is regulated by the interplay of activating and inhibitory surface receptors. The mechanisms by which these receptors transduce their signals and the integration of positive and negative signals are not completely understood. 2B4 (CD244) is an important activating NK cell receptor. Ligand engagement results in the recruitment of 2B4 to membrane microdomains, which is essential for the function of this receptor.

Here we successfully established a new approach to investigate membrane microdomains without destroying the membrane's natural composition, as it has often been criticized for the classical cold non-ionic detergent lysis followed by sucrose density gradient centrifugation. NK cell receptors were stimulated by antibodies coupled to magnetic beads. NK cells were then physically disrupted in a nitrogen-cavitation bomb and membrane fragments surrounding the engaged receptor including the associated signaling machinery were immunoisolated by separation of the magnetic beads. By comparing bead contents of activating (2B4) with inhibitory (NKG2A) NK cell receptors using 2D-DIGE, several proteins with significant difference emerged, which were subsequently identified by mass spectrometry. Important candidates for cytoskeletal remodeling and signal transduction were identified to be specifically associated with 2B4, which gave us a first hint for the formation of multimolecular complexes and their role in the early steps of NK cell activation.

In a second project we analyzed the glycosylation of 2B4. We demonstrated that 2B4 is heavily and differentially glycosylated in primary human NK cells and NK cell lines. The differential glycosylation of 2B4 could be attributed to sialic acid residues on *N*- and *O*-linked carbohydrates. Glycosylation plays an important role in receptor-ligand recognition and interaction but may also lead to repulsion between molecules. Using a recombinant fusion protein of the extracellular domain of 2B4 we demonstrated that *N*-linked glycosylation of 2B4 is essential for binding to its ligand CD48. In contrast, sialylation of 2B4 had a negative impact on ligand binding as the interaction between 2B4 and CD48 was increased after the removal of sialic acids. This was confirmed in a functional assay system, where the desialylation of NK cells or the inhibition of *O*-linked glycosylation resulted in increased 2B4-mediated lysis of CD48 expressing tumor target cells. These data demonstrate that glycosylation has an important impact on 2B4-mediated NK cell function and suggest that regulated changes in glycosylation during NK cell development and activation might be involved in the regulation of NK cell responses.

ZUSAMMENFASSUNG

Natürliche Killer (NK) Zellen repräsentieren die erste lymphoide Subpopulation in der Immunabwehr gegen Tumore und virale Infektionen. Die Aktivität der NK Zellen wird durch eine Vielzahl von aktivierenden und inhibierenden Oberflächenrezeptoren reguliert. Die Signaltransduktion dieser Rezeptoren als auch das Zusammenpiel zwischen beiden Rezeptortypen ist bis heute noch nicht vollständig verstanden. 2B4 (CD244) ist ein aktivierender Rezeptor, der für die Regulation von NK Zellen von großer Bedeutung ist. Seine Aktivierung führt zur Rekrutierung in spezialisierte Membranbereiche, so genannte „lipid rafts" oder Membran Mikrodomänen. Die klassische Methode zur Untersuchung dieser „lipid rafts" beruht auf der Verwendung von kaltem, nicht-ionischen Detergenz mit anschließender Saccharose-Dichtegradientenzentrifugation.

In dieser Arbeit wurde eine neue Technik zur Untersuchung von Membran Mikrodomänen etabliert, bei der es nicht zu einer Zerstörung der natürlichen Membran-zusammensetzung kommt, was ein oft genannter Kritikpunkt für die Verwendung von Detergenzien ist. NK Zell Rezeptoren wurden durch Antikörper gebundene, magnetische Kügelchen stimuliert. Anschließend erfolgte die Zerstörung der Zelle mit Hilfe einer Stickstoff-Bombe sowie die Immunisolierung der Rezeptor umgebenden Membranfragmente inklusive angrenzenden Signalmoleküle durch magnetische Separierung der Kügelchen.

Ein Vergleich der immunisolierten Proteine von aktivierenden (2B4) mit inhibierenden (NKG2A) NK Zell Rezeptoren mittels 2D-DIGE führte zur Entdeckung mehrerer Proteine, die spezifisch mit 2B4 assoziiert waren, und die anschließend durch Massenspektrometrie identifiziert wurden. Hierbei handelte es sich unter anderem um Proteine, die eine wichtige Aufgabe bei der Signaltransduktion oder bei der Umorganisation des Zytoskeletts erfüllen und somit einen ersten Einblick in den Aufbau multimolekularer Komplexe und deren Rolle zur NK Zell Regulierung geben.

In einem zweiten Projekt untersuchten wir die Glykosylierung von 2B4 und konnten zeigen, dass 2B4 sowohl in NK Zelllinien als auch in primären NK Zellen differenziell glykosyliert ist. Die unterschiedliche Glykosylierung von 2B4 konnte auf an *N*- und *O*-gebundene Sialinsäuren zurückgeführt werden. Glykosylierung spielt eine wichtige Rolle bei Rezeptor-Liganden Erkennung und deren Interaktion, kann aber auch zur Abstoßung von Molekülen führen. Durch die Verwendung eines rekombinanten Fusionsproteins konnten wir zeigen, dass *N*-verknüpfte Kohlenhydrate essentiell für die Bindung von 2B4 an seinen Liganden CD48 sind. Im Gegensatz dazu übt die Sialylierung von 2B4 einen negativen Einfluss auf die Ligandenbindung aus, da die Interaktion zwischen 2B4 und CD48 nach Entfernung von Sialinsäuren erhöht wurde. Dieser Effekt konnte durch

funktionelle Tests bestätigt werden, da eine Desialylierung von NK Zellen oder die Inhibierung der *O*-Glykosylierung zur Verstärkung der 2B4-vermittelten Lyse von CD48 exprimierenden Zielzellen führte.

Diese Daten zeigen, dass die Glykosylierung von 2B4 einen wichtigen Einfluss auf die NK Zell Funktion besitzt. Veränderungen der Glykosylierung während NK Zell Entwicklung und Aktivierung könnten daher an der Regulation von NK Zell Antworten beteiligt sein.

1 INTRODUCTION

1.1 Natural killer cells

Natural killer (NK) cells were first discovered in 1975 as bearing the ability to lyse leukaemia cells *in vitro* without previous sensitization (Herberman *et al.*, 1975a; Herberman *et al.*, 1975b; Kiessling *et al.*, 1975a; Kiessling *et al.*, 1975b). On the basis of this experiment the term "natural cytotoxicity" was defined, although by now it is commonly known that NK cells are much more diverse in functionality. NK cells were first characterized as being $CD56^{+}CD3^{-}$, but recently it was recommended to use the marker NKp46 as being more specific over species barriers (Walzer *et al.*, 2007a; Walzer *et al.*, 2007b).

NK cells develop from the same progenitor as T and B cells and therefore represent the third lymphoid subpopulation (Colucci *et al.*, 2003). Unlike T and B cells, NK cells do not exhibit somatic recombination but regulate their activity through germline encoded activating and inhibitory receptors. Because of their ability of being active without prior stimulation, NK cells belong to the first defense against viruses, pathogens and malignantly transformed cells. These characteristics led to the classification of NK cells to the innate immune system. NK cells comprise 5–15 % of circulating lymphocytes, but are also present in other tissues such as the gut, the lung and liver, as well as in the pregnant uterus, where they may have specialized functions (Tabiasco *et al.*, 2006). The importance of NK cells became clear in patients born without or with impaired function of this lymphocyte subpopulation. These patients suffer from recurrent illnesses and have particular problems in controlling herpes viral infections despite their functional adaptive immune response (Biron *et al.*, 1999; Janka, 2007; Nichols *et al.*, 2005; Orange *et al.*, 2002).

NK cell function can be divided into two parts: (1) Cytotoxicity, which can be performed in a perforin or a death receptor mediated manner. NK cells possess large numbers of preformed cytotoxic granules, containing perforin and various granzymes. Upon contact of NK cells with an appropriate target cell, granules are transported to the contact zone (also termed NK cell immunological synapse, NKIS) (Davis *et al.*, 1999; Eriksson *et al.*, 1999b) where they are released into the synaptic cleft and lead to target cell apoptosis in a perforin and granzyme dependent manner. A more uncommon mechanism of target cell elimination by NK cells that also is slower in kinetic and less efficient, is the triggering of death receptors. Expression of tumor necrosis factor (TNF) related apoptosis inducing ligand (TRAIL) and Fas ligand (CD178) by effector NK cells triggers the appropriate death receptors on a target cell, leading to their apoptosis (Chavez-Galan *et al.*, 2009). (2) The second function of NK cells is their ability to produce cytokines and

therefore to communicate with other cells of the innate and adaptive immune system. Important NK cell cytokines include interferon (IFN)-γ, tumor necrosis factor (TNF)-α as well as granulocyte-macrophage colony-stimulating factor (GM-CSF) (Biron *et al.*, 1999). Especially IFN-γ and TNF-α are crucial for the T cell mediated protection against intracellular pathogens and cancer (Cooper *et al.*, 2004; Moretta, 2002). NK cell helper function is also important for their crosstalk with dendritic cells (DCs), either by direct contact or by cytokine release (Degli-Esposti and Smyth, 2005).

More than 48 distinct NK cell subsets have been defined, whose function and regulation are hardly known (Jonges *et al.*, 2001). However, two distinct subsets of NK cells have been well characterized: $CD56^{high}$ $CD16^{-}$ cells are specialized in cytokine production whereas $CD56^{dim}$ $CD16^{+}$ cells are the major cytotoxic NK cell subset (Colucci *et al.*, 2003). Recently, a new subset termed NK-22 has been identified which is essential for mucosal homeostasis. These NK cells bear the capacity to produce IL-22 and thereby contribute more to the homeostasis of the mucosal epithelia rather than to the classical NK cell functions like cytotoxicity and IFN-γ production (Cella *et al.*, 2009; Malmberg and Ljunggren, 2009).

1.2 Regulation of NK cell activity: "missing" and "induced" self

In the early 1960s, it was a common hypothesis that transplanted tumor cells were rejected only when grafts express "foreign" MHC molecules which serve as antigens for a cytotoxic T cell response. 1964 Cudkowicz and Stimpfling found that F1-hybrid mice (derived from crossing of two inbred strains) were often resistant to tumor grafts of the parental origin (Cudkowicz and Stimpfling, 1964). This F1 hybrid resistance, which could not be correlated with a foreign antigen expression, was associated with NK cell activity soon after their discovery in 1975 (Kiessling *et al.*, 1977). The F1 resistance led to the formation of the "missing-self" hypothesis (Karre, 2008; Karre *et al.*, 1986). This model postulates that the absence or reduced expression of "self" MHC class I molecules leads to the recognition of and target cell lysis by NK cells. The theory was further supported by the identification of inhibitory NK cell receptors with specificity for self-MHC class I molecules (Karlhofer *et al.*, 1992; Moretta *et al.*, 1993). Target cells, which only had minor expression levels of MHC class I molecules, as often observed in tumors, virally infected cells or in the case of transplanted grafts, trigger the activation of NK cells due to their inability to deliver inhibitory signals (Ljunggren and Karre, 1990).

For a long time, the theory of "missing-self" served as the only explanation of NK cell regulation. However, it became clear that the absence of inhibitory signals alone is not sufficient to induce target cell lysis. NK cells need to be triggered by activating receptors, too. This led to the model of the "induced-self" mechanism, whereby ligands lead to an

activation of NK cells despite the existence of an inhibitory signal (Watzl, 2003). We now know that the mechanism of NK cell regulation is much more complex, implying receptor expression as well as the balance and integration of signals delivered from activating and inhibitory receptors (see also Figure 1) (Lanier, 2005).

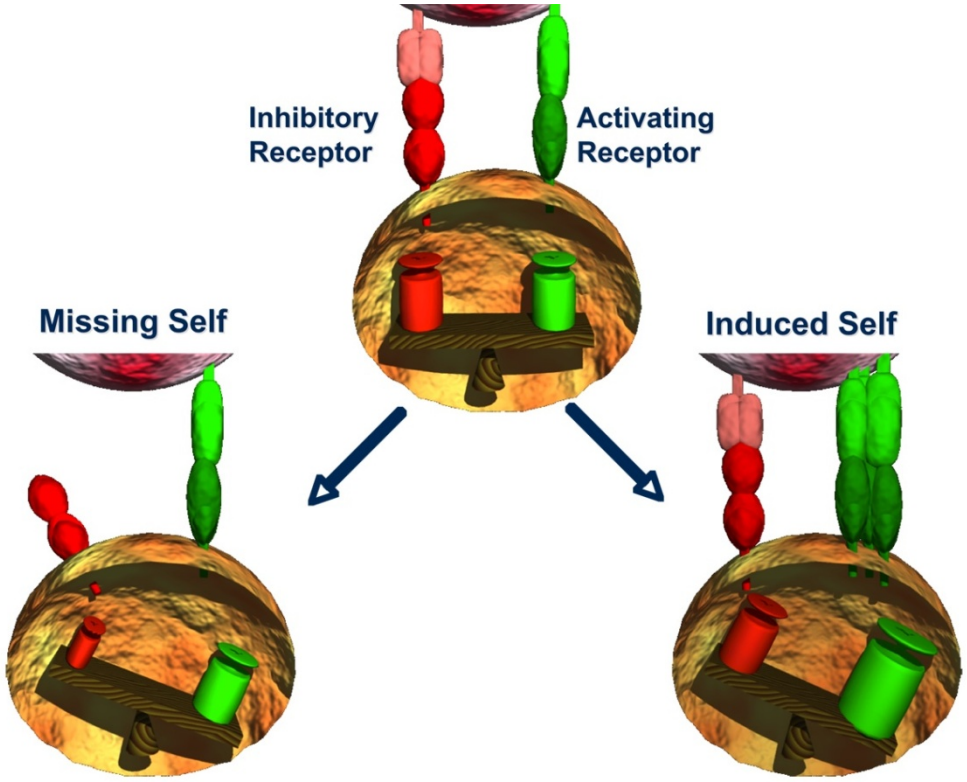

Figure 1: Illustration of missing and induced self. The NK cell (bottom) can bind via its activating and its inhibitory receptors to the attached target cell (top). The balance between the signals can shift to NK cell activation by the loss of inhibitory ligands (missing self) or by enhanced expression of activating ligands (induced self) on the target cell.

1.3 Inhibitory receptors

The first inhibitory NK cell receptors identified were the C-type lectin like Ly49 receptors in the mouse (Karlhofer *et al.*, 1992). The human homologs are the killer cell immunoglobulin-like receptors (KIRs), which belong to the immunoglobulin (Ig)-superfamily. The KIRs are type I transmembrane proteins and are divided into two groups based on their intracellular domain. Receptors with a long cytoplasmic domain (L) bear one or two immunoreceptor tyrosine-based inhibition motifs (ITIM) in their cytoplasmic tail and therefore act as inhibitory receptors. Short cytoplasmic forms (S) of KIRs lack this ITIM and instead associate with the immunoreceptor tyrosine-based activating motif (ITAM) bearing adaptor molecule DNAX activation protein (DAP)12 and function as activating receptors. Furthermore, both, activating and inhibitory KIRs contain two or three extracellular domains (D). Therefore, according to the number of extracellular domains and the length of the cytoplasmic tail, KIRs are classified as

KIR2D(S/L) or KIR3D(S/L). KIR receptors specifically recognize certain human leukocyte antigen (HLA)-A, -B or -C allotypes, but unlike T cells, not in a peptide specific way, although the peptide can contribute to KIR binding (Rajagopalan and Long, 1997, 2010). It has been shown that inhibitory KIRs exhibit a higher affinity to HLA molecules as their corresponding activating part, which may be a mechanism to avoid the risk of autoimmunity (Katz *et al.*, 2001; Vales-Gomez *et al.*, 1998).

In addition to these Ig-like receptors, human NK cells express receptors of the C-type lectin-like family, namely NKG2, which form heterodimers with CD94 and some of them are inhibitory. The family comprises of NKG2A, -C, -E and -F. CD94/NKG2C heterodimers serve as activating receptors and transduce their signal via the adaptor molecule DAP12. NKG2A bears an ITIM in its cytoplasmic tail and therefore can deliver an inhibitory signal. The sequence of NKG2E is very similar to NKG2C and therefore it is assumed that it acts as an activating receptor, too, but up to now, an association with DAP12 couldn't be shown (Lanier, 2005). Both, CD94/NKG2A and CD94/NKG2C complexes bind specifically to the non-classical MHC class I molecule HLA-E, which presents peptides derived from leader peptides of other MHC class I molecules. It is therefore a marker for the overall expression of MHC class I molecules. From this, the question arises, how NK cells decide which receptor - inhibitory or activating - is bound and stimulated. It has been shown that the inhibitory heterodimer comprising of CD94/NKG2A has a higher affinity for HLA-E molecules than that consisting of CD94/NKG2C (Vales-Gomez *et al.*, 1999). Furthermore, the peptides bound by HLA-E molecules may impair the binding affinity of CD94/NKG2C, too (Michaelsson *et al.*, 2002). Hence, mechanisms to avoid autoimmunity may be a common feature of receptor families comprising of both, inhibitory and activating receptors, with similarity in their extracellular domains.

An overview of the human inhibitory receptors is given in Figure 2.

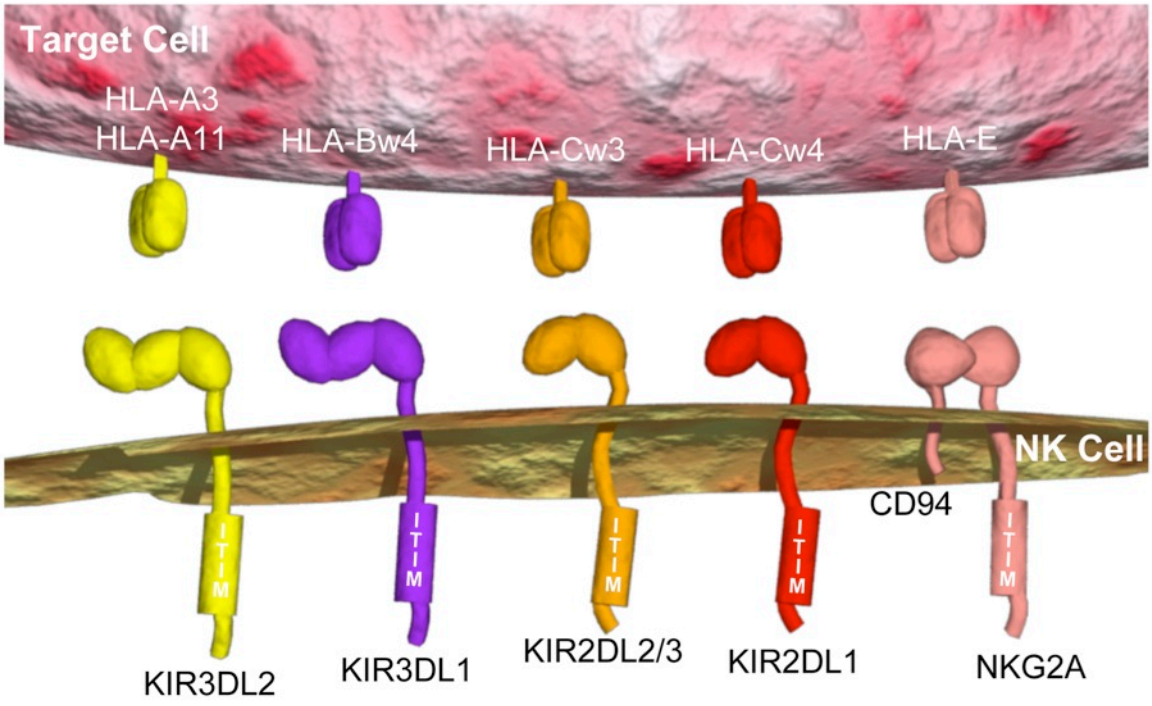

Figure 2: Overview of the human inhibitory receptors and their ligands. Inhibitory KIRs and CD94/NKG2 complexes carry an ITIM in their cytoplasmic domain. KIRs are receptors of the Ig superfamily that bind to different HLA allotypes, while CD94/NKG2 receptors belong to the C type lectin like family and recognize HLA-E.

1.4 Activating receptors

The group of activating NK cell receptors is much more heterogeneous than that of inhibitory receptors. Beside the activating KIRs and CD94/NKG2 complexes, many activating receptors have been described, however, some of their ligands remain obscure.

Among the activating receptors, the low affinity receptor for IgG, CD16 (FcγRIII) plays a special role. It transduces its signals via the ITAM containing accessory FcεRI-γ and CD3ζ chains and mediates antibody-dependent cellular cytotoxicity (ADCC). Therefore, it enables NK cells to recognize and eliminate pathogens or cells opsonized by antibodies by specific binding of the antibody's Fc part to CD16. This mechanism is essential for antibody based therapies, like e.g. the treatment of B-cell non-Hodgkin lymphoma with rituximab (Anderson *et al.*, 1997; Reff *et al.*, 1994).

Another important group for the activation of NK cells are the natural cytotoxicity receptors (NCRs) consisting of NKp30 (CD337), NKp44 (CD336) and NKp46 (CD335). Even though their cellular ligands are unknown, NKp44 and NKp46 are assumed to recognize viral hemagglutinin (Arnon *et al.*, 2001; Mandelboim and Porgador, 2001). Apart from viral hemagglutinin, NKp30 has been shown to bind to human leukocyte antigen-B-associated transcript 3 (Bat3) (Pogge von Strandmann *et al.*, 2007) and B7-H6, a protein expressed specifically by tumor cells (Brandt *et al.*, 2009). Because NCRs

lack intracellular signaling motifs on their own, they need to signal via adaptor molecules like CD3ζ (NKp30, NKp46), FcεRI-γ (NKp46) and DAP12 (NKp44) (Moretta *et al.*, 2001). This is mediated by a positively charged amino acid residue in the transmembrane region of the NCRs that is pivotal for their interaction with ITAM bearing adaptor molecules.

The C-type lectin NKp80 was recently characterized to be stimulated by activation-induced C-type lectin (AICL, also CLEC2B), a myeloid-specific receptor expressed by monocytes, macrophages and granulocytes (Welte *et al.*, 2006), but the signaling pathway remains to be resolved. DNAX accessory molecule 1 (DNAM)-1 binds the molecules poliovirus receptor (PVR) (CD155) and Nectin-2 (CD112) and also activates NK cells (Gilfillan *et al.*, 2008). NKG2D belongs to the C-type lectin family, and recognizes MHC class I related chain (MIC) molecules A and B as well as UL-16 binding proteins (ULBPs). These ligands are upregulated during cellular stress and trigger the human homodimer NKG2D to signal via its adaptor molecule DAP10, whereas the murine receptor is also able to interact with DAP12 (Eagle and Trowsdale, 2007).

The signaling lymphocyte activation molecule (SLAM) related receptors (SRRs) comprise another group of activating NK cell receptors. Because the (co)activating receptor 2B4 (CD244) which belongs to this subfamily, is of special interest in this thesis, the SRRs will be described below.

Figure 3 summarizes the activating NK cell receptors and their ligands.

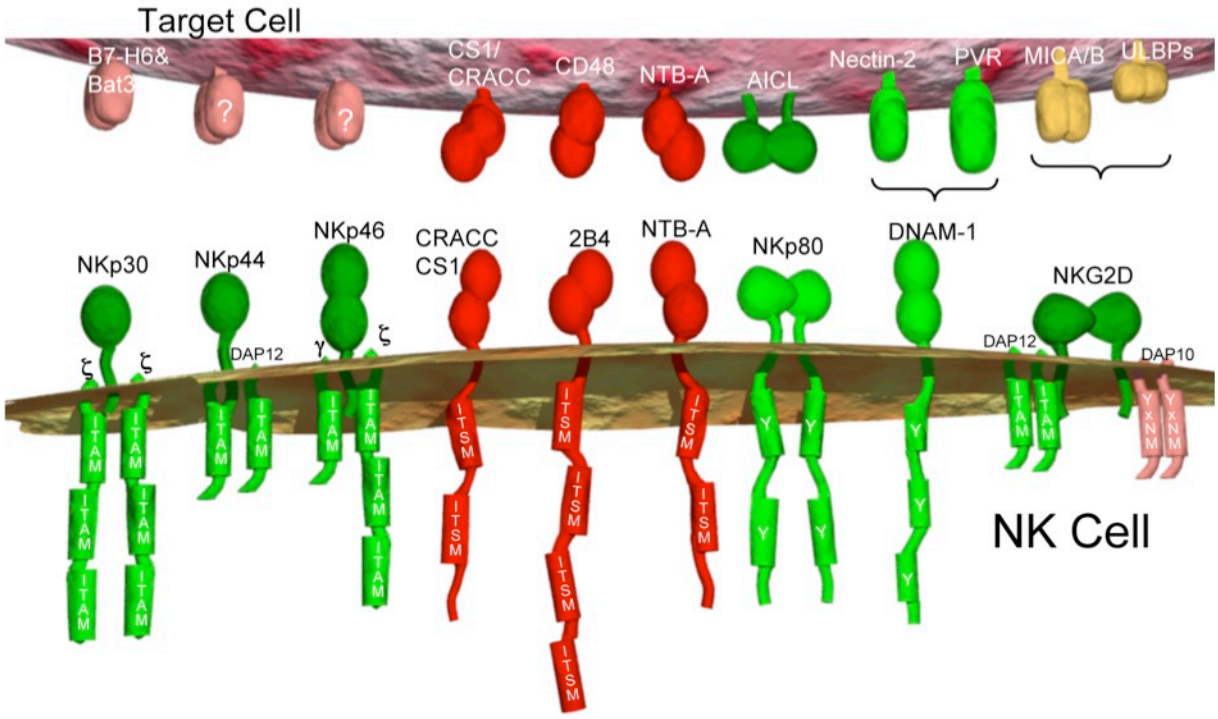

Figure 3: Overview of activating receptors and their ligands. Signaling motifs of the receptors or their respective adaptor chains are indicated. CD3ζ is symbolized by ζ and FcεRI-γ by γ. Human NKG2D interacts only with DAP10.

1.5 The SLAM family of immunoglobulin-like receptors

1.5.1 SLAM-related receptors (SRR)

The signaling lymphocyte activation molecule (SLAM) related receptors (SRRs) are a group of activating NK cell receptors consisting of six transmembrane proteins belonging to the Ig super family. This family comprises of SLAM (CD150), 2B4 (CD244), NK, T and B cell antigen (NTB-A), CD2-like receptor activating cytotoxic cells (CRACC, CS1) (CD319), CD84, and Ly-9 (CD229) (Bhat *et al.*, 2006; Claus *et al.*, 2008; Ma *et al.*, 2007; Veillette, 2006). The SRR family members are broadly expressed in the hematopoietic system. SRRs are expressed as type I transmembrane proteins with an amino-terminal V-type and a membrane proximal C2-type Ig-like domain. Ly-9 is an exception, as it comprises four Ig-like domains with an arrangement of V-C2-V-C2. With the exception of 2B4, SRRs interact homophilic. 2B4 interacts with CD48, a glycosylphosphatidylinositol- (GPI-) anchored molecule, broadly expressed on immune cells (Brown *et al.*, 1998b; Latchman *et al.*, 1998). In contrast to many other activating NK cell receptors described above, SRRs contain a distinct signaling motif, which differs also in its sequence from the common ITAM. SRRs contain different numbers of the so called immunoreceptor tyrosine-based switch motifs (ITSMs) and deliver their activating signal via SLAM-associated protein (SAP), Ewings sarcoma-Fli1-activated transcript 2 (EAT-2) and EAT-2 related transcript (ERT, only in mice) (Latour and Veillette, 2004). These small molecules consist of a Src homology 2 (SH2) domain, with which they can bind to phosphorylated tyrosines of the ITSMs. The importance of SRRs and SAP became clear in patients suffering from X-linked lymphoproliferative disease (XLP), where the affected individuals carry a mutation in the gene encoding for SAP. In XLP, B and T cells as well as monocytes show a large expansion due to a dysregulated immune response initiated by Epstein-Barr virus (EBV) infection. In addition to transducing signals via activating molecules, SRRs are also able to associate with the phosphatases SHP-1/-2 and SHIP, thereby transmitting inhibitory signals. The finding of binding signaling molecules with opposite effects led to the term *switch motif* (Bottino *et al.*, 2001; Eissmann *et al.*, 2005).

Only 2B4, NTB-A and CRACC are expressed on NK cells. Whereas activating signals of 2B4 and NTB-A depend on functional SAP as seen in XLP patients, CRACC seems to be independent of this adaptor molecule as CRACC signaling is not impaired in the disease (Bouchon *et al.*, 2001).

1.5.2 The 2B4 receptor (CD244)

The SRR 2B4 is one of the best characterized surface receptors on NK cells, maybe due to the fact that it is expressed on all NK cells, rather than only on distinct subpopulations.

The identification of its ligand CD48 makes it possible to analyze the function of 2B4 due to possible stimulation with its natural ligand instead of antibody-mediated crosslinking.

The receptor has first been described in murine lymphocytes with a non-MHC class I restricted NK cell like activity (Garni-Wagner *et al.*, 1993). Rodents express two receptors with different length of their cytoplasmic domains due to different splicing variants (Mathew *et al.*, 1993). The short form (2B4S) transduces an activating signal, whereas the long form (2B4L) exhibits inhibitory activity (Lee *et al.*, 2004; Mooney *et al.*, 2004; Schatzle *et al.*, 1999).

Human 2B4 is a 365 amino acid type 1 transmembrane protein with a calculated molecular weight of 39 kDa and a pI of 9.16. It was first described in 1999 (Kubin *et al.*, 1999; Nakajima *et al.*, 1999; Tangye *et al.*, 1999). It has been reported that two isoforms of 2B4, h2B4-A and h2B4-B, could be expressed in human NK cells. These receptors differ by the addition of five amino acids between the distal IgV and the membrane proximal C2 domain of h2B4-B. This difference may impair the binding affinity for CD48 and therefore result in differential cytotoxic activity (Mathew *et al.*, 2009), but this has to be confirmed in further studies.

After engagement, human 2B4 induces cytotoxicity as well as cytokine production by triggering different signaling pathways (Chuang *et al.*, 2001). In addition, 2B4 can also enhance signals induced by other NK receptors such as NKp30 and NKp46, thereby acting as a costimulator (Sivori *et al.*, 2000). In this case, 2B4 crosslinking enhances receptor mediated signals to such an extent that in most cases a synergistical effect is observed. This means that the signal's outcome is rather an amplification than the pure addition of both signals alone (Bryceson *et al.*, 2006).

In contrast to its activating feature, it has been shown that under certain circumstances 2B4 may act as an inhibitory receptor. During development, activating receptors like NKp46 and NKp30 are expressed before HLA class I-specific inhibitory receptors. This critical state may impair the self-tolerance of NK cells. 2B4 was shown to prevent hyperresponsiveness by functioning as inhibitory receptor providing a fail-safe mechanism for NK cell development (Sivori *et al.*, 2002). The inhibitory function of 2B4 may be based on the absence of SAP as it has been reported to be responsible for the impaired immune response in XLP patients. However, the expression level of the receptor itself may also influence the balance between inhibition and activation of 2B4. It has been observed that a high receptor expression leads to an inhibitory, rather than to an activating response. Similarly, low expression of SAP or extensive antibody-mediated crosslinking induce inhibition. This dual role enables the immune system to adjust an adequate response by regulating a single receptor signaling pathway (Chlewicki *et al.*, 2008).

1.6 Signaling pathways

Engagement of 2B4 by its ligand CD48 or antibody-mediated crosslinking leads to the recruitment of the receptor into so called "lipid rafts", resulting in the phosphorylation of its ITSM domains by Src-family kinases (Watzl and Long, 2003; Watzl *et al.*, 2000). Raft recruitment has been shown to be essential for phosphorylation of 2B4 (Watzl *et al.*, 2003). Upon phosphorylation, SAP associates with the ITSMs of 2B4, whereas the membrane proximal ITSM is essential for 2B4 signaling (Eissmann *et al.*, 2005). EAT-2 and in mice also ERT have been shown to be recruited to phosphorylated 2B4, too. All three adaptor molecules bear an SH2 domain which is sufficient for receptor binding. SAP also binds the Src kinase FynT (Chen *et al.*, 2006) which leads to an increased receptor phosphorylation, whereas contrary findings for EAT-2 and ERT are discussed (Calpe *et al.*, 2006; Clarkson *et al.*, 2007; Roncagalli *et al.*, 2005). The interaction of SAP with FynT occurs in an unusual SH2-SH3-domain dependent manner, involving the residue arginine-87 on SAP (Latour *et al.*, 2003). While the phosphorylation of 2B4 occurs independently of SAP, the presence of SAP is crucial for signal transduction (Meinke, 2010). A defect in SAP expression or a mutation on R87 impairs the 2B4 mediated signaling pathway completely and leads to the XLP disease. The association of EAT-2 with 2B4 is still under investigation. Veillette and colleagues proposed an inhibitory outcome of the 2B4-EAT-2 association (Valiante and Trinchieri, 1993; Veillette *et al.*, 2007) whereas in our hands EAT-2 binding to 2B4 is impaired in the absence of SAP (Meinke, 2010). It is assumed that the affinity of EAT-2 to the ITSM of 2B4 is much lower than that of SAP and can be counteracted by EAT-2 overexpression or SAP mediated receptor recruitment. An additional adaptor molecule is 3BP2 which interacts with the fourth ITSM domain of 2B4 and whose phosphorylation leads to Vav signaling, ERK activation and NK cell cytotoxicity (Bottino *et al.*, 2000).

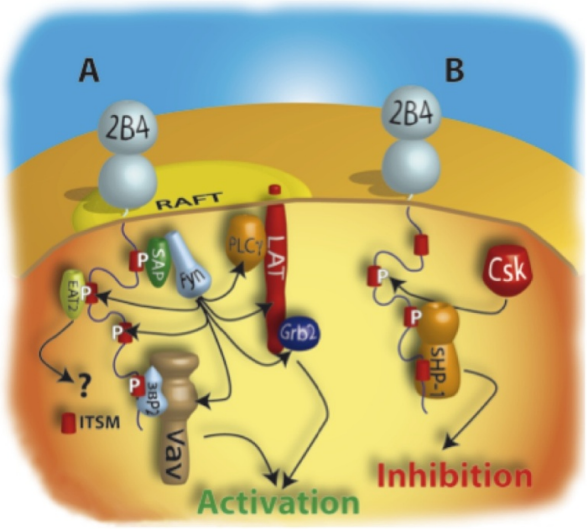

Figure 4: The model of 2B4 signal transduction. A Early signaling events in 2B4-mediated lymphocyte activation **B** A possible mechanism for 2B4-mediated inhibitory signals in the absence of functional SAP, e.g. in XLP patients. Picture by courtesy of Claus *et al.*, 2008.

Inhibitory signals of 2B4 may occur due to binding of the phosphatases SHIP, SHP-1 and -2 to the third phosphorylated ITSM domain. Those phosphatases dephosphorylate other signaling molecules and thereby inhibit the receptor's downstream signaling. Furthermore, the enzymes block the binding sites for SAP (Eissmann *et al.*, 2005; Tangye *et al.*, 1999). How the ITSM domain of 2B4 is phosphorylated remains unclear. Another mediator of inhibitory signals is Csk. This kinase was found to associate with 2B4 and to phosphorylate its ITSM domain. Nevertheless, Csk inhibits Src-family kinases and thereby abolishes NK cell activation (Eissmann *et al.*, 2005).

Further studies with antibody mediated crosslinking of 2B4 molecules revealed the tyrosine phosphorylation of many substrates, including Vav1, SHIP-1, c-Cbl, 3BP2, p38 MAPK, ERK1/2 and PLC-γ (Chen *et al.*, 2004; Lanier, 2008; Watzl *et al.*, 2000). However, results depend strongly on the experimental setup and cell type used. This also may contribute to the controversial results concerning SAP and EAT-2 mediated signaling described above.

The phosphorylated ITIM of engaged inhibitory receptors bind the phosphatases SHIP, SHP-1 and -2, which in turn dephosphorylate several intracellular proteins (Tomasello *et al.*, 2000; Watzl *et al.*, 2000). Vav1 seems to be a key substrate for SHP-1. Thus, by controlling Vav1 phosphorylation, the decision of whether an activating signal proceeds downstream or not appears to be made. Vav1 phosphorylation therefore seems to be the first switch-like process in NK cells (Stebbins *et al.*, 2003; Urlaub, 2009). The process of inhibition is spatially restricted to the inhibitory immunological synapse, also termed the supramolecular inhibition cluster - SMIC (Orange, 2008). Thus, the NK cell gains the possibility to still act on target cells lacking inhibitory ligands, whereas inhibition by further contacted cells is assured (Eriksson *et al.*, 1999b).

1.7 Membrane microdomains and their role in activation of NK cells

Lipid rafts play an important role in the signal transduction of NK cells (Davis *et al.*, 1999; Fassett *et al.*, 2001; Lou *et al.*, 2000; Watzl *et al.*, 2003). Lipid rafts are membrane microdomains enriched in cholesterol and glycosphingolipids, such as sphingomyelin and GM1, but contain also special proteins. In contrast to the surrounding lipid bilayer, rafts are highly ordered and tightly packed, due to the high concentration of more ordered lipid acyl chains. Additionally, cholesterol binds to sphingomyelin via hydrogen bonds and thereby leads to a tightly packed lipid layer, also known as the "condensing effect" (Lichtenberg *et al.*, 2005).

The concept of "lipid rafts" has often been linked with the terms liquid-ordered (lo) or detergent resistant membranes (DRM). However, recent studies provide differences between those terms (Lichtenberg *et al.*, 2005). Liquid ordered phases are formed within

lipid bilayers as a result of local enrichment in sterols, e.g. cholesterol that hinders the formation of gauche conformations. The increased lipid acyl chain order forms a more compact state of lipids (Brown and London, 1997). Some of these lo phases are indeed detergent resistant, which means that they could prevent detergent incorporation into the lipid bilayer (Xu *et al.*, 2001).

So, what exactly are "lipid rafts"? These special membrane microdomains can be defined as organized membrane areas existing *in vivo*. Lipid rafts constitute lo-phase domains and may be partially separated from the surrounding plasma membrane by detergent. Consequently, by using the term "lipid raft", the respective examination method has to be considered.

Lipid rafts serve as signal platforms, as they separate membrane components from each other and thus create distinct areas with defined lipid and, of special interest, protein composition (Brown and London, 1998a). Among them are proteins with saturated acyl chains (including GPI-anchored proteins, myristoylated and palmitoylated proteins). These include important signaling proteins, such as Src-family kinases and heterotrimeric G protein alpha subunits (Hope and Pike, 1996; Simons and Ikonen, 1997; Zhang *et al.*, 1998) but also the GPI-linked CD48, the ligand of 2B4. Some integral membrane proteins extending through both lipid layers are also found in lipid rafts. Furthermore, constitutively and transiently raft associated proteins exist. Constitutive association seems to depend on S-palmitoylation (Dykstra *et al.*, 2003) as has been shown for linker for activation of T cells (LAT) (Zhang *et al.*, 1998) as well as the T cell coreceptors CD4 and CD8 (Arcaro *et al.*, 2000; Parolini *et al.*, 1999). Despite this, some integral membrane proteins are normally excluded from lipid rafts and only translocate into the specialized membrane microdomain after ligation as e.g. the T cell receptor (TCR), B cell receptor (BCR), FcεR1 receptor and the NK cell activating receptors 2B4 and NKG2D (Dykstra *et al.*, 2003; Endt *et al.*, 2007; Masilamani *et al.*, 2006; Simons and Toomre, 2000; Watzl *et al.*, 2003).

These observations led to two models of raft-organization: In the first model, proteins are already localized in small lipid rafts, which are able to form stable and bigger complexes after receptor engagement (Lingwood and Simons, 2010; Pralle *et al.*, 2000; Simons *et al.*, 1997). The second model proposes only a small fraction of proteins to be constitutively localized in lipid rafts. Crosslinking of separated proteins induces clustering and thereby higher affinity for lipid rafts followed by recruitment of signal complexes into membrane microdomains (Brown *et al.*, 1998a; Harder *et al.*, 1998). It remains open, which of both models is correct or if both concepts may be right concerning particular membrane proteins.

It has been demonstrated that the activating receptor 2B4 is recruited into DRMs upon engagement by crosslinking (Bottino *et al.*, 2000) or by mixing NK cells with CD48

expressing target cells (Watzl *et al.*, 2003). Thereby, the ITSM domains of 2B4 become phosphorylated by Src-kinases, which leads to NK cell activation (Bhat *et al.*, 2006). Raft recruitment depends on phosphorylated Vav1, which induces the exchange from GDP to GTP of Rac1, which in turn leads to reorganization of the actin cytoskeleton. Blocking actin polymerization impairs the receptor recruitment as well as its phosphorylation, suggesting cytoskeletal rearrangement upstream of DRM recruitment and phosphorylation (Watzl *et al.*, 2003). Cholesterol depletion, resulting in the disruption of lipid rafts, highlights the requirement of specialized membrane microdomains for 2B4 functionality as it interferes with receptor phosphorylation and thereby completely blocks target cell lysis by NK cells (Hillyard *et al.*, 2007; Watzl *et al.*, 2003).

NK cells bear the risk to be permanently stimulated due to constitutively expressed activating receptors and thereby leading to uncontrolled target cell lysis. At this point, inhibitory receptors come into play. DRM recruitment of 2B4 can be blocked by inhibitory KIR engagement, whereby the ITIM-bound SHP-1 seems to act upstream of 2B4 receptor phosphorylation (Watzl *et al.*, 2003; Watzl *et al.*, 2000). The same is true for the NKG2D receptor. Stimulation of this activating receptor results in its recruitment into DRM, whereas this can be blocked by engagement of the inhibitory CD94/NKG2A heterodimer (Endt *et al.*, 2007).

KIR inhibitory receptors are not found in lipid rafts, leading to the assumption that they interfere from outside with the formation of NKIS (Fassett *et al.*, 2001). Nonetheless, the formation of an inhibitory synapse has been described as counterpart for the activating synapse leading to the discrimination between supramolecular activating cluster (SMAC) and supramolecular inhibitory cluster (SMIC). SMICs have been reported to be built after engagement of inhibitory KIRs, followed by their recruitment into the center of the contact area (Davis *et al.*, 1999; Vyas *et al.*, 2002). SMICs differ from the SMAC in that they exclude lipid raft components and do not accumulate actin filaments (Lou *et al.*, 2000; McCann *et al.*, 2003). Instead, the phosphatase SHP-1 is recruited to SMICs, which can block the recruitment of activating receptors into lipid rafts (Vyas *et al.*, 2004).

The interplay between inhibitory KIR and activating receptors is summarized in Figure 5.

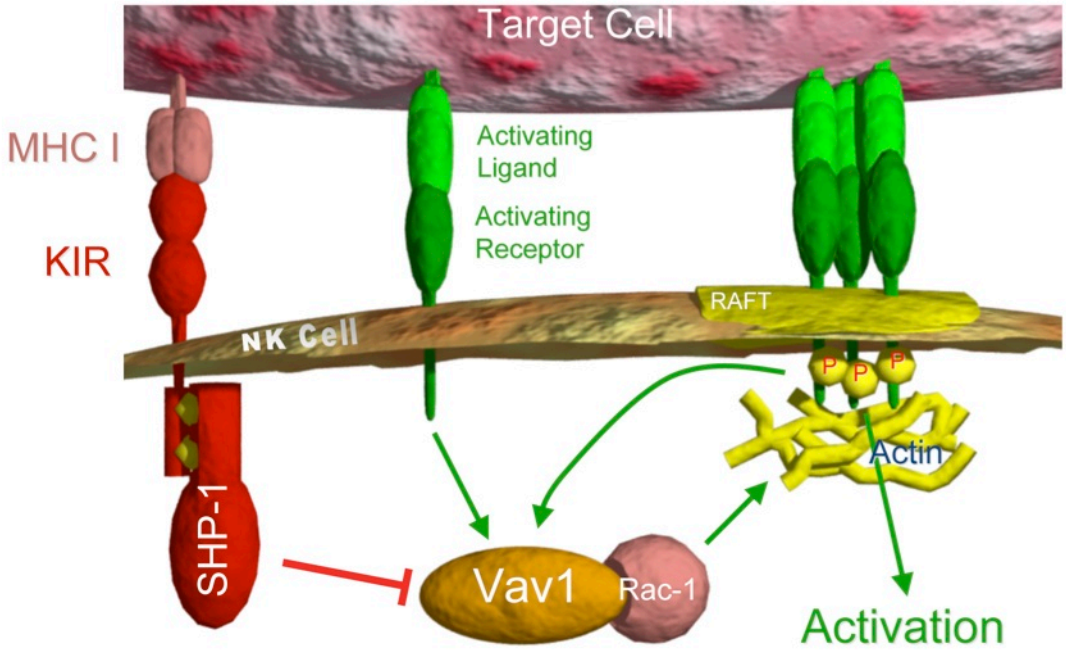

Figure 5: Crosstalk between activating and inhibitory signals. Upon triggering of activating receptors Vav1 gets phosphorylated and initiates a positive feedback loop of actin reorganization and recruitment of more activating receptors. Inhibitory receptors can block phosphorylation of Vav1 via the phosphatase SHP-1.

1.8 Studying lipid rafts

Most definitions and studies concerning lipid rafts are based on the method of cold non-ionic detergent lysis and subsequent sucrose density gradient centrifugation. Therefore lipid rafts are defined as DRMs. However, this method has often been criticized to cause artifacts: (a) Classification of lipid raft marker proteins is dependent on detergent, temperature, and cell type and therefore varies with the experimental setup (Chamberlain, 2004; Schuck *et al.*, 2003). (b) The use of detergent may also isolate molecules from intracellular membranes (Chamberlain, 2004). (c) The detergent may influence protein and lipid content due to rearrangement of intermolecular associations (Heerklotz, 2002). (d) It has been demonstrated that Triton X-100 enhances formation of lo domains or induces fusion of existing rafts (Simons and Vaz, 2004), thereby provoking false-positive conclusion. (e) Weak lipid-protein interactions may not be strong enough to resist detergent-mediated lysis (Schuck *et al.*, 2003). (f) Cofractionation of two proteins in DRMs does not prove the colocalization of those proteins in the same rafts (van der Goot and Harder, 2001). Hence, non-invasive methods are needed to study the natural composition of lipid rafts. Several techniques have been used to shed light on membrane microdomains. Flow cytometry became a useful tool to study lipid rafts since the discovery that the subunit B of cholera toxin (CTXB) binds to GM1 with high affinity. However, it has to be considered, that CTXB induces small aggregates on ice, which became extensively larger after incubation at 37 °C (Hammond *et al.*, 2005). Additionally to CTXB several fluorescently labeled lipid derivates exist, which can either mark the lo-

(raft) or ld- (non-raft) phase. Fluorophore-conjugated antibodies against cholesterol or other well-accepted raft-markers as GPI-anchored proteins like CD48, the ligand of 2B4, may be an option to localize membrane microdomains (Kiss *et al.*, 2008). Imaging approaches using two-photon or confocal microscopy bear the advantage to visualize lipid domains in a nearly physiological manner, whereby optical approaches are limited by the resolution of the microscope used. Further non-invasive fluorescence-based methods with higher resolution are the often used Förster resonance energy transfer (FRET) microscopy (Rao and Mayor, 2005; Sharma *et al.*, 2004), and the recently applied stimulated emission depletion (STED) far-field fluorescence nanoscopy (Eggeling *et al.*, 2009). Whereas the novel method of STED became attractive to study single molecules trafficking in nanosized areas, energy transfer methods are restricted to a pair of interacting proteins. Both techniques, as well as all visualization methods, are not applicable to the analysis of multimolecular complexes. A new method to study the composition of membrane microdomains was developed by Harder and Kuhn (Harder and Kuhn, 2001) based on the observation that TCR signaling complexes accumulate in the contact zone towards an anti-TCR coated magnetic bead (Hartgroves *et al.*, 2003). Polarized cells were subsequently disrupted using nitrogen cavitation. Thereby, nitrogen is dissolved under high pressure into cells. Sudden release of pressure induces the nitrogen to become gaseous again. This is accompanied by an extension of the gas, which in turn results in stretching of the lipid membrane until the cell is ruptured. This mechanical approach bears several advantages: Firstly, the sample is rather chilled than warmed-up due to its adiabatic pressure release. Secondly, no detergent is used, preventing the mentioned lipid and protein disruptions. At least, the use of inert gas enables steady-state conditions without oxidation or changes in pH. By using this method of immunoisolation, protein as well as lipid composition surrounding the TCR signaling complexes have been successfully analyzed (Harder and Kuhn, 2000; Hartgroves *et al.*, 2003; Zech *et al.*, 2009).

1.9 Glycosylation of proteins

Glycosylation is a diverse and highly regulated mechanism of posttranslational modification of proteins and lipids. Glycans are involved in many key biological processes including receptor activation, signal transduction, endocytosis as well as cell adhesion and molecular trafficking. In recent years, the knowledge about glycosylation and its function expanded enormously. Glycobiology became a popular field to understand structure, chemistry, biosynthesis, and biological function of glycans and their derivatives as well as their interrelation with other biological functions. The "glycome" is the complete quantity of sugars in an organism comparable with the term "proteome". The

glycome differs highly between species and serves as self-nonself recognition mechanism among them, but also among organisms themselves. Indeed, pathogens are often recognized via their sugar moieties and faults in glycosylation cause developmental defects and severe diseases. The diversity of glycosidic modification makes identification and functional relation difficult and leads to the estimation that the variability of the human glycome exceeds that of the proteome. Especially the immense structure repertory and the multiplicity of linkages and combinations facilitate the linkage with each other and with different macromolecules and thereby increase the spectrum of complexity (Kottgen *et al.*, 2003; Ohtsubo and Marth, 2006). The spectra of macromolecules is formed by diverse junctions of monosaccharides, mainly composed of D-glucose (Glc), D-galactose (Gal), D-mannose (Man), L-fucose (Fuc), D-xylose (Xyl), glucuronic acid and iduronic acid, as well as the amino sugars *N*-acetylglucosamine (GlcNAc), *N*-acetylgalactosamine (GalNAc) and the sialic acids (SA/Neu5Ac). However, despite the multiplicity of glycan structure, its synthesis is based on common cellular mechanism involving glycosyltransferases and glycosidases.

Protein glycosylation includes *N*- and *O*-glycans as well as glucosaminoglycans (proteoglycans). In the following sections, the synthesis of *N*- and *O*-glycans as well as their involvement in cellular mechanisms will be described in detail.

1.10 Structure and biosynthesis of *N*-glycans

N-glycosidically bound carbohydrates are linked via *N*-acetlyglucosamine to the asparagines residues within the N-!P-[S/T] sequence motif (where !P is any amino acid except proline). However, Zielinska *et al.* have shown that *N*-glycosylation is not restricted to this consensus sequence or the uncommon N-X-C motif but can also be found on yet unknown positions (Zielinska *et al.*, 2010). Furthermore, only 30 % of all available motifs within a protein are glycosylated with some of them showing only incomplete glycosylation (Mellquist *et al.*, 1998).

The biosynthesis of *N*-glycans starts in the cytosolic compartment of the rough ER (rER) (for details see also Figure 6). Herewith, an oligosaccharide precursor is formed by the transfer of GlcNAc from UDP-GlcNAc to dolichol phosphate (Dol-P). This step can be inhibited by tunicamycin. This mixture of homologous nucleoside antibiotics inhibits the GlcNAc phosphotransferase (GPT) to catalyze the initial step of *N*-glycosylation. The rest of the sugar core is added subsequently till the Dol-P-P-$(GlcNAc)_2$-$(Man)_5$ tree is completed. The oligosaccharide "flips" into the lumen of the rER, where it is completed by the addition of 4 Man and 3 Glc residues.

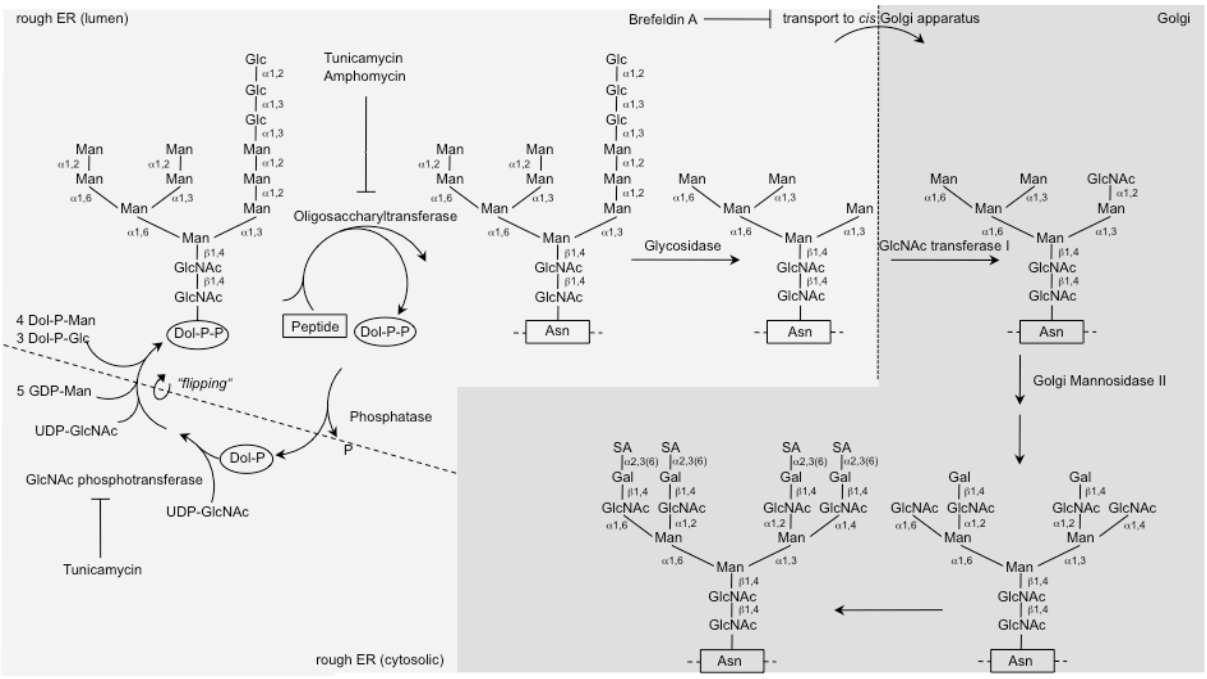

Figure 6: Process of *N*-glycosylation. UDP-GalNAc is transferred to Dol-P (oval) in the cytoplasm at the rough ER (light gray) membrane. After addition of GlcNAc and 5 Man to the growing sugar tree, the structure "flips" (dashed line) to the inside of the rER, where further sugar moieties are added and the tree subsequently is transferred to a peptide's Asn residue (box). After several Man and Glc residues have been removed, the peptide is transferred (dotted line) to the Golgi (dark gray), where further Man residues are removed and GlcNAc and Gal are added. Addition of the GlcNAc marks conversion to the complex type. The resulting branched *N*-glycan structure can be further elongated by the sequential addition of Gal, Fuc and SA. An exemplified tree is shown. For abbreviations see text. Inhibitors are included.

The assembled precursor molecule is subsequently transferred by oligosaccharyl-transferase cotranslationally to the nascent polypeptide. This step can also be inhibited by tunicamycin as well as amphomycin. Two glycosidases (α1,2-glucosidase I, α1,3-glucosidase II) remove the terminal Glc residues. Both enzymes can be inhibited by further chemicals, as well. After additional removal of one Man residue by α1,2-mannosidase the glycosidic tree is transported from the rER to the Golgi compartment. This transport is receptor mediated and can be inhibited by Brefeldin A (Kleene and Schachner, 2004; Moremen *et al.*, 1994). Here, the glycosidic tree is terminated depending on its final destination, which is determined by the amino acid sequence of the protein. The processing mostly begins with the ablation of further mannose residues and stepwise addition of GlcNAc, Gal and finally Neu5Ac. This leads to the formation of different "antennae". The transfer of sialic acid residues terminates the glycosidic tree, as they cannot serve as target for glycosyltransferases or glycosidases, generally. The trimming and processing mechanisms in the Golgi compartment is highly complex and ends in different oligosaccharide structures: high mannose types, ending with unsubstituted Man residues, hybrid types and complex types. The latter are mostly secreted or cell surface *N*-glycans.

Despite their large modification variability, *N*-glycans possess a common core structure, resulting from the transfer of the oligosaccharide precursor (Beyer *et al.*, 1979; Kleene *et al.*, 2004; Kornfeld and Kornfeld, 1985). Even though many of the mutations affecting *N*-glycosylations are lethal (Freeze and Westphal, 2001), in recent years, it has become evident that defects in the attachment of carbohydrates to proteins are implicated in a number of human diseases. Among these, the congenital disorders of glycosylation (CDGs) refer to a large number of syndromes that include severe morphogenic and metabolic defects. Molecular causes for some of the syndromes included have been well investigated. The most prevalent ones are due to a mutation in the *PMM2* gene. These mutations diminish the production of the dolichol-oligosaccharide precursor, which is essential for the initiation of *N*-glycosylation (Ohtsubo *et al.*, 2006; Spiro, 2002). Furthermore, *N*-glycans have been shown to be involved in modulating the conformation and activity of integrins and extracellular matrix (ECM) proteins (Janik *et al.*, 2010). Thus, improper glycosylation of cell surface proteins involved in cell adhesion as e.g. integrins, can result in different adhesion behavior. This in turn has been shown to lead to enhanced metastatic potential of tumor cells (Zhao *et al.*, 2008).

Proper *N*-linked glycosylation therefore is a tightly regulated and controlled process that determines the fate of molecules and whole organisms (Ohtsubo *et al.*, 2006).

1.11 Structure and biosynthesis of *O*-glycans

In contrast to *N*-linked glycans, the synthesis of *O*-linked glycans is less well established. The main types of *O*-linked glycans are those of the mucin and the proteoglycan type. Both are generated relatively late during protein processing in the Golgi compartment (Ungar, 2009). Mucin type *O*-glycans are attached to serine or threonine residues and at later stages during protein processing. However, a consensus sequence has not been elucidated, so far. GalNAc represents the first sugar to be linked to serine or threonine. It is transferred from UDP-GalNAc to the hydroxyl group of Ser or Thr by a large family of up to 20 different GalNAc transferases in *cis* Golgi compartments (Tarp and Clausen, 2008). The chemical compound Benzyl-α-*N*-GalNAc (BADG) competes with endogenous galactosyltransfer and thus inhibits the proceeding of *O*-linked glycosylation (Kuan *et al.*, 1989). Starting from the first GalNac, there are several different possibilities to further elongate the *O*-linked glycan in *trans* Golgi vesicles by different glycosyltransferases, depending on the linkage and the sugars used (details for the synthesis are shown in Figure 7) (Tarp *et al.*, 2008). There are four different starting structures (core1-4) and they are often elongated by the addition of further Gal, GlcNAc or GalNAc residues and usually are terminated by Fuc, Neu5Ac, or both (Dall'olio, 1996). Modifications and mutations in *O*-glycosylation were shown to potentially promote tumor cell growth and survival by influencing cell adhesion (Hollingsworth and Swanson, 2004) by impairing

e.g. the cytotoxicity of NK cells (Ogata *et al.*, 1992) or of T lymphocytes (van de Wiel-van Kemenade *et al.*, 1993).

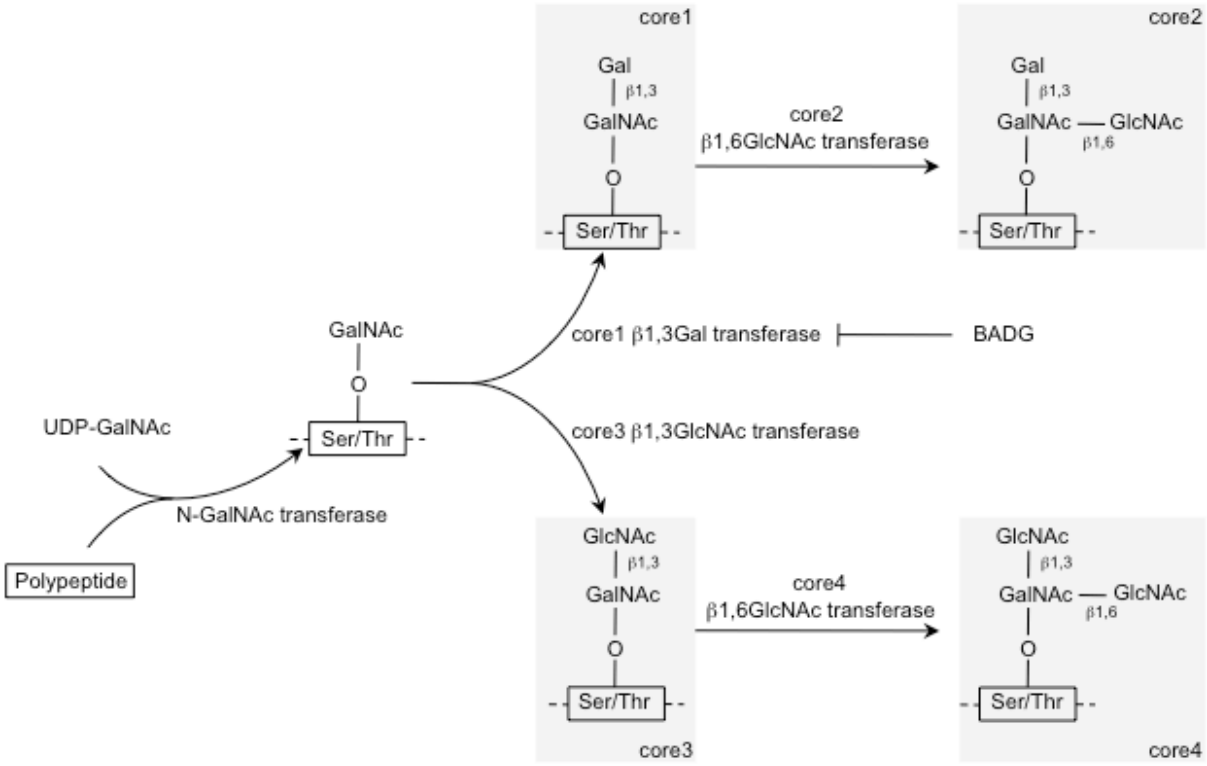

Figure 7: Synthesis of mucin type *O*-glcans. Mucin type glycans are attached to serine or threonine. GalNAc represents the first sugar to be linked to Ser or Thr of a polypeptide (boxed). It is transferred from UDP-GalNAc to the hydroxyl group of Ser or Thr by a large family of up to 20 different GalNAc transferases in *cis* Golgi compartments (Tarp *et al.*, 2008). Starting from this GalNac, there are several different possibilities to further elongate the *O*-linked glycan in *trans* Golgi vesicles by different glycosyltransferases. If Gal is linked via β1,3 linking to the *O*-3 position the so called core 1 structure is formed, which is the basis for most of the mucin-type *O*-linked glycans. In mammals, this reaction is carried out by a single core1 Gal transferase. Further attachment of GlcNAc via β1,6 linking to the initial GalNAc by one of three GalNAc transferases results in the core2 structure (Tarp *et al.*, 2008). In contrast β1,3 linking of GlcNAc to the initial GalNAc leads to the core3 structure. Core3 may serve as substrate for an enzyme catalyzing the core 4 reaction. Here, GlcNAc is added in a β1,6 linkage to GalNAc similar to synthesis of the core 2 structure (Tarp *et al.*, 2008). These four starting structures often are elongated by the addition of further Gal, GlcNAc or GalNAc residues and usually are terminated by Fuc, Neu5Ac, or both. BADG competes for sugar elongation, where indicated. For abbreviations see text.

1.12 Sialic acids (SA)

Sialic acids are derivates of neuraminic acid. The monosaccharides with a nine-carbon backbone contain a carboxylgroup, which leads to the addition of one negative charge at physiological pH. Diversity of sialic acids is generated by different substitutions based on the neuraminic acid moiety. About 50 sialic acid types are known. The most frequent synthesized forms are *N*-acetylneuraminic acid (Neu5Ac), followed by *N*-glycolylneuraminic acid (Neu5Gc) and *O*-acetylated derivatives, mostly *N*-acetyl-9-*O*-

acetylneuraminic acid (Neu5,9Ac2) (Varki and Schauer, 2009). Sialic acids are mainly found at the end of glycoproteins and glycosphingolipids. In *N*-glycans, sialic acids are mainly linked α2,3 or α2,6 to Gal, in *O*-glycans they are usually linked to GalNAc (Blix *et al.*, 1956). A special sialylation moiety is found on the neuronal cell adhesion molecule NCAM (CD56). Herewith, a large glycopolymer consisting of α2,8 linked sialic acids is found, which can reach up to 100 sugar residues (Finne *et al.*, 1983). Due to their terminal position and negative charge, sialic acids exhibit the ability to interact with other molecules and thereby serve as recognition site, but also may inhibit intermolecular and therefore intercellular interaction (Schauer, 2009).

The influenza virus from birds and pigs is able to recognize and bind α2,3 linked sialic acids via its hemagglutinin. The viral Neuraminidase is important for viral release, as it cleaves the carbohydrate bond and therefore enables the viral core to bud from the cell surface. In contrast, human influenza virus mainly recognizes α2,6 linkages. Hence, a mutation in the hemagglutinin gene could enable the avian virus to infect human cells, leading to a pandemic effect.

It has recently been shown that sialylation has an important role during the maturation from double positive to CD8 single positive cells: Immature $CD8^+$ T cells sustain a low level of sialylation whereas naïve T cells are highly sialylated. This core1-*O*-linked sialylation plays an important role, as it decreases the cognate binding of CD8 towards MHC class I molecules. Another example that glycosylation, in particular sialylation, plays a major role in regulating lymphocyte activity is the complex mechanism of CD22 signaling (also known as Siglec-2). It modulates BCR signaling by inhibiting its downstream events and thereby preventing a constant activation of B cells. It became clear that CD22 interacts with α2,6 sialic acid residues of IgM, the main part of the BCR, on the same surface. This *cis* interaction leads to tyrosine phosphorylation of CD22 and finally to BCR signal inhibition (Jin *et al.*, 2002; Kelm *et al.*, 2002). However, *trans* interaction of CD22 with its ligand is able to control the BCR activation strength. Maybe CD22 moves in concert with IgM into the contact zone, where its engagement results in a direct down-modulation of the BCR (Lanoue *et al.*, 2002). As α2,6 sialic acids are ubiquitously synthesized by human cells, the CD22 *trans* interaction could be a mechanism to avoid autoimmunity.

1.13 Glycan binding proteins - Siglecs

Carbohydrates seem to be rather involved in fine tuning, or act as molecular switches (Schauer, 2009), as the affinity of proteins for carbohydrates is relatively low (K_d valued in micromolar to low millimolar range). However, the specificity is relatively high.

Furthermore, the avidity of glycan-binding proteins is enormous, as some of them can bind multiple glycan moieties.

Lectins are a group of glycan binding proteins first identified in plants. Lectins can be devided into 5 groups (R-, L-, C-, P- and I-type,) due to their ligand recognition characteristics. Siglecs (sialic acid binding Ig-like lectins) belong to the I-type lectins as they recognize carbohydrates via an Ig-domain. They are mostly expressed on hematopoietic cells and contain a cytoplasmic ITIM domain, thereby transmitting inhibitory signals (Sperandio *et al.*, 2009). NK cells express Siglec-7 and -9, which are able to suppress NK cell activation (Yamaji *et al.*, 2005). Recently, it has been shown that the mucin MUC16, which is highly expressed by epithelial ovarian cancers, is recognized by Siglec-9 in a sialic acid dependent manner (Belisle *et al.*, 2010). This interaction is thought to suppress NK cell activity and thereby dampen an anti-tumor response.

In summary, glycans are involved in many cellular and also metastatic processes and represent an enormous role in altering protein-protein or protein-carbohydrate recognition. Protein glycosylation is highly ordered and regulated and defects in glycosylation are lethal or results in severe diseases. Sometimes, glycans are the only variation between otherwise identical glycoproteins. These differences can occur within one and the same cell, resulting in a "microheterogeneity" (Ohtsubo *et al.*, 2006), which does not necessarily abolish or induce recognition, but may modify the interaction with other molecules. Determining the regulation of glycosylation, their alterations and outcome in cell-cell communication will provide profound insights into the role of glycans in mammalian diseases and immunity.

2 AIMS OF THE THESIS

NK cells represent a tool for the immune system to act against malignant and virus infected cells. It is therefore important to understand the early signaling events after the triggering of activating NK cell receptors and the mechanisms regulating receptor affinity.

In a first approach a bead-based isolation method to analyze membrane microdomains surrounding NK cell receptors and its adjacent cytoplasmic parts should be established. As mentioned before, many observations aimed at the use of detergents to characterize regions of mostly activating immune cell receptors. However, the use of detergents is discussed controversial to result in artifacts due to artificial membrane disruption. Furthermore, the commonly used methods fail to authentically depict the *in vivo* situation and does not allow for analysis comparing activating and inhibitory receptor signaling. To analyze a more natural composition of membrane microdomains surrounding NK cell receptors, the antibody coated bead based system developed by Harder and Kuhn (Harder *et al.*, 2001) should be modified to study the outcome of NK cell stimulation. This method would also enable us to investigate inhibitory NK cell receptors, as those are not recruited into DRMs and thereby fail to be examined by chemical disruption methods. After successful establishment, the system should be used to investigate time-dependent changes of adjacent proteins, as well as differences between activating and inhibitory receptors with respect to associated molecules.

The second aim was to investigate posttranslational modifications of 2B4 and their outcome in NK cell activation. 2B4 represents a highly glycosylated protein with several proposed *N*-glycosylation sites (Tangye et al., 1999 and this thesis). However, up to now, the influence of 2B4 associated glycans remains elusive. Since glycans can have multiple implications for ligand recognition and functional outcome, we proposed influences of 2B4 associated glycans as well. Characterization of glycosidic alterations of 2B4 expressed by different NK cell lines and also primary NK cells as well as their modification should give us information about the carbohydrate composition and their influence in receptor affinity. By using glycosylation inhibitors, we aim to test how glycosylation may impair 2B4 mediated target cell killing.

3 MATERIAL AND METHODS

3.1 Materials

3.1.1 Mouse monoclonal antibodies

Name	Conjugate	Source, Reference
IgG control, MOPC21	none, PE	Sigma, Taufkirchen, Germany
anti-2B4 (C1.7)	none, PE	Immunotech, Marseille, France
anti-NKG2D (149810)	none, PE	RnD Systems, Minneapolis, USA
anti-NKp30 (p30-15)	none, PE	(Hoffmann *et al.*, 2007) + BioLegend, Uithoorn, The Netherlands
anti-NKG2A/CD159a (Z199)	none	Beckman Coulter, Fullerton, USA
anti-CD45	none	BD Pharmingen, Germany
anti-CD48 (MEM-102)	none, PE	Santa Cruz Biotechnology, Germany + BD Pharmingen, Germany
anti-Vav1 (VAV-30)	none	Abcam, Cambridge, USA
anti-phospho-tyrosine, 4G10	biotin	Upstate cell signaling solutions, Charlottesville, VA, USA
anti-ILZ	none	Stark *et al.*, 2005

3.1.2 Rabbit polyclonal antibodies

Name	Source, Reference
anti-2B4	Watzl *et al.*, 2000
anti-phospho Vav1 pY160	Biosource, Camarillo, CA

3.1.3 Secondary antibodies

Name	Conjugate	Source, Reference
goat-anti-mouse IgG	none	Dianova, Hamburg, Germany
goat-anti-mouse IgG	HRPO	Jackson ImmunoResearch Laboratories, USA
goat-anti-mouse IgG	PE	Jackson ImmunoResearch Laboratories, USA
goat-anti-rabbit IgG	HRPO	Santa Cruz Biotechnology, Heidelberg, Germany
goat-anti-human IgG	Biotin	Jackson ImmunoResearch Laboratories, USA

3.1.4 Recombinant proteins

Name	Tag	Source
2B4-ILZ	ILZ followed by 6xHis (C-terminal)	Stark *et al.*, 2005 and this thesis
rhSiglec7-Fc Chimera	Fc	RnD Systems, Minneapolis, USA

3.1.5 Cells

All culture media, fetal calf serum (FCS), non-essential amino acids and sodium pyruvate were purchased from Gibco (Invitrogen, Carlsbad, CA); donor horse serum was purchased from Biochrom (Berlin, Germany), human serum from PromoCell (Heidelberg, Germany), PHA-P from Sigma and purified human IL-2 from Hemagen Diagnostics (Columbia, USA). If not indicated otherwise, all cells were grown with 10 % (v/v) FCS and 1 % (v/v) penicillin/streptomycin (Gibco, Invitrogen).

Cell type	Origin	Culture Medium
NKL	human NK cell line	RPMI, 100 U/ml IL-2
NK92C1	human NK cell line from malignant non-Hodgkin lymphoma	Alpha MEM, 12.5 % (v/v) FCS, 12.5 % (v/v) donor horse serum, 2-mercaptoethanol
primary human NK cells	isolated from peripheral blood mononuclear cells (PBMC) by negative selection	IMDM, 10 % (v/v) human serum, 10 % (v/v) non-essential amino acids, 10 % (v/v) sodium pyruvate, 100 IU/ml IL-2
HeLa	cervical cancer cell line	DMEM
HEK-293T (HEK)	human embryonic kidney cell line	DMEM
HEK-2B4	HEK-293T cells, stably transfected with human 2B4	DMEM + 1 µg/ml puromycin
HEK-CD48	HEK-293T cells, stably transfected with human CD48	DMEM + 1 µg/ml puromycin
HeLa-CD48	cervical cancer cell line, stably transfected with human CD48	DMEM + 1 µg/ml puromycin
HeLa-Mock	cervical cancer cell line, stably transfected with human CLEC12B	DMEMµ + 1 µg/ml puromycin

3.1.6 Enzymes

Name	Use	Source
CIP (Calf Intestinal Phosphatase)	depohosphorylation of proteins	New England Biolabs, Frankfurt, Germany
PNGaseF (Peptide-*N*-Glycosidase F)	de-*N*-glycosylation of proteins	Sigma, Germany
Neuraminidase (*Arthrobacter ureafaciens* α2-3,6,8,9-Neuraminidase)	desialylation of proteins and cells	Merck-Calbiochem, Darmstad
O-Glycosidase (Endo-α-N-Acetyl galactosaminidase)	de-*O*-glycosylation of proteins	New England Biolabs, Frankfurt

3.1.7 Inhibitors

Name	Use	Source
BADG (Benzyl-2-acetoamido-2-deoxy-α-D-galactopyranoside; dissolved in DMSO)	inhibitor for *O*-glycosylation	Merck, Calbiochem
TM (tunicamycin)	inhibitor for *N*-glycosylation	Merck, Calbiochem

3.1.8 Plasmids

Name	Comment	Source
2B4-ILZ	expression construct for 2B4-ILZ fusion protein	Stark et al 2005
dIgC2 (2B4-deltaIgC2)	expression construct for human 2B4, deleted of the membrane proximal C2 type Ig domain	Claus *et al*, unpublished results
Y1,2,3,4F (2B4-Y1,2,3,4F)	expression construct for human 2B4 with all ITSM tyrosins mutated to phenylalanine	Eissmann *et al.*, 2005

3.1.9 Kits

Isolation of human NK cells	NK Cell Negative Isolation Kit, Invitrogen (formerly Dynal, Oslo, Norway)
Quantification of protein concentration	EZQ Protein Quantitation Kit, Molecular Probes, Invitrogen
Quantification of surface molecules	Qifikit, Dako
IFN-γ measurement	Human IFN-γ ELISA, Bender Med Systems, Vienna
Silverstaining	SilverSNAP Silver Stain Kit II, Thermo Scientific
CyDye DIGE Fluor minimal dye labeling kit	GE-Healthcare, Freiburg, Germany

3.1.10 Buffers

Triton X-100 lysis buffer:	150 mM	NaCl
	20 mM	Tris-HCl, pH 7.4
	10 % (v/v)	Glycerol
	0.5 % (v/v)	Triton X-100
	2 mM	EDTA
	10 mM	NaF
	1 mM	PMSF
	1 mM	Na-orthovanadate (for studies on protein phosphorylation)
PBS (pH 7.4):	137 mM	NaCl
	8.1 mM	Na_2HPO_4
	2.7 mM	KCl
	1.5 mM	KH_2PO_4
PBST:	1 x	PBS
	0.05 % (v/v)	Tween 20
PBST/NaCl:	1 x	PBS
	0.05 % (v/v)	Tween 20
	0.5 M	NaCl
Blocking buffer for Western blot:	1 x	PBST
	5 % (w/v)	nonfat dry milk powder, Saliter, Obergünzburg
PBS/pervanadate:	1 x	PBS
	10 mM	H_2O_2
	200 µM	Na-orthovanadate
Western blot transfer buffer:	24 mM	Tris
	129 mM	Glycin
	20 % (v/v)	MeOH
5xRSB (reducing sample buffer): *(for 1x and 2x RSB, dilute with 50 % Glycerol)*	10 % (w/v)	SDS
	50 % (v/v)	Glycerol
	25 % (v/v)	2-Mercaptoethanol
	0.1 % (w/v)	Bromphenol Blue
	0.3125 mM	Tris-HCl, pH = 6.8
Stripping buffer (pH 2.2) for Western blot:	200 mM	Glycin
	0.1 % (w/v)	SDS
	1 % (v/v)	Tween 20

Immunoisolation:

IMDM Hepes + FCS:	1x	IMDM
	1 % (v/v)	Hepes
	50 mM	FCS
1000xCLAP (protease inhibitor, dissolved in DMSO):	10 mg/ml	Chymostatin
	10 mg/ml	Leupeptin
	10 mg/ml	Antipain
	10 mg/ml	Pepstatin
		(all Sigma, Germany)
100xDNAse:	50 % (v/v)	Glycerol
	150 mM	NaCl
	10 mg/ml	DNase (≥2,000 Kunitz units/mg)
		(Sigma, Germany)
HB (HBuffer):	250 mM	Sucrose
	10 mM	Na-Hepes pH 7.2
	10 mM	NaF
	50 mM	NaCl
	1 mM	Na-orthovanadate
HB^+ ($HBuffer^+$):	1x	HB
	1x	CLAP
	1x	DNase
	prepare immediately before use	

2D-Gelelectrophoresis:

CHAPS/ASB-14 lysis buffer	7 M	Urea
	1 M	Tris-Base
	2 M	Thiourea
	4 % (w/v)	detergent (ASB-14 or CHAPS)
CHAPS/ASB-14 2xSB (sample buffer) stock solution	7 M	Urea
	2 M	Thiourea
	2 % (w/v)	detergent (ASB-14 or CHAPS)
Rehydration Solution	(2,5 ml)	2x SB stock
	2 % (50 µl)	IPG Buffer, pH 3-10 or pH 3-11 *(BioRad)*
	2 % (50 mg)	DTT
DeStreak Rehydration Solution (for 2D-DIGE)	(3 ml)	DeStreak Rehydration Solution *(GE Healthcare)*
	2 % (60 µl)	IPG Buffer, pH 3-11 *(BioRad)*

SDS equilibration buffer pH 7.0:	75 mM	Tris, pH 8.8
	6 M	Urea
	30 % (v/v)	Glycerol
	2 % (w/v)	SDS
Equilibration buffer I:	SDS equilibration buffer incl. 0.5 % (w/v) DTT	
Equilibration buffer II:	SDS equilibration buffer incl. 4.5 % (w/v) Iodacetamid	
10xSDS electrophoresis running buffer pH 8.3	250 mM	Tris-HCl
	19.2 mM	Glycine
	1 % (w/v)	SDS
Fixation solution	50 % (v/v)	Methanol
	7 % (v/v)	Acetic acid
Washing solution	10 %	Methanol
	7 %	Acetic acid

Protein purification:

HBS (2x)(pH 7.0):	13 g/l (w/v)	Hepes
	16 g/l (w/v)	NaCl
	3 mM	Na_2HPO_4
ILZ wash buffer (pH 8.0):	50 mM	NaH_2PO_4
	300 mM	NaCl
	20 mM	Imidazole
	0.05 % (v/v)	Tween 20
ILZ elution buffer (pH 8.0):	50 mM	NaH_2PO_4
	300 mM	NaCl
	250 mM	Imidazole
	0.05 % (v/v)	Tween 20

MOPS buffer (20 x) (Invitrogen)

TAE (10 x) (Invitrogen)

3.1.11 Chemicals and reagents

Most chemicals were purchased from Roth (Karlsruhe, Germany), Sigma-Aldrich (Seelze, Germany), Merck (Darmstadt, Germany).

Name	Source
BSA	Serva, Heidelberg, Germany
Chromium-51	Hartmann Analytik, Braunschweig
Dynabeads: Protein G, Pan mouse IgG, goat-anti-mouse	Dynal, Invitrogen
recombinant human IL-2	NIH cytokine repository
recombinant human IL-15	R&D Systems, Minneapolis, USA
IPG buffer / ampholytes	Bio-Rad
ReadyStrip IPG pH3-10 (7 cm)	Bio-Rad
Immobiline Dry Strip pH3-11 NL (24 cm)	GE-Healthcare, Freiburg, Germany
LSM solution	PAA, Pasching, Germany
Ni^{2+}-NTA Agarose	Qiagen, Hilden, Germany
Phosphatebuffer G7-Reactionbuffer	NEB Biolabs
PVDF Blot membrane	Millipore
Puromycin	Sigma, Germany
Precision Plus Protein Standard	BioRad, Hercules, CA
Protein G agarose	Invitrogen
NuPAGE Gels	Invitrogen
Streptavidin-HRPO	Jackson ImmunoResearch Laboratories, USA
Streptavidin-PE	Jackson ImmunoResearch Laboratories, USA
SuperSignal West Pico and Dura	Thermo
SYPRO Ruby Protein Gel Stain	Molecular Probes, Invitrogen
TrypLE Express	Invitrogen
X-ray films	Perbio/Pierce, Rockford, IL

3.2 Methods

3.2.1 Cell culture

All cells were grown at 37 °C and 5 % CO_2 in a humidified incubator under sterile conditions. Cell lines were splitted on a regular basis every two to three days. Cell culture flasks were exchanged every week. Cells were frozen in FCS containing 10 % DMSO at -75 °C and stored in liquid nitrogen. Cell lines were thawed on a regular basis. FCS and human serum were heat inactivated by incubation on 56 °C for 30’ prior to use.

3.2.2 NK cell isolation

Human polyclonal NK cells were isolated from whole blood or buffy coats. First peripheral blood mononuclear cells (PBMC) were purified by density centrifugation over LSM solution. Then NK cells were isolated using the NK cell negative isolation kit from Dynal (Invitrogen). NK cells were between 90 % and 99 % $NKp46^+$, $CD3^-$ and $CD56^+$. After isolation, NK cells were plated on 96 well round bottom plates at $1x10^6$-$2x10^6$ cells/ml with $5x10^5$ cells/ml irradiated JY cells. Growing cells were expanded 1:1 with IMDM medium supplemented as described above.

3.2.3 Cell stimulation

3.2.3.1 Cell stimulation with beads

Dynabeads were washed three times with IMDM Hepes+FCS medium and resuspended in the initial volume or at least 50 µl. Human-anti-mouse coupled Dynabeads comprise of $4x10^8$ beads/ml. 2 µg of mouse antibody was added per 10^7 beads and incubated for 1 h at room temperature at a rotating wheel. After three washes, the Dynabeads were resuspended at $4x10^8$ beads/ml in medium. Cells were harvested, washed three times and prepared as cell pellet in a 1.5 ml Eppendorf microcentrifuge or 15 ml Falcon tube. Antibody-coated Dynabeads were added at a ratio of 1:2 to the loosened cells, mixed carefully and incubated 5'-10' on ice. Cell-bead conjugates were transferred to 37 °C or to 4 °C for the desired time and reaction was stopped by adding 1-5 ml ice-cold HB and incubation for 5' on ice. Cell-bead conjugates were pelleted by centrifugation for 2' at 500xg at 4 °C.

3.2.3.2 Pervanadate stimulation

Protein phosphorylation was induced by using the phosphatase inhibitor pervanadate. Cells were resuspended at $2x10^7$ cells/ml in PBS/pervanadate solution and incubated for 10' at 37 °C.

3.2.4 Quantification of cell-bead contacts

Cell-bead conjugates were performed as described in 3.2.3.1. Cells and beads were counted using a conventional hemocytometer in four 1 mm^2 chambers, respectively. Contacts per bead were calculated as (contacts between cells and beads)/(total bead number) and contacts per cell were calculated as (contacts between cells and beads)/(total cell number).

3.2.5 Chromium-release assay

Cell lines were grown to mid log phase, primary NK clones were used at 3-4 weeks of age. Usually, $1x10^5$ NKL, $5x10^4$ NK92C1 or $2{,}5x10^4$ primary NK cells per well were used at highest effector:target ratio. $5x10^5$ HeLa-CD48 or HeLa-Mock target cells were labeled in 100 µl medium with 100 µCi ^{51}Cr (3,7 MBq) for 1 h at 37 °C. Cells were washed twice in medium and resuspended at $5x10^4$ cells/ml in medium. 5000 target cells/well were used in all assays. Maximum release was determined by incubation of target cells in 1 % Triton X-100. For spontaneous release, targets were incubated without NK cells in medium alone. All samples were done in triplicates. Plates were incubated for 4 h at 37 °C, 5 % CO_2. Supernatant was harvested and ^{51}Cr release was measured in a gamma counter. Percent specific release was calculated as ((experimental release - spontaneous release) / (maximum release - spontaneous release)) x 100.

3.2.6 Flow cytometry

3.2.6.1 Cell staining

Surface staining of cells was performed in 96 V-well plates. About $2x10^5$ cells were resuspended in 50 µl fluorescence-activated cell sorting (FACS)-buffer (PBS containing 2 % FCS) containing 10 µg/ml of the respective primary antibody or indicated concentrations of fusion protein and incubated on ice for 20'. After washing with FACS-buffer, cells were resuspended in 50 µl PE conjugated goat-anti-mouse secondary antibody diluted 1:200 in FACS-buffer. Cells were incubated on ice for 20' in the dark to protect the fluorophore, washed again and resuspended in FACS-buffer containing 2 % formaldehyde. Samples were analyzed on a BD FACScan or BD FACSCalibur and results were evaluated using the FlowJo Software from Treestar.

3.2.6.2 Quantification of surface molecules

Surface molecules were quantified using the Qifikit (Dako) according to the manufacturer's instructions. In brief, cell staining was performed as described but additionally, calibration beads were stained with the same solution of secondary antibody. Based on the mean fluorescence intensity (MFI) of the calibration bead populations a standard curve was generated and used to calculate molecule numbers on the stained cells.

3.2.7 Deglycosylation of NK cells

Desialylation of cells was done using 1 µl Neuraminidase for $1x10^6$ cells/100 µl PBS rotating 2 h at 37 °C, 5 % CO_2. To inhibit elongation of *O*-glycosyl chains, cells were incubated with 2.5 mM BADG 48 h at 37 °C, 5 % CO_2. De-*N*-Glycosylation was performed by incubating cells 12 h with 0.5 µg/ml tunicamycin at 37 °C, 5 % CO_2.

Cells were washed once with CTL medium (IMDM with 10 % FCS and penicillin/streptomycin) and used for flow cytometry, cytotoxicity assays or cell lysis.

3.3 Protein biochemistry

3.3.1 Nitrogen cavitation

Nitrogen cavitation was done with a pre-cooled apparatus and magnetic stirrer. Before adding the samples, the magnetic stirrer was set on full power and all valves were closed. Cell-bead conjugates were resuspended in up to 10 ml but at least 1 ml of freshly prepared HB^+ and transferred into the cavitation chamber. After closing the bomb and attaching all filling connections, the pressure was set to 1000 psi for 5' - 7', if not indicated differently. Samples were released by slowly opening the release valve and immediately retrieved using a 15 ml Falcon tube inserted in a magnet. The cavitation chamber was rinsed with 1 ml of HB and the tube filled up to 10 ml with HB. The tube was closed and inverted several times to release the beads from the foam. After an incubation period of 5' in the magnet at 4 °C, the supernatant was removed completely by aspirating the foam first followed by decanting the supernatant. Washing was repeated twice with 10 ml HB and transferred into a 1.5 ml eppendorf tube by resuspending beads in 1 ml HB^+. Beads were finally resuspended in 1 ml HB and counted using the Casy Cell Counter Model TT, "dried" by using the magnet and spinning down at 10,000 rpm at 4 °C and resuspended in an appropriate volume of buffer (such as 2×RSB, CHAPS-, ASB-14 lysis buffer or similar) for the subsequent analysis procedure.

3.3.2 Nitrogen cavitation – sample preparation for 2D-DIGE

For 2D-DIGE five samples of anti-2B4 and anti-NKG2A stimulation method were prepared. Therefore, $3x10^8$ NKLs were stimulated for 5' either with $1.5x10^8$ anti-NKG2A or anti-2B4 coated magnetic beads and disrupted via nitrogen cavitation. The washed beads were counted and proteins were solubilized / eluted in CHAPS lysis buffer with the ratio [bead number]:[volume of lysis buffer] of 4:1. The pH was set to 9.0 and samples were frozen subsequently. For concentration determination 1 µl sample was taken and diluted 1:8 with buffer. Protein concentration was analyzed using the EZQ Protein Quantitation Kit, the protein amount was calculated and samples were adjusted to 4 µg/µl. Samples were labeled using the CyDye DIGE minimal fluor protocol, separated via 2D-technique and gels were scanned and analyzed using the DeCyder software.

3.3.3 Cell lysis with Triton X-100

For Western blot analysis $1\text{-}2x10^7$ cells/ml were lysed to obtain the required protein concentrations. Pelleted cells were resuspended in 0.5 % Triton X-100 lysis buffer supplemented with 1 mM PMSF and if necessary 1 mM Na-orthovanadate and incubated on ice for 20'. Lysates were clarified by centrifugation for 15' at 20,000xg and 4 °C. If cells were stimulated with beads previously, beads were recovered before centrifugation, washed three times with Triton X-100 lysis buffer and resuspended in appropriate volume of buffer (such as 2×RSB, CHAPS-, ç14-lysis buffer or similar) for the subsequent analysis procedure.

3.3.4 Immunoprecipitation

Lysates of up to $2x10^7$ cells were incubated for 1 h with 20 µl of goat-anti-mouse Dynabeads coated with 1.6 µg Isotype mAb (MOPC21) for preclearing and subsequently with specific antibody to isolate protein of interest. Samples were washed three times with ice-cold lysis buffer and residual buffer was removed completely using a magnet followed by spinning down the beads and aspirating remaining buffer. Beads were eluted by incubation in 2xRSB at 95 °C for 5' or in ASB-14 or CHAPS containing lysis buffer by shaking at 18 °C for 20', respectively. Samples were frozen at -20 °C until they were analyzed by SDS- or 2D-PAGE and Western blot.

3.3.5 Fusion proteins

2B4-ILZ fusion proteins were produced and purified as described previously (Stark *et al.*, 2005; Watzl, 2006). Prior to protein elution from the agarose-beads, samples were divided and left untreated (2 h 4 °C) or enzymatically deglycosylated: For desialylation beads were incubated for 2 h at 37 °C with 17 µl Neuraminidase in PBS. Additional de-*O*-glycosylation was achieved in a second approach using 10 µl *O*-Glycosidase together with the amount of Neuraminidase mentioned before. For ablation of *N*-glycosidic bound carbohydrates the same amount of beads were incubated overnight at 37 °C with 17 µl of PNGaseF in 50 mM Phosphatebuffer G7-Reactionbuffer. After treatment, beads were washed twice and proteins were eluted as described (Stark *et al.*, 2005; Watzl, 2006). Protein concentration was quantified using the EZQ Protein Quantitation Kit. Purity was controlled via SDS-PAGE and silverstaining and successful deglycosylation via 2D-gelelectrophoresis and Western blot, respectively. For 2D-gelelectrophoresis 100 ng 2B4-ILZ fusion proteins were supplemented with ASB-14 lysis buffer up to 20 µl and processed as described below.

3.3.6 Enzymatic deglycosylation and dephosphorylation of proteins

Immunoprecipitated proteins were enzymatically treated directly on the magnetic beads. For dephosphorylation $8x10^6$ beads were resuspended in 20 µl 1x NEB buffer 3 (New England Biolabs) and incubated 1 h at 37 °C with 2 µl Calf Intestine Phosphatase (CIP – New England Biolabs, Frankfurt). The same amount of beads were resuspended in 20 µl of 50 mM sodiumphosphate-buffer pH 7.4 with 1 µl of one of the following deglycosylation enzymes: PNGaseF for de-*N*-glycosylation (overnight 37 °C), Neuraminidase for desialylation (2 h, 37 °C) and Neuraminidase + *O*-Glycosidase for de-*O*-glycosylation (2 h, 37 °C).

3.3.7 Protein quantification

Protein concentration was determined using a customized BSA standard and the EZQ Kit according to the manufacturer's instructions. The membrane was analyzed on a FLA-2000 (Inter Departmental Equipment, Haifa, Israel) using 473 nm excitation wavelength and 580 nm emission filter.

3.3.8 SDS-polyacrylamid gel electrophoresis (SDS-PAGE)

After adding reducing sample buffer, samples were boiled for 5’ at 95 °C and centrifuged for 1’ at 20,000 x g. Samples to a maximal volume of 25 µl and 5 µl of Precision Plus Protein Standard (BioRad) were loaded on 10 % or 12 % NuPage gels (Invitrogen) and separated for 1 h 15’ at 150 V in 1 x MOPS buffer.

3.3.9 2D-gelelectrophoresis (2D-PAGE)

Bead eluates of 2B4-ILZ fusion proteins or receptors prepared by immunoisolation or immunoprecipitation were supplemented with 2xSB to a final volume of 100 µl and incubated for 20’ 18 °C and afterwards mixed with 100 µl Rehydration Solution. For isoelectric focusing (IEF) ReadyStrip IPG pH3-10 were used with the following conditions: 50 µA per gel at 20 °C for all steps, active rehydration at 50 V for 12 h, focusing: 15’ 250 V (ramp: rapid), 2 h 4000 V (ramp: linear), 5 h 4000 V (ramp: rapid). About 10 000 Vh were reached. IPG strips were equilibrated first in equilibration buffer I (containing 0.5 % (w/v) DTT), then in equilibration buffer II (with 4.5 % (w/v) iodacetamid, instead of DTT). Strips were placed on 4-12 % NuPAGE Bis-Tris ZOOM gels and overlayed carefully with melted 1 % low melting agarose prepared with 1xMOPS containing bromphenolblue. Proteins were separated for 1 h 15’ at 150 V in 1xMOPS buffer and transferred to a polyvinylidene difluoride (PVDF) membrane as described below.

3.3.10 Western blot

After SDS-PAGE proteins were transferred to a PVDF membrane for 1.5 h at 200 mA in Western blot transfer buffer. PVDF membranes were activated with methanol and washed with transfer buffer prior to use. After Western blotting, membranes were incubated for 1 h at RT in blocking buffer and washed for at least three times in PBST. Membranes were incubated with the primary antibody for 1 h at RT or overnight at 4 °C. The membrane was washed at least three times with PBST/NaCl and incubated with the appropriate horseradish-peroxidase (HRPO)-conjugated secondary antibody for 1 h at room temperature. Secondary antibodies were diluted 1:5,000 - 1:40,000 in blocking buffer. After incubation with the secondary antibody, the membrane was extensively washed with PBST and developed using either SuperSignal West Pico or Dura and X-Ray films.

3.3.11 2D-DIGE (two-dimensional difference gelelectrophoresis)

CyDye DIGE Fluor minimal dyes were prepared according to the manufacturer's instructions (Ettan DIGE System User Manual, GE Healthcare). 50 µg protein were labeled with 1 µl of Cy3 or Cy5 working dye solution (400 pmol) and incubated on ice for 30' in the dark. Sample labeling was randomized by equal distribution of Cy3 and Cy5 to the different samples. The reaction was stopped by adding 1 µl of 10 mM lysine and incubation for 10' on ice in the dark. A master mix of internal standard was prepared by mixing an appropriate volume of each sample to be sufficient for the final number of gels. Therefore, every protein from each sample is represented in the internal standard, which is present on all gels. The master mix of the internal standard was splitted into the corresponding number and stained as if they were samples, using Cy2 working dye solution. Samples were used immediately or stored up to 2 weeks at -80 °C. Cy3 and Cy5 samples and Cy2 internal standards were combined and an equal volume of rehydration solution was added and left on ice for 15'. DeStreak Rehydration Solution was added to a final volume of 450 µl and used for passive rehydration of Immobiline Dry Strips pH3-11 NL, for at least 10 h at RT in the dark. First dimension IEF was done according to the manufacturer's instruction with the following setup: 1 h 200 V (step n hold), 1 h 500 V (step n hold), 9 h 1000 V (gradient), 1 h 1000 V (step n hold), 3 h 8000 V (gradient), 3 h 8000 V (step n hold). About 45 950 Vh were reached. 12 % acrylamid gels were casted according to the manufacturer's instructions. Strips were equilibrated in 1.5 ml equilibration buffer I and II for 15' each. Strips were placed on the gels and overlaid carefully with melted 0.5 % low melting agarose prepared in SDS electrophoresis running buffer containing bromphenolblue. Gel cassettes were inserted in an Ettan DALT*twelve* electrophoresis system filled with 1xSDS electrophoresis buffer in the lower chamber and 3xSDS electrophoresis buffer in the upper chamber. Proteins were separated with 1 W per gel followed by increasing the power up to 5 W per gel until the bromphenolblue dye front reach the end of the gel. Gel cassettes were scanned immediately using a Typhoon Variable Mode Imager according to the manufacturer's instructions or stored for one day in 1xSDS electrophoresis buffer at 4 °C in the dark. Gels were fixed in fixation solution over night, stained with SYPRO Ruby over night and washed 30' in wash solution and two times for 5' in H_2O. Image analysis was performed using the DeCyder 2D software and protein spots with significant difference in abundance (see also 4.1.4) were picked of three gels and combined for mass spectrometry analysis.

4 RESULTS

4.1 Membrane microdomains surrounding NK cell receptors

4.1.1 Establishing a new system: activation by antibody coated magnetic beads and cell disruption by nitrogen cavitation bomb

4.1.1.1 2B4, NKp30 and NKG2D expression by NK cells

To get an idea of the expression level of different NK cell receptors we analyzed NKL and NK92C1 cells via flow cytometry. In Figure 8A the surface expression of the NK cell receptors 2B4, NKp30 and NKG2D is measured using directly labeled antibodies. NKL expressed a moderate amount of 2B4, almost no NKp30 and NKG2D at a high level (Figure 8A, grey line). NK92C1 expressed a slightly higher amount of 2B4 than NKL, but a significantly higher level of NKp30, whereas the surface expression of NKG2D was moderate (Figure 8A, black line). To determine the number of receptors expressed on cell surface, a FACS based assay using commercially available calibration beads (Qifikit) was used. This kit allows for quantitative evaluation of surface epitopes by comparing fluorescences to calibrated beads. Figure 8B illustrates a representative experiment. Comparable with the directly stained cells in Figure 8A, NKG2D was expressed higher by NKL cells, whereas 2B4 and NKp30 were mainly expressed by NK92C1 cells. NKG2A, as part of the CD94/NKG2A inhibitory heterodimer, showed with a value of $5x10^4$ the greatest amount of molecules per cell.

Therefore, both assays depict the same receptor expression profile of NKL and NK92C1 cells, respectively.

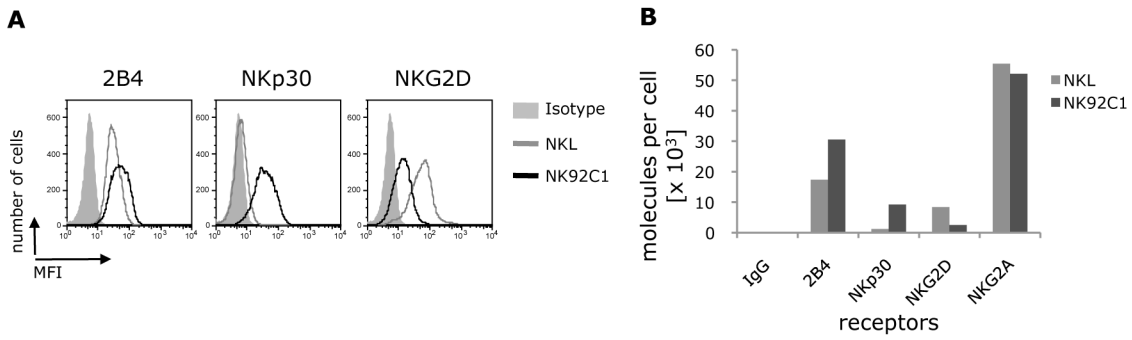

Figure 8: Receptor expression on NK cell lines. A NKL (grey line) and NK92C1 (black line) cells were stained with directly labeled antibodies against 2B4, NKp30 and NKG2D and analyzed via flow cytometry. Isotype control of stained NKL cells is shown as filled histogram. **B** Representative quantification of surface molecules on NKL (grey bars) and NK92C1 (black bars) cells. Total amounts of molecules were determined using a FACS based calibration assay (Qifikit). Calculation was done according to the manufacturer's instructions.

4.1.1.2 Binding of antibody coated magnetic beads to cells

Analyzing membrane receptors and their associated cytoplasmic regions requires the precise binding and stimulation with antibody coated magnetic beads and exclusion of unspecific cell interaction.

In our system, ongoing stimulation of cells is stopped by adding ice-cold HB buffer after a defined period of incubation at 37 °C. To obtain a "zero" value, where cell-bead contacts are made, but no receptor activation takes place, incubation was performed at 4 °C. While maximal binding with specific antibody-coated beads should be achieved, isotype loaded beads should not bind at any condition. We tested different buffers for their ability to facilitate maximal binding of anti-2B4 coated magnetic beads to NKL cells at 4 °C and analyzed cell-bead contacts as described in materials and methods (Figure 9).

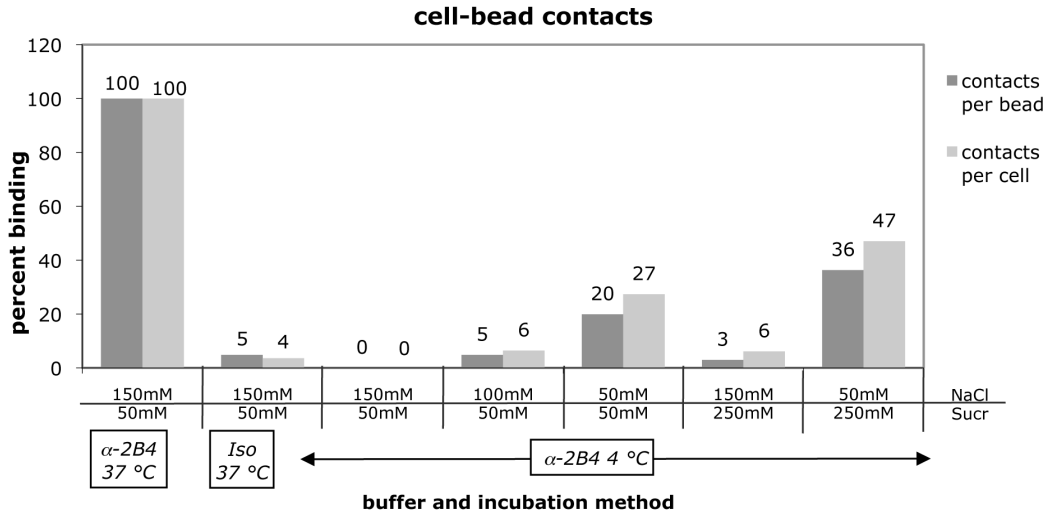

Figure 9: Cell-bead contact formation using different buffers. NKL cells were incubated with anti-2B4 (α-2B4) or isotype (Iso) coated beads for 10' at the indicated temperatures and contact formation was stopped with HB buffer containing the indicated amounts of NaCl and sucrose (Sucr). Contacts per bead (dark grey bars) and contacts per cell (light grey bars) were analyzed and calculated as described in materials and methods. Contacts after incubation of cells with anti-2B4 coated magnetic beads at 37 °C, stopped with an HB buffer containing 150 mM NaCl and 50 mM sucrose were set as 100 % and other values were calculated accordingly.

Beads always comprise half of the number of NK cells. This means that the bead to NK cell ratio was set to 1:2 in all experiments. The number of beads and cells as well as contacts between both were counted and the ratio of contacts per bead and the ratio of contacts per cell was determined. 10' of incubation at 37 °C serves as positive control. These values were set as 100 %, whereas incubation with isotype coated beads under the same conditions serves as negative control.

At 37 °C almost every bead was connected to at least one NK cell, whereas not every NK cell was able to form a contact (data not shown). This setup was chosen to reduce side

effects resulting from two or more NK cell synapses on one cell. Incubation at 4 °C diminished contact formation by NK cells.

A good binding of anti-2B4 coated magnetic beads by NKL could be observed by using HB buffer completed with 150 mM NaCl and 50 mM sucrose at 37 °C. In contrast, almost no contacts were found using isotype loaded beads (5 and 4 %) or at an incubation temperature of 4 °C for stimulating beads (0 %) (Figure 9, first three bars). Utilizing buffers with decreasing amount of NaCl from 150 mM over 100 mM to 50 mM increased the contact ratio from 0 % up to 5/6 % or 20/27 %, respectively. Increasing the sucrose content from 50 mM to 250 mM also led to an increase of contact formation at 4 °C (Figure 9).

Thus, best binding of anti-2B4 coated magnetic beads to NKL cells at 4 °C occurs by stopping the interaction with HB buffer containing 50 mM NaCl and 250 mM sucrose. This buffer did not increase isotype control binding (data not shown) and therefore used for the following stimulation and isolation methods.

Different surface expression levels as shown in Figure 8 may influence the binding capacity of NK cells to antibody coated magnetic beads. To examine, if NKL and NK92C1 discriminate between different antibody coated beads, cells were stimulated for 5’ at 37 °C and cell-bead contacts were counted. As illustrated in Figure 10A, the bead:cell ratio was adjusted to 0.5 (black bars) as described in materials and methods. NK cells constantly formed less than one contact to the magnetic beads (ratio < 1.0, light grey bars).

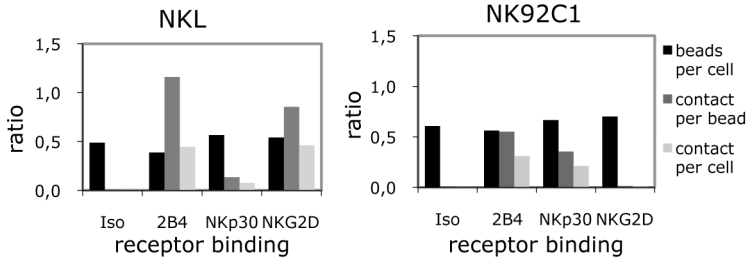

Figure 10: Binding of antibody coated magnetic beads to NK cells. Differentially antibody coated magnetic beads were incubated with NKL or NK92C1 cells for 5’ at 37 °C and contact formation was blocked with ice cold HB buffer as described in materials and methods. Black bars indicate ratio between beads and cells, dark grey bars contacts per bead and light grey bars contacts per cell.

However, the beads sometimes were attached to more than one cell, as seen by an average contact per bead ratio greater than 1.0 (dark grey bars). Isotype loaded magnetic beads did neither bind to NKL cells nor to NK92C1 cells. Despite this, a good binding could be observed using anti-2B4 and anti-NKG2D-coated beads for NKL cells, as well as anti-2B4 and anti-NKp30 beads for NK92C1 cells. When comparing the results with the FACS staining in Figure 8 this is an interesting observation due to the fact, that

2B4 was expressed in higher quantity by NK92C1 cells but anti-2B4 coated beads were better attached to NKL cells. According to the FACS data, NKL cells bound anti-NKp30 coated beads very weakly, whereas no binding of anti-NKG2D coated beads to NK92C1 cells could be observed, even if low expression of this receptor was detectable.

Hence, surface expression as detected by FACS-based assays is not necessarily in agreement with binding behavior of NK cells to antibody coated beads. We chose to carry our experiments on in NKL cells, as the 2B4/NKL pair appeared to be the optimally suited system for our study.

4.1.1.3 Bead based stimulation leads to a functional and specific outcome

To test if engaged receptors induce signaling, $2x10^6$ NKLs were stimulated with isotype or anti-2B4 coated magnetic beads for 7' at 37 °C and disrupted via nitrogen cavitation as described in materials and methods and schematically in Figure 11A. Incubation with isotype coated magnetic beads and recovering of those did not lead to any receptor isolation. However, using anti-2B4 coated magnetic beads to stimulate NKLs, the receptor could be isolated successfully (Figure 11B (1) vs. (2), middle panel). The same was true for immunoprecipitation of 2B4 from the remaining cell lysates (Figure 11B (3), (4), middle panel), which means that not all receptors were engaged by this method. In contrast to the receptors remaining unstimulated, the engaged ones exhibited phosphorylation as demonstrated by reprobing the membrane with anti-phosphotyrosine antibody (Figure 11B (1) vs. (2), top panel). Thus, only the stimulated 2B4 is phosphorylated. The remaining receptors are not affected by coincubation of cells with magnetic beads. Interestingly, 2B4-immunoprecipitations from lysates of isotype stimulated samples seem to contain more residual receptors than the receptor stimulated and immunoisolated and thereby "receptor-diminished" lysates.

In order to test for functionality of antibody coated bead stimulation, NKL cells were incubated for 16 hours with magnetic beads and supernatants were analyzed for IFN-γ. As seen in Figure 11B, only the anti-2B4 coated magnetic beads stimulated NKL cells to produce IFN-γ. Neither uncoated (Ctrl) nor isotype loaded beads were able to activate NKL cells, even after overnight incubation.

In summary binding *of* as well as stimulation *with* antibody coated magnetic beads occurs receptor specific and leads to receptor specific as well as functional NK cell stimulation.

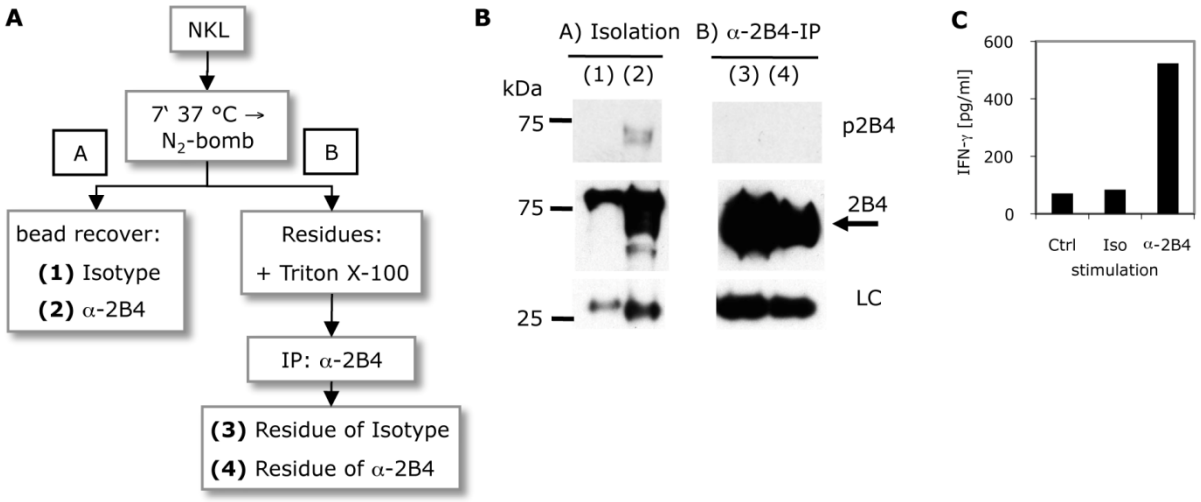

Figure 11: Bead based stimulation leads to specific and functional outcome. A Flow chart illustrating sample preparation. NKL cells were stimulated with isotype (1) or anti-2B4 (α-2B4) (2) coated magnetic beads for 7' at 37 °C and disrupted via nitrogen cavitation. Beads were recovered and washed [A]. The remaining cell residues were additionally treated with Triton X-100 for 20' at 4 °C and remaining 2B4 receptors were immunoprecipitated [B]. **B** Samples prepared as described in A were analyzed by Western blotting. Membranes were probed with anti-phosphotyrosine antibody to detect receptor phosphorylation (middle panel) and with antibodies against 2B4 (upper panels). LC determines the light chain of the anti-2B4 antibodies used for immunoisolation or immunoprecipiation (C1.7 see materials and methods) and was visualized by the anti-mouse secondary antibody. Depicted is one representative result of two experiments. **C** NKL cells were stimulated 16 hours with unloaded (Ctrl) or antibody coated (Iso=isotype, anti-2B4) magnetic beads and IFN-γ amount was measured and calculated as described in materials and methods.

4.1.1.4 2B4 stimulation by antibody coated magnetic beads leads to receptor phosphorylation and signal molecule recruitment

One of the first signaling events after 2B4 engagement is the rapid phosphorylation of the receptor by Src kinases. To test, if in our system 2B4 phosphorylation takes place in a time dependent manner, we incubated NKL and antibody coated beads for up to 10' at 37 °C and analyzed the bead-content after lysis with TX-100 buffer (Figure 12A). Phosphorylation of 2B4 occurred as soon as after 5' and increased up to 10' of stimulation. The isotype coated beads did not isolate any receptor molecules.

A further important feature of 2B4 is its function as costimulatory receptor for other activating receptors, for example NKG2D. Mostly, costimulation by 2B4 results in a synergistical enhancement, which means an amplification of the signal rather than the mere addition of both signals alone. The guanine exchange factor (GEF) molecule Vav1 acts as decision point during activation of NK cells by integrating the in-coming signals from different receptors into further downstream events. Vav1 is recruited via the adaptor molecule growth factor-bound protein (Grb)2 to the cytosolic domain of the NKG2D adaptor molecule Dap10, thereby completing the signaling complex. 2B4 is able to enhance Vav1 phosphorylation, however it transduces signals by other adaptor molecules (SAP, 3BP2) as NKG2D.

To test, if receptor engagement in our system could confirm previously reported signaling pathways we stimulated NKL cells for 5’ at 37 °C with antibody coated magnetic beads and analyzed the bead content after TX-100 lysis via SDS-PAGE and Western blotting, respectively. Stimulation of 2B4 alone led to the expected receptor phosphorylation (Figure 12B – second lane) as already seen before (Figure 12A + Figure 11). However, even if SAP association was reported to be crucial for 2B4-mediated signaling, it could not be detected in our setup (data not shown). Vav1 association was detectable, whereas its phosphorylation could not be confirmed. Furthermore, a tyrosine phosphorylated protein with molecular weight of 16 kDa appeared. In contrast to this, stimulation with anti–NKG2D coated magnetic beads led to proper receptor and Vav1 isolation as well as adequate Vav1 phosphorylation (Figure 12B – lane 3). A phosphorylated protein at 16 kDa could be detected, too, whereas an additional band appeared at 14 kDa.

So far, we analyzed the outcome of single receptor stimulation. To test, if 2B4 stimulation is able to contribute to proper Vav1 phosphorylation, we used double antibody coated beads to stimulate both receptors simultaneously. However, by using double antibody coated beads, only half of the bead surface is coated with anti-NKG2D antibodies and therefore receptor engagement is diminished per se. Using anti-NKG2D and isotype double coated beads could give an idea to which extent NKG2D engagement is able to lead to Vav1 phosphorylation. As seen in Figure 12 lane 4, Vav1 association still occured, whereas phosphorylation of the GEF was diminished. Interestingly, NKG2D isolation was not impaired even if only half of the bead surface is covered with anti-NKG2D antibody. Furthermore, the stimulation seems to be insufficient to isolate the small phosphoproteins that have been seen before. As we now have a reference with which we can compare additional 2B4 engagement, we coated beads with anti-2B4 and anti-NKG2D at once. As expected, simultaneous engagement of both receptors led to less 2B4 receptor isolation as compared to single stimulation (Figure 12 lane 2+5). The amounts of the NKG2D receptor as well as of Vav1 were comparable with the anti-NKG2D/isotype double coated beads. Interestingly, Vav1 was phosphorylated to a greater extend as when using the anti-NKG2D/isotype control and even more in comparison to single anti-NKG2D coated magnetic beads. According to single stimulation, a 16 kDa phosphoprotein could be coisolated again.

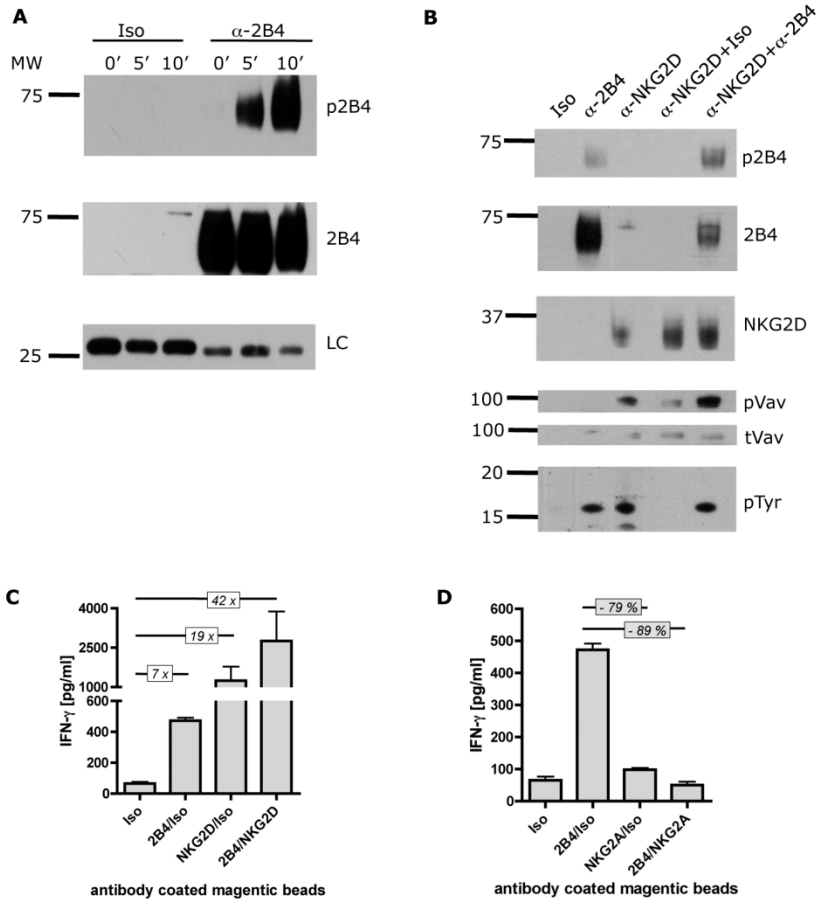

Figure 12: Outcome of 2B4 stimulation. A NKL cells were stimulated with isotype or anti-2B4 coated magnetic beads for 0', 5' or 10' at 37 °C and lysed with Triton X-100 lysis buffer. Beads were recovered and protein contents were analyzed by Western blotting. Membranes were probed with anti-phosphotyrosine antibody to detect 2B4 phosphorylation (p2B4), anti-2B4 (α-2B4) to visualize receptor amount, as well as anti-mouse secondary antibodies to detect the light chain (LC) of the anti-2B4 coated magnetic beads, respectively. **B** NKL cells were stimulated with antibody coated beads (indicated on top) for 5' at 37 °C and lysed with Triton X-100 lysis buffer. Contents of the recovered beads were analyzed by Western blotting. 2B4 phosphorylation (p2B4) as well as the tyrosine phosphorylation (pTyr) were detected after reprobing the membrane with the 4G10 antibody. **C+D** IFN-γ amount after overnight stimulation. NKL cells were stimulated for 12 h with the indicated antibody coated beads and supernatants were tested for IFN-γ production using the BMS ELISA as described in materials and methods. In **C** the outcome of costimulation and in **D** the outcome of inhibition are shown. Results are representative for at least three experiments.

In summary, the outcome of costimulation by double antibody coated magnetic beads could be verified already on the level of enhanced Vav1 phosphorylation. But does this synergy among 2B4 and NKG2D also lead to enhanced NK cell stimulation?

To answer this question, the same setup was used to stimulate NKL cells over night and to analyze the released IFN-γ amount. Incubation of cells with anti-2B4/isotype loaded beads resulted in a 7-fold and use of anti-NKG2D/isotype loaded beads in an even 19-fold cytokine secretion compared to the isotype control (Figure 12C). Synergistic stimulation of 2B4 and NKG2D together resulted in a 42-fold induction of IFN-γ secretion, which cannot be the result of a merely additive effect of each receptor itself.

Important for the regulation of NK cells is an efficient inhibition to suppress activation and thereby prevent uncontrolled cytotoxicity. As depicted in Figure 12D, engagement of the inhibitory receptor NKG2A did not induce the secretion of IFN-γ, in contrast to 2B4 engagement. More importantly, by triggering the inhibitory NKG2A receptor in concert with 2B4 via double coated beads, we could further decrease the released IFN-γ up to -89 %. Consequently, in addition to the synergy among the activating receptors 2B4 and NKG2D, the inhibition of NK cells via engagement of the inhibitory receptor NKG2A could be confirmed.

4.1.1.5 Size reduction of membrane microdomains

One critical point for the identification of downstream signaling events occurring after receptor engagement, is the size and thereby the definition of membrane microdomains. The method of immunoisolation used here is a less invasive technique concerning the "natural" composition of membrane microdomains. However, a critical point is the inhomogeneity and the unknown size of the isolated membrane fragments after nitrogen cavitation. To investigate, if we could reduce the amount of contaminating membrane proteins, we chose to focus on the association of CD45, a critical non-lipid raft marker, and varied the pressure onto the cells in the nitrogen cavitation bomb to reduce the size of extracted fragments. As seen in Figure 13, increasing the pressure from 500 up to 1200 psi did not lead to a complete ablation of CD45 from the anti-2B4 isolated lipid isles. Nevertheless, at 1000 psi the amount of CD45 was reduced sufficiently without any reduction in 2B4 amount. Therefore we decided to continue the experiments with a pressure size of 1000 psi.

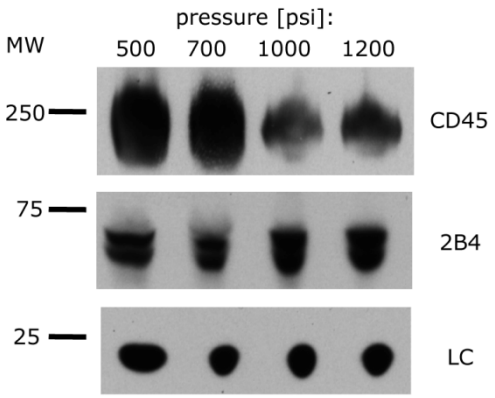

Figure 13: Size reduction of membrane microdomains. NKL cells were stimulated with anti-2B4 coated magnetic beads for 5' at 37 °C and subsequently disrupted via nitrogen cavitation with varied pressure (500 – 1200 psi) to minimize size of membrane fragments. Beads were recovered and protein contents were analyzed by Western blotting. Membranes were probed with anti-CD45 and anti-2B4 and appropriate secondary antibodies to detect the characteristic non-raft marker CD45, the engaged 2B4 receptor and light chain (LC) of the anti-2B4 coated magnetic beads, respectively.

4.1.2 Phosphoproteomics: A multiplicity of different phosphorylated proteins

Protein phosphorylation is an important post-translational modification, which is essential for many cellular functions (Gnad *et al.*, 2007). Analysis of this key mechanism can be performed by separating proteins with 2D-gelelectrophoresis and subsequently detection of phosphotyrosines via immunoblotting. Stimulation of 2B4 triggers many signaling molecules in order to achieve NK cell activation. Neither the mechanism, nor the chronology of these processes are completely understood. The method of immunoisolation using the nitrogen cavitation bomb enables us to analyze spatially restricted events directly after receptor triggering.

NKL cells were stimulated with anti-2B4 coated magnetic beads at 37 °C for 2’ or 10’ and subsequently disrupted via nitrogen cavitation. Samples were divided into two parts and proteins were separated by 2D-gelelectrophoresis to check each sample separately for protein amount and phosphorylation status using silver staining and anti-phosphotyrosine Western blotting, respectively.

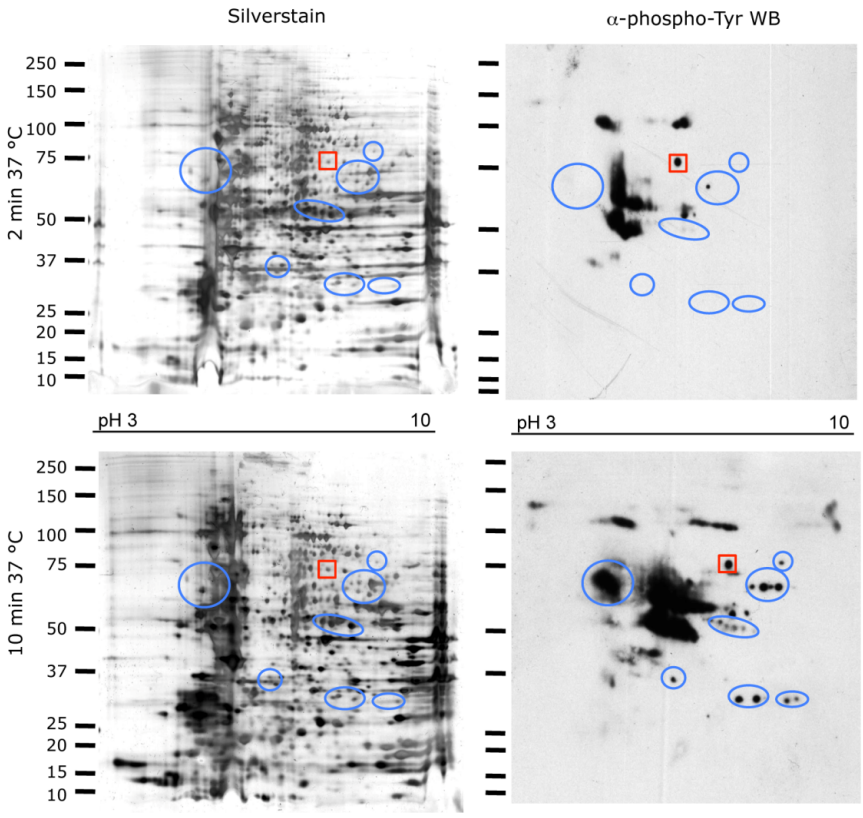

Figure 14: Phosphoproteomics. NKL cells were stimulated with anti-2B4 coated magnetic beads for 2’ (top) or 10’ (bottom) at 37 °C and disrupted via nitrogen cavitation. Beads were recovered as described in materials and methods. Samples were divided into two parts and bead contents were separated using 2D-gelelectrophoresis. One gel of each sample was silver stained (left panel), the other one analyzed via Western blotting using the 4G10 antibody to detect phosphotyrosine (right panel). Red squares indicate spots appearing in both samples (2’ and 10’) with both silver staining and Western blot. Blue circles mark distinct outcomes of stimulation, mainly detectable in the anti-phosphotyrosine Western blot.

As illustrated in Figure 14, left panel, the protein content after 2' of stimulation does not or only marginally differ from the composition of longer stimulated cells. However, protein phosphorylation increased and also shifted to more low-molecular mass proteins as shown in Figure 14, right panel. Some spots appeared in the silver staining as well as in the anti-phosphotyrosine Western blot of both differentially stimulated samples (red square) whereby other spots could be detected with silver staining although the phosphorylation occured only after a longer time of stimulation (blue circles). Therefore, time dependent stimulation with antibody coated magnetic beads and subsequent disruption of cells by nitrogen cavitation results in the immunoisolation of the same amount of membrane microdomain adjacent proteins. In contrast, phosphorylation as indicator of proceeding signaling cascade increases as expected.

4.1.3 Effect of inhibition and activation - 2D-PAGE

The activating NK cell receptor 2B4 is recruited into DRMs after receptor engagement (Watzl *et al.*, 2003; Watzl *et al.*, 2000). To identify proteins involved in raft recruitment, immunoisolation using the nitrogen cavitation bomb should help to gain further insights into the natural composition of 2B4 containing membrane microdomains as well as adjacent signaling molecules. As not only raft associated proteins are isolated with this method, we need a receptor which is not recruited into lipid rafts. It has been shown, that the inhibitory receptor CD94/NKG2A is excluded from lipid rafts, even after receptor ligation (Sanni *et al.*, 2004). Therefore we decided to compare immunoisolated samples of the activating receptor 2B4 with those of the inhibitory NK cell receptor CD94/NKG2A. To get an idea, which proteins are uniquely involved in 2B4 mediated signaling we separated immunoisolated proteins with 2D-gelelectrophoresis. Additionally we also could get information about signaling pathways after engagement of inhibitory NK cell receptors.

NKL cells were stimulated with anti-2B4 or anti-NKG2A coated magnetic beads and immunoisolated proteins were separated via 2D-PAGE followed by silver staining. As shown in Figure 15, many proteins could be isolated by this mechanical cell disruption method.

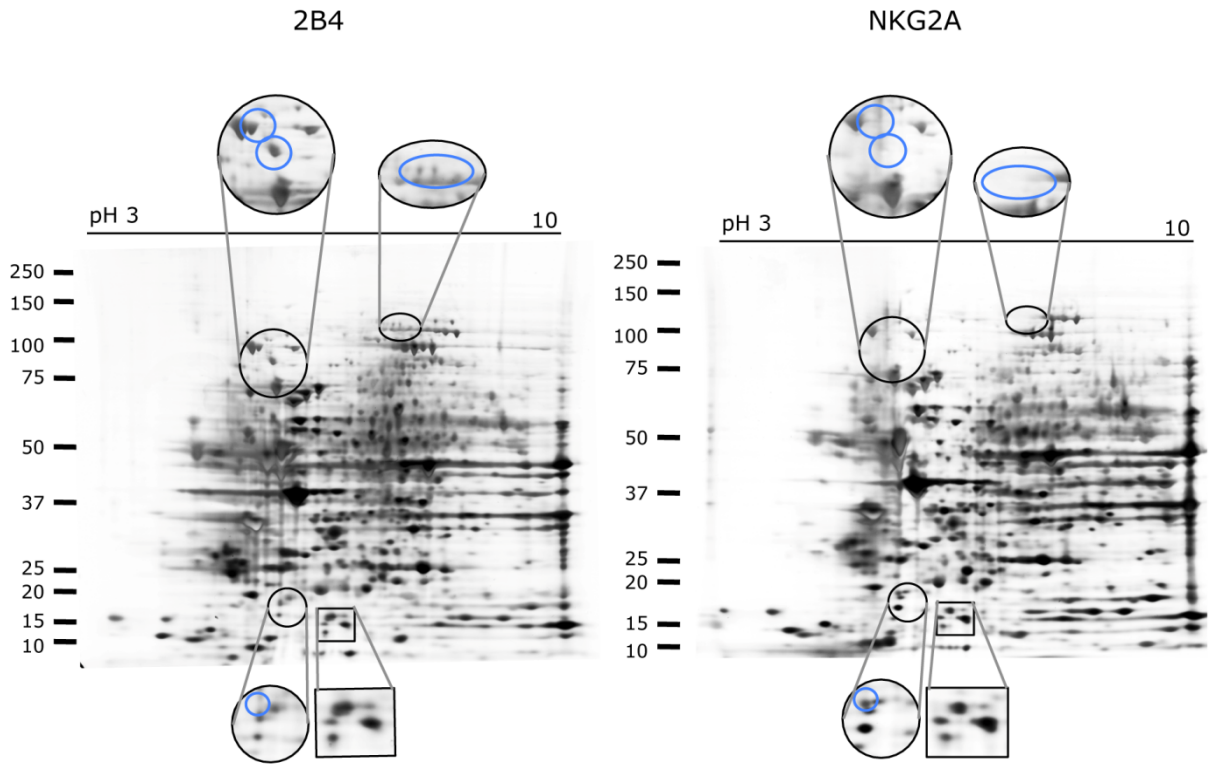

Figure 15: Inhibition versus activation. NKL cells were stimulated 5' at 37 °C with antibody coated magnetic beads to engage 2B4 or NKG2A (as part of the inhibitory receptor CD94/NKG2A) and disrupted via nitrogen cavitation. Beads were eluted in CHAPS-containing lysis buffer and samples were separated using 2D-gelelectrophoresis. Gels were silver stained. Differences are indicated and shown in higher magnification with blue circles whereas one example for spot similarity is given by an enlarged square.

Although most spots were comparable between both samples (marked by a square) significant differences were visible (marked by a circle). In evidence, spots completely disappeared or seemed to be isolated in a greater amount when comparing both gels. To improve sensitivity and accuracy and thereby getting more precise and "true" information about the differences between activating and inhibitory signals, we switched to two-dimensional difference gelelectrophoresis (2D-DIGE).

4.1.4 Effect of inhibition and activation - 2D-DIGE

An advantage of 2D-DIGE is the comparison of two samples in one gel by utilizing an internal standard. This also allows for the comparison between gels with only minor gel-to-gel variation. We optimized our system for ideal means of protein concentration and solubilization and performed 2D-DIGE experiments with the settings obtained. We chose to compare five samples in parallel after stimulation via anti-NKG2A or anti-2B4 coated magnetic beads.

Figure 16 shows an example for one protein of interest (POI), whereas the colors blue and green mark the NKG2A and 2B4 sample, respectively.

Figure 11

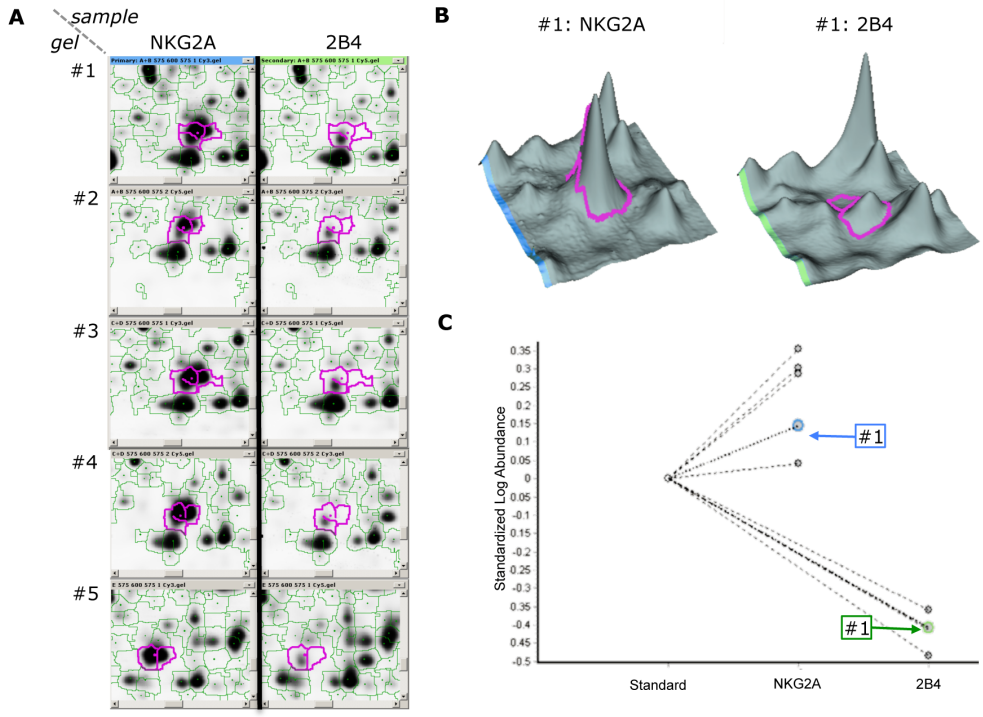

Figure 16: Inhibition versus activation: Analysis of one protein of interest (POI) using the DeCyder software. NKG2A (representing NK cell inhibition) and 2B4 (representing NK cell activation) samples were prepared as described in materials and methods. Spots were detected and quantified using the DeCyder software. Shown is one representative POI analyzed in the Biological Variation Analysis (BVA) module to perform statistical analysis to assess treatment difference. The NKG2A sample of gel#1 is marked blue and the 2B4 sample of gel#1 is marked green. **A** demonstrates the purple marked POI in the image view. Samples of NKG2A stimulated cells are shown on the left side, whereby the right panel represents samples of 2B4 stimulated cells. Each pair, read from top to bottom, represent one gel, indicated by numbers. **B** shows the same POI of gel#1 as in A in three-dimensional view. **C** compares the depicted POIs shown in A with the internal standard of every gel, set zero. Each circle represents a different sample of a different gel, whereas the NKG2A and 2B4 sample of gel#1 are colored as before.

In Figure 16A the image view illustrates a magnification with a purple marked POI. Even though most protein spots do not differ, differences in spot intensities between the NKG2A and 2B4 samples are obvious. Figure 16B demonstrates the same POI of gel#1 as three-dimensional view. By using an internal standard on each gel, the samples are quantitatively comparable. This is shown with a graphical view in Figure 16C, where the standards of every gel were set to zero and the POI intensities were calculated accordingly. The POI shown already in Figure 16A+B is marked again blue for NKG2D and green for 2B4.

A total of 23 spots were statistically relevant. To define a protein of interest, t-test values smaller than 0.05 were chosen. The resulting list was sorted by average ratio and spots were confirmed when it was greater than 1.2. Some spots were added manually, even if

the average ratio was not greater than ±1.1, when they seemed relevant in graphical view. Because the sample material was limited and no preparative gel was prepared, proteins were picked out of three analytical gels and pooled to get the required amount of protein for MALDI or ESI analysis.

4.1.5 Inhibition and stimulation: proteins involved in signaling processes

Table 1 summarizes the identified proteins, which may be relevant for the analyzed processes. The complete list of identified proteins is attached at the end of this thesis. Most proteins were identified by ESI spectrometry due to limited protein amount and overlapping spectra of several proteins as a result of the picking strategy.

Sample ID[a]	Protein Name[b]	T-test[c]	Av. Ratio[d]	Prot. score[e]	Prot. Mass [Da][f]	pI[f]	No. of hits[g]		Prot. Nr.
2**	ezrin [Hs]	0.021	1.38	236	74118	6.46	5		1
3	protein phosphatase 3, catalytic subunit, alpha isoform isoform 1 [Hs]	$7.1x10^{-4}$	2.44	39	58262	5.90	1	k	7
3	phospholipase C-alpha (protein disulfide-isomerase A3) [Hs]	$7.1x10^{-4}$	2.44	34	57044	6.38	2	m	8
4*	chaperonin containing TCP1, subunit 2 [Hs]	$1.8x10^{-3}$	1.54	460	57794	6.01	14		1
7**	FK506 binding protein 5 [Hs]	0.035	1.50	514	51693	5.70	14		1
7**	chaperonin containing TCP1, subunit 2 [Hs]			108	57753	5.97	3		4
11	Rho GDP dissociation inhibitor (GDI) beta [Hs]	0.045	1.16		23031	4.9	52%		
12	calpain, small subunit 1 [Hs]	$7.9x10^{-3}$	1.27		28469	4.9	25%		
17**	chaperonin containing TCP1, subunit 2 [Hs]	$6.6x10^{-5}$	4.77	94	57753	5.97	1	k	6
17**	chaperonin [Hs]			40	59004	5.48	1	k	11
18	chaperonin [Hs]	0.019	1.16	42	59004	5.48	1	k	8
18	chaperonin containing TCP1, subunit 2 [Hs]			34	57753	5.97	1	k	9
21*	growth factor receptor-bound protein 2 isoform 1 [Hs]	$6.2x10^{-6}$	-4.51	175	23655	6.31	9		3
32	FK506 binding protein 5 [Hs]	$1.8x10^{-3}$	2.72	109	51693	5.70	4		6

Table 1: Identified proteins chosen by their relevance.
[a]Due to picking strategy (see text) and ESI analysis, some protein spots exhibit more than one protein, whereas the table depicts only the cytoplasmic and possible relevant proteins. The complete list is attached at the end of this thesis. *marks the identification of Ig [*mus musculus*] identifications, which were of low significance but with always lower number of hits than the depicted protein. **markes the identification of Ig [*mus musculus*] peptides, however being non-significant due to less number of hits.
[b]Protein name derived from PubMed. [HS] means *homo sapiens*.
[c]*p* value calculated using the Student's T-test.
[d]Average ratio between 2B4 and NKG2A (>1 greater extend in the 2B4 samples; <-1 greater extend in the NKG2A samples.
[e]Probability-based Mascot scores
[f]Theoretical molecular mass (Da) and pI from the ExPASy database.
[g]Number of hits resulting from ESI analysis. Percent values indicates sequence coverage of MALDI analysis.
[k] illustrates that only one peptide was identified which might not be significant
[m] single peptide score non-significant, sum of single peptide scores significant

In Table 2 the identified proteins are grouped according to their relevance for localization or function.

Sample ID[a]	Protein Name[b]	T-test[c]	Av. Ratio[d]	Subcellular location[e]	Function[e]
2**	ezrin [Hs]	0.021	1.38	cytoplasm / peripheral membrane	cytoskeleton remodeling
11	Rho GDP dissociation inhibitor (GDI) beta [Hs]	0.045	1.16	cytoplasm	GTPase activation
12	calpain, small subunit 1 [Hs]	$7.9x10^{-3}$	1.27	cytoplasm / peripheral membrane	cytoskeleton remodeling
21*	growth factor receptor-bound protein 2 isoform 1 [Hs]	$6.2x10^{-6}$	-4.51	cytoplasm	signal transduction
3	protein phosphatase 3, catalytic subunit, alpha isoform isoform 1 [Hs]	$7.1x10^{-4}$	2.44	cytoplasm, nucleus	cell cycle, cell devision
3	phospholipase C-alpha (protein disulfide-isomerase A3) [Hs]	$7.1x10^{-4}$	2.44	cytoplasm, ER, golgi	isomerase, protein transport
4*	chaperonin containing TCP1, subunit 2 [Hs]	$1.8x10^{-3}$	1.54	cytoplasm	protein folding
7**	FK506 binding protein 5 [Hs]	0.035	1.50	cytoplasm, nucleus	protein folding
7**	chaperonin containing TCP1, subunit 2 [Hs]	0.035	1.50	see above	see above
32	FK506 binding protein 5 [Hs]	$1.8x10^{-3}$	2.72	see above	see above
17**	chaperonin containing TCP1, subunit 2 [Hs]	$6.6x10^{-5}$	4.77	see above	see above
17**	chaperonin [Hs]			see above	see above
18	chaperonin [Hs]	0.019	1.16	see above	see above
18	chaperonin containing TCP1, subunit 2 [Hs]			see above	see above

Table 2: Identified proteins sorted by localization and function
[a]Due to picking strategy (see text) and ESI analysis, some protein spots exhibit more than one protein, whereas the table depicts only the cytoplasmic and possible relevant proteins. The complete list is attached at the end of this thesis. *marks the identification of Ig [*mus musculus*] identifications, which were of low significance but with always lower number of hits than the depicted protein. **markes the identification of Ig [*mus musculus*] peptides, however being non-significant due to less number of hits.
[b]Protein name derived from PubMed. [HS] means *homo sapiens*.
[c]*p* value calculated using the Student's T-test.
[d]Average ratio between 2B4 and NKG2A (>1 greater extend in the 2B4 samples; <-1 greater extend in the NKG2A samples.
[e]Informations about subcellular location and function from UniProtKB and NCBI databases

The relevant proteins ezrin, Rho GDP dissociation inhibitor (Rho GDI) beta, calpain, small subunit 1 as well as growth factor receptor-bound protein2 isoform 1 (Grb2) will be further debated in the discussion part.

4.2 Glycosylation of 2B4 and its effect in ligand binding and function

Glycosylation is an important posttranslational modification of lipids and proteins. Their diversity reflects their multiple biological functions beginning with the recognition of pathogens, cell differentiation, development, trafficking, cell-cell communication and also intracellular processes. 2B4 is an important activating receptor for the regulation of NK cell response. 2B4 contains several *N*-glycosylation sites (Tangye *et al.*, 1999) which may impair or influence positively the interaction with its ligand CD48. The second part of this thesis aims for the characterization of posttranslational modifications especially glycosylation of the activating NK cell receptor 2B4 and its influence in functionality.

4.2.1 2B4 is a highly glycosylated receptor

To study, if different NK cells exhibit different posttranslationally modified 2B4 receptors we immunoprecipitated the protein from different NK cells and stably 2B4 transfected HEK-293T (HEK-2B4) cells and analyzed it via 2D-gelelectrophoresis and Western blotting. The 2B4 receptor migrated at an apparent molecular weight of about 70 kDa in all cells analyzed and showed distinct spots over a broad pH range (Figure 17A). The spot pattern between 2B4 molecules from primary NK cells, the NK cell line NKL and HEK-2B4 cells were comparable whereas the NK cell line NK92C1 expressed a more alkaline receptor.

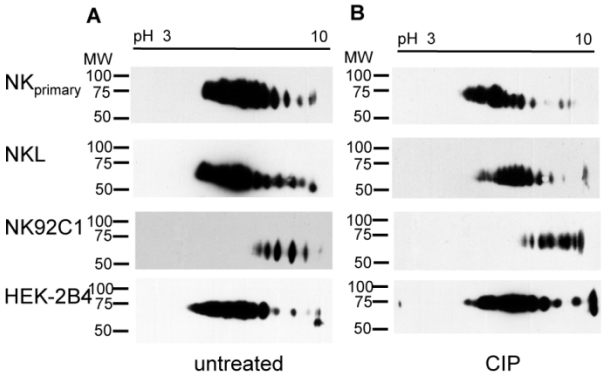

Figure 17: 2B4 is highly glycosylated. 2B4 was immunoprecipitated from primary NK, NKL, NK92C1, HEK-2B4 cells and analyzed using 2D-gelelectrophoresis and anti-2B4 Western blotting. Samples were left untreated (**A**) or dephosphorylated using Calf Intestinal Phosphatase (CIP) (**B**). Representative results of four experiments are shown.

2B4 contains four ITSM domains important to fulfill its function. Phosphorylation replaces neutral hydroxyl groups with negatively charged phosphates. This results in a shift towards acidic pH. To test whether the differences in pH could be due to background phosphorylation of the four cytoplasmic ITSM domains, immunoprecipitated 2B4 proteins were dephosphorylated using Calf Intestinal Phosphatase (CIP). While this treatment led to a complete dephosphorylation of 2B4 as evident by anti-phosphotyrosine blotting (data not shown), it only resulted in a marginal shift of the whole spot pattern towards a

more basic pH (Figure 17B). This indicates that phosphorylation has only minor influence in the diversity of 2B4 receptor spot pattern.

To further confirm that phosphorylation is only partially responsible for the diverse spot pattern of 2B4, we expressed wildtype 2B4 (wt) as well as a construct with tyrosine to phenylalanine mutations in all ITSM (Y1,2,3,4F) in HEK-293T cells. As illustrated in Figure 18A the mutation of all ITSM tyrosines led only to minor reduction in spot diversity compared to the 2B4 wildtype construct. Pervanadate treatment of HEK-293T cells again resulted in a shift towards acidic pH for the wildtype construct, whereas the mutant form did not change its spot distribution (Figure 18B). Furthermore, the absence of all four ITSM tyrosines in the mutant form did not lead to phosphorylated 2B4 as depicted by the anti-phosphotyrosine Western blot (Figure 18C).

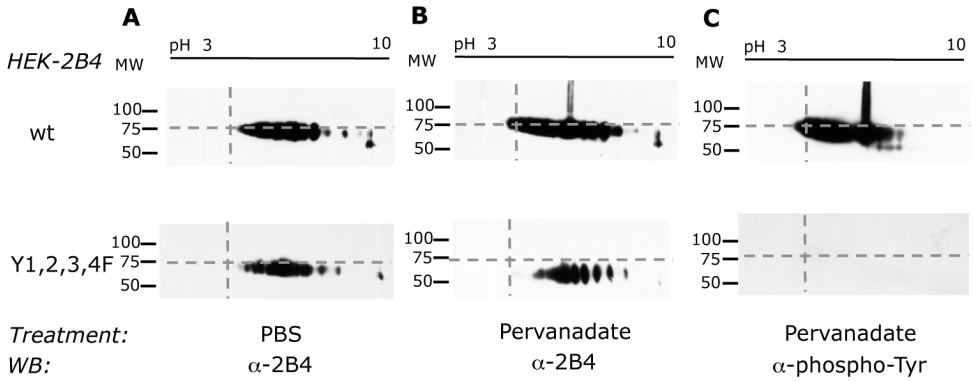

Figure 18: Spot pattern of 2B4 is not due to phosphorylation. HEK-2B4 cells or HEK cells transfected with 2B4-ITSM mutant (Y1,2,3,4F) were incubated 10' at 37 °C in PBS (PBS (**A**)) or in PBS containing Pervanadate (Pervanadate (**B**+**C**)) to block phosphatase activity. Cells were lysed and 2B4 was immunoprecipitated. Samples were separated using 2D-gelelectrophoresis and analyzed via Western blotting. Blottet membranes were probed with anti-2B4 antibody (α-2B4 (**A**+**B**)) and reprobed with 4G10 antibody to detect phosphotyrosines (α-phospho-Tyr (**C**)).

Hence, phosphorylation of the ITSM domains of 2B4 leads to a further shift of the spot pattern towards acidic pH, whereas complete dephosphorylation does not lead to an abolishment of spot diversity. These results allow for the assumption, that 2B4 is a highly glycosylated receptor.

4.2.2 2B4 is highly **N-*glycosylated***

Human 2B4 contains eight possible *N*-glycosylation sites. To test whether 2B4 is *N*-glycosylated and if *N*-glycosylation differs between the examined cell populations, the immunoprecipitated receptor was dephosphorylated using CIP or additionally de-*N*-glycosylated using PNGaseF. Removal of *N*-glycans reduced the mass of 2B4 to the predicted molecular weight of 39 kDa (Figure 19A, B). Interestingly, the spot patterns between the different cell lines were comparable after PNGaseF treatment (Figure 19B).

This suggests that *N*-linked carbohydrates on 2B4 differ between NK92C1 and the other NK cells analyzed. It further shows that *N*-linked sugars account for the 30 kDa difference between calculated and apparent molecular weight of the 2B4 receptor. However, the 2B4 receptor still migrated as distinct spots covering a broad pH range after the removal of *N*-glycans. This suggested the presence of additional sugar moieties that are highly charged and of small size.

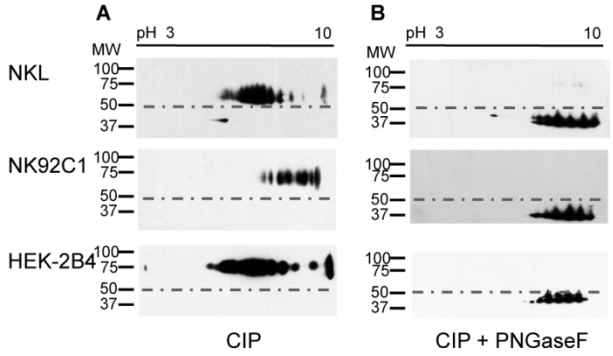

Figure 19: 2B4 is highly *N*-glycosylated. Immunoprecipitated 2B4 from NKL, NK92C1 or HEK-2B4 cells was either dephosphorylated using CIP (**A**) or additionally de-*N*-glycosylated using PNGaseF (**B**) and further analyzed using 2D-gelelectrophoresis and anti-2B4 Western blotting. Representative results of at least three experiments are shown.

4.2.3 2B4 contains sialic acids and O*-linked carbohydrates*

Sialic acids are highly negatively charged and therefore shift the pH of proteins towards acidic pI with only minor change in molecular mass. To test for the presence of sialic acids on 2B4, we desialylated immunoprecipitated 2B4 using Neuraminidase. Desialylation shifted the pH of immunoprecipitated 2B4 to its calculated pI of 9.61 (Figure 20A, B). Additional removal of *O*-linked glycans did not change the pI further (Figure 20C). Instead, we sometimes observed a slight increase in molecular weight of the 2B4 receptor. These data show that the distinct spot pattern of 2B4 is caused by sialic acid residues on *N*- and *O*-linked sugars.

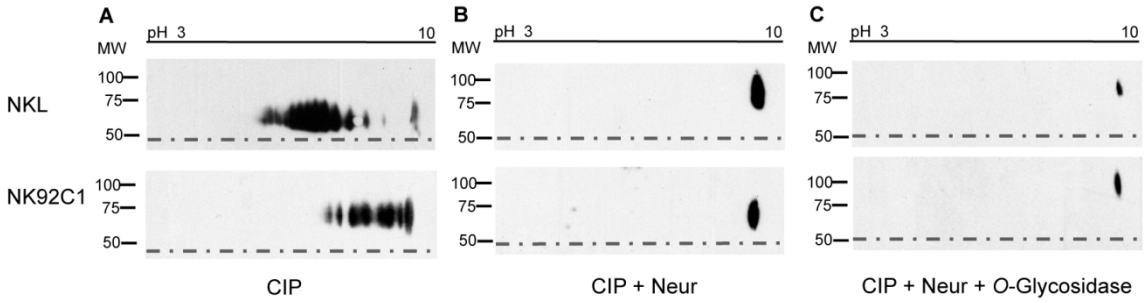

Figure 20: 2B4 contains sialic acids and *O*-linked carbohydrates. Immunoprecipitated 2B4 from NKL or NK92C1 cells was either dephosphorylated using CIP (**A**) or additionally desialylated using Neuraminidase (Neur) (**B**) or further de-*O*-glycosylated using *O*-Glycosidase (**C**). Treated proteins were separated using 2D-gelelectrophoresis and analyzed via anti-2B4 Western blotting. Representative results of at least two experiments are shown.

4.2.4 The IgC2 domain has minor influence on glycosylation

Human 2B4 consists of two Ig domains: the membrane distal V-type (IgV) and the proximal C2-type (IgC2) domain. Deletion of the C2-type domain could give information, how either of the domains contribute to the molecular weight of 2B4 by different amounts of glycosylation. 2B4 has an experimentally observed molecular weight of 70 kDa and a calculated weight of 39 kDa. Experimental data illustrate, that deletion of the proximal domain led to a decrease of molecular weight from 70 kDa to 50 kDa and a significant shift of the pH values to a more basic range (Figure 21). Furthermore, a smear at 40 kDa as well as a vertical band on the cathode emerged.

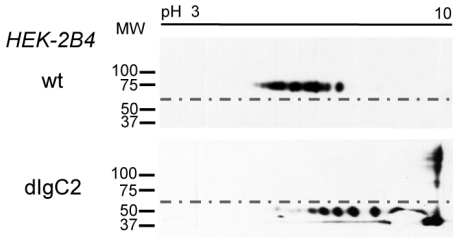

Figure 21: The IgC2 domain has minor influence in glycosylation. Immunoprecipitated 2B4 from HEK-2B4 cells or HEK cells transfected with an IgC2 deletion mutant of 2B4 (dIgC2) were analyzed using 2D-gelelectrophoresis and anti-2B4 Western blotting. Representative results of at least two experiments are shown.

Ablation of the membrane proximal IgC2 domain resulted in a decrease of *calculated* molecular weight from 39 kDa to 32 kDa. Therefore, amino acids of the C2-type domain contribute to 7 kDa. The *examined* molecular weight of wildtype 2B4 is 70 kDa. Deletion of the IgC2 domain resulted in a remaining molecular weight of 50 kDa; a difference of 20 kDa composed of 7 kDa protein and 13 kDa glycosylation. Glycosylation of wildtype 2B4 leads to a mass addition of 31 kDa. As calculated yet, the glycosylation of the membrane proximal C2-type domain contributes to only 13 kDa mass addition. Hence, the glycosylation of the distal IgV domain constitutes the remaining 18 kDa and is therefore mainly responsible for the observed molecular weight of 2B4.

Human 2B4 contains eight possible *N*-glycosylation sites. Three of them are found in the distal V-type Ig domain, four of them in the membrane proximal C2-type Ig domain and one near the transmembrane region. This is interesting, as the distal IgV domain seems to be mainly responsible for the alterations in molecular weight of 2B4, even if it contains less *N*-glycosylation sites than the membrane proximal IgC2 domain.

4.2.5 The binding affinity of 2B4 to its ligand CD48 is affected by glycosylation

The *N*-glycosylation sites within 2B4 are in close proximity to the binding site of its ligand CD48. According to the structure of murine 2B4 (Velikovsky *et al.*, 2007) the *N*-linked carbohydrates may lie outside of the binding interface. However, they could still be involved in ligand binding due to their large size and highly negative charge. Additionally, also *O*-linked carbohydrates, for which no consensus motives are known, could have an impact on the function of the 2B4 receptor. To test how these carbohydrates could

influence the binding affinity of 2B4 to its ligand CD48 we expressed the extracellular Ig-like domains of 2B4 linked to an isoleucine zipper (ILZ) motif as a recombinant soluble fusion protein in HEK cells. These 2B4-ILZ fusion proteins showed a glycosylation pattern similar to the 2B4 receptor found in stably transfected HEK cells and primary human NK cells (Figure 22A top). Also the difference between the apparent molecular weight of 2B4-ILZ of about 55 kDa and the calculated molecular weight of 27 kDa can be explained by the addition of about 30 kDa due to glycosylation of the 2B4 fusion protein. Desialylation as well as de-*O*-glycosylation of the fusion protein shifted the pI to more alkaline pH and removal of *N*-linked carbohydrates resulted in a mass shift towards the calculated molecular weight (Figure 22A). This demonstrates that the glycosylation of the 2B4-ILZ fusion protein is comparable to the 2B4 receptor expressed on NK cells.

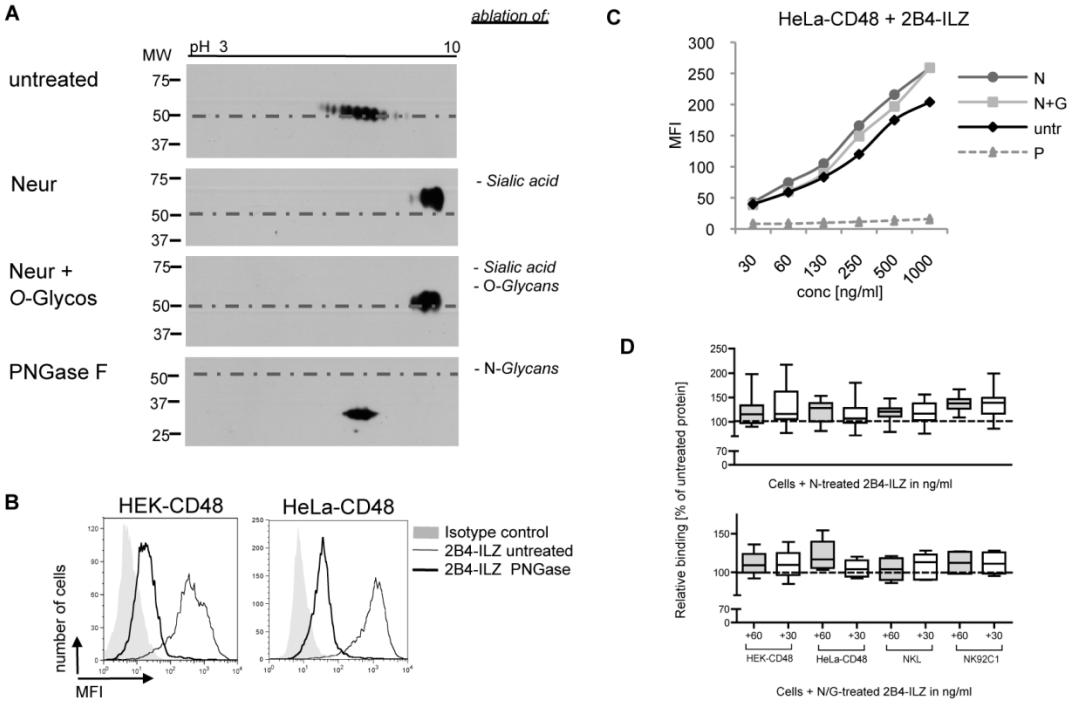

Figure 22: Binding of 2B4 to CD48 is affected by glycosylation. (**A**) 2B4-ILZ fusion proteins were left untreated or treated with Neuraminidase (Neur) and/or *O*-Glycosidase (*O*-Glycos) or PNGaseF as described in materials and methods. Successful deglycosylation was controlled by 2D-gelelectrophoresis and anti-2B4 Western blotting. (**B**) Binding of PNGaseF treated 2B4-ILZ fusion protein to CD48 expressing HEK and HeLa cells (thick line) in comparison with untreated protein (thin line) and isotype control (grey area). (**C**) Concentration dependent binding of differentially treated fusion proteins to HeLa-CD48 cells. Neuraminidase (N, circles), Neuraminidase and *O*-Glycosidase (N+G, square), untreated (untr, diamonds), and PNGaseF (P, triangles) treated 2B4-ILZ fusion proteins were used at the indicated concentration in a FACS-based binding assay to HeLa-CD48 cells. (**D**) Binding of 60 ng/ml (grey bars) or 30 ng/ml (white bars) of Neuraminidase- (top) or Neuraminidase and *O*-Glycosidase- (bottom) treated 2B4-ILZ fusion proteins to HEK-CD48, HeLa–CD48, NKL or NK92C1 cells. Data are presented in percent binding of treated versus untreated protein for at least four independent experiments.

We next asked the question how the removal of the different sugars from the 2B4-ILZ fusion protein would affect its binding to its ligand CD48. For this we used the fusion protein to stain HEK and HeLa cells stably transfected with CD48. Removal of *N*-linked carbohydrates by PNGase treatment almost abolished the specific binding of 2B4-ILZ to HEK-CD48 and HeLa-CD48 cells (Figure 22B,C). This demonstrates that *N*-linked sugars on 2B4 are essential for its binding to CD48. Interestingly, we observed a somewhat increased binding of 2B4-ILZ to HeLa-CD48 cells after removing sialic acid residues or additionally *O*-linked sugars (Figure 22C,D). This increase was consistently seen for many different CD48 expressing cells and suggests that sialic acid residues on 2B4 may have a negative impact for its binding to CD48.

4.2.6 Inhibition of N*-glycosylation with tunicamycin impairs cytotoxicity of NK cells*

To test if 2B4 glycosylation also has an impact on 2B4-mediated NK cell activation, we deglycosylated NK cells differentially to alter 2B4 bound carbohydrates. As PNGaseF failed to deglycosylate whole NK cells, we chose inhibitors to interfere with glycosyltransferases and thereby impair the posttranslational modification.

It would be interesting, if the decreased binding of de-*N*-glycosylated 2B4-ILZ fusion proteins to CD48 expressing cells (Figure 23) could be repeated with NK cells, impaired in *N*-glycosylation. To interfere with *N*-glycosylation on NK cells, we chose tunicamycin which abrogates the transfer of *N*-acetylglucosamine-1-phosphate (GlcNAc-1-P) from UDP-GlcNAc to dolichol-P by blocking the GlcNAc phosphotransferase. Tunicamycin treatment of NK cells for 24 h led to a reduction of viability of both NK cell lines tested when compared to control treated cells, as seen by a shift in the forward and side scatter (FSC and SSC) population (Figure 23A, left panel). To test if tunicamycin impairs protein expression itself, we controlled the surface expression of the receptors 2B4 and CD48 via flow cytometry. As depicted in Figure 23A, right panel, 2B4 as well as CD48 expression were slightly diminished. Nevertheless, the ablation of sialic acids as result of de-*N*-glycosylation decreased even more, indicating a greater reduction of surface glycosylation than receptor downmodulation. Hence, as receptor expression and viability seemed to be only slightly impaired by tunicamycin, we tested their ability to lyse Mock- or CD48- transfected HeLa cells as targets for different NK cells. The presence of CD48 clearly enhanced the lysis of HeLa cells by the NK cell lines NKL and NK92C1, demonstrating the specific NK cell activation through 2B4 (Figure 23B). In contrast, the killing activity of tunicamycin treated NKL as well as NK92C1 cells against CD48 expressing target cells was significantly reduced back to the level of control target cells. To analyze, if the observed effects could be traced back to de-*N*-glycosylation, 2B4 immunoprecipitates of NKL and NK92C1 cells were examined via Western blotting (Figure

23C). Interestingly, only NK92C1 cells revealed a reduction in molecular weight up to 39 kDa. NKL cells did not depict any reduction in molecular weight of 2B4. Herewith, only a slight decrease in band intensity at 70 kDa could be observed. Thus, the reduction of killing capacity of tunicamycin treated NK seems to be mainly caused by the increased apoptosis of these cells after tunicamycin treatment and not by efficient de-*N*-glycosylation.

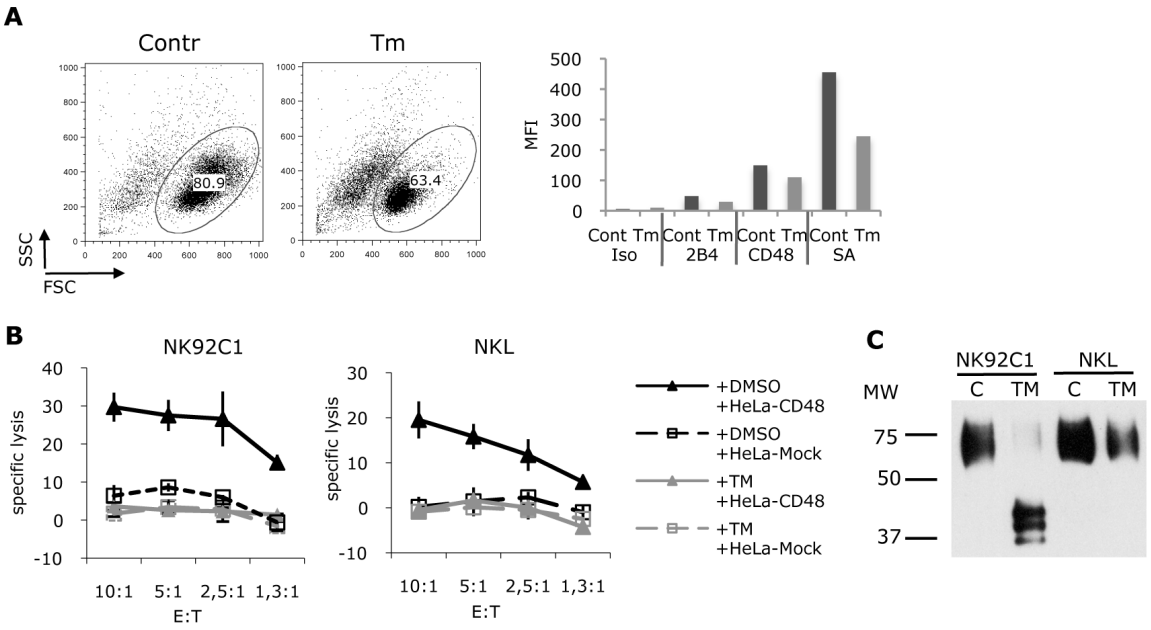

Figure 23: Tunicamycin inhibits NK cell cytotoxicity. NK cells were treated with DMSO as control or tunicamycin for 12 h at 37 °C. (**A**) Control (Cont) or tunicamycin (Tm) treated NKL cells were analyzed via flow cytometry. Left panel represent the forward / sideward scatter dot blot. Viable cells were gated and percentage values are shown. The graph on the right shows the surface staining of indicated receptors. Sialic acids (SA) were stained using rhSiglec7-Fc Chimera**.** (**B**) Treated NK cells were used as effector cells in a 4 h chromium release assay against HeLa-CD48 or HeLa-Mock cells. One representative experiment of three is shown. (**C**) Treated NK cells were lysed and immunoprecipitated 2B4 was analyzed using SDS-PAGE followed by anti-2B4 Western blotting.

4.2.7 Inhibition of O-glycosylation as well as removal of sialic acids increase the killing activity of NK cells

As tunicamycin seemed to bear further effects than inhibition of *N*-glycosylation, we turned our attention to sialic acids and *O*-glycosylation.

Successful removal of sialic acid from the surface of NK cells was performed by Neuraminidase treatment. The analysis of the immunoprecipitated 2B4 receptor from the treated cells by 2D-gelelectrophoresis followed by Western blotting showed a clear shift towards basic pH, demonstrating the effectiveness of the treatment (Figure 24A). Compared to control-treated NK cells, Neuraminidase treated NK cells showed enhanced killing capacity against CD48 expressing target cells (Figure 24B). While the extent of the enhanced lysis varied between experiments, we consistently observed better 2B4-mediated killing by Neuraminidase treated NK cells.

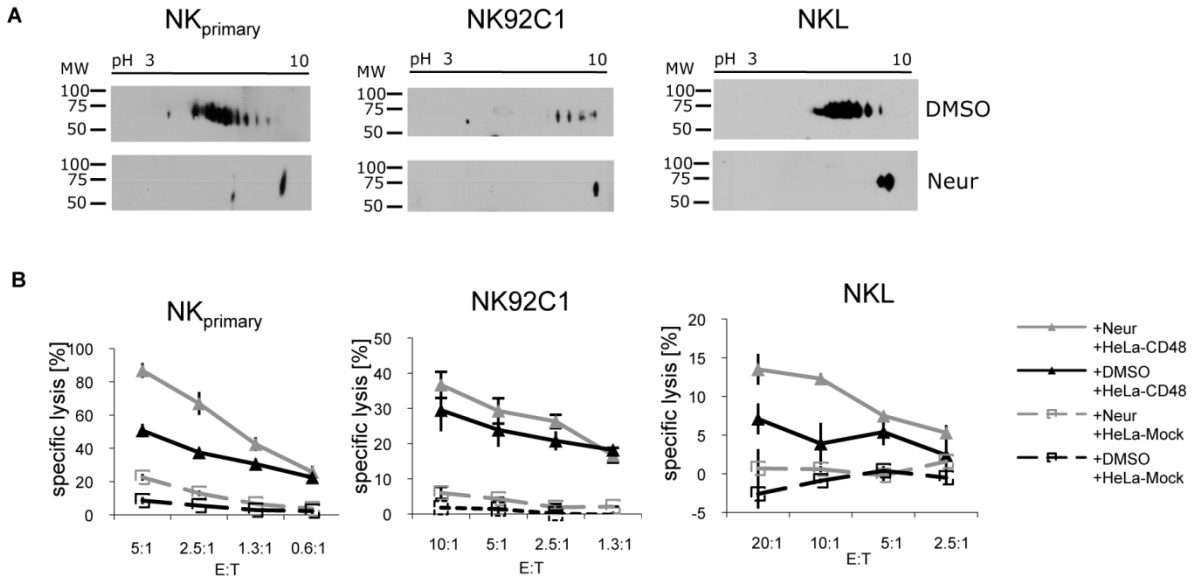

Figure 24: Desialylation of NK cells results in increased 2B4-mediated target cell lysis. NK cells were treated with DMSO as control (DMSO) or Neuraminidase for 2 h at 37 °C (Neur). (**A**) Treated NK cells were lysed and immunoprecipitated 2B4 was analyzed using 2D-gelelectrophoresis followed by anti-2B4 Western blotting. (**B**) Treated NK cells were used as effector cells in a 4 h chromium release assay against HeLa-CD48 or HeLa-Mock cells. One representative experiment of at least four is shown.

To interfere with *O*-glycosylation we cultured the NK cells with the inhibitor BADG (benzyl-α-*N*-GalNAc). BADG competes with endogenous GalNAc-*O*-Ser/Thr for galactosyltransferase and therefore prevents the elongation of *O*-glycosyl chains. Analysis of 2B4 from the treated cells showed a loss of negative charge as well as slight decrease in molecular mass due to loss of *O*-glycosidic bound carbohydrates (Figure 25A). As seen before for desialylated NK cells the BADG treated effector cells showed enhanced killing activity against CD48 expressing target cells, too (Figure 25B).

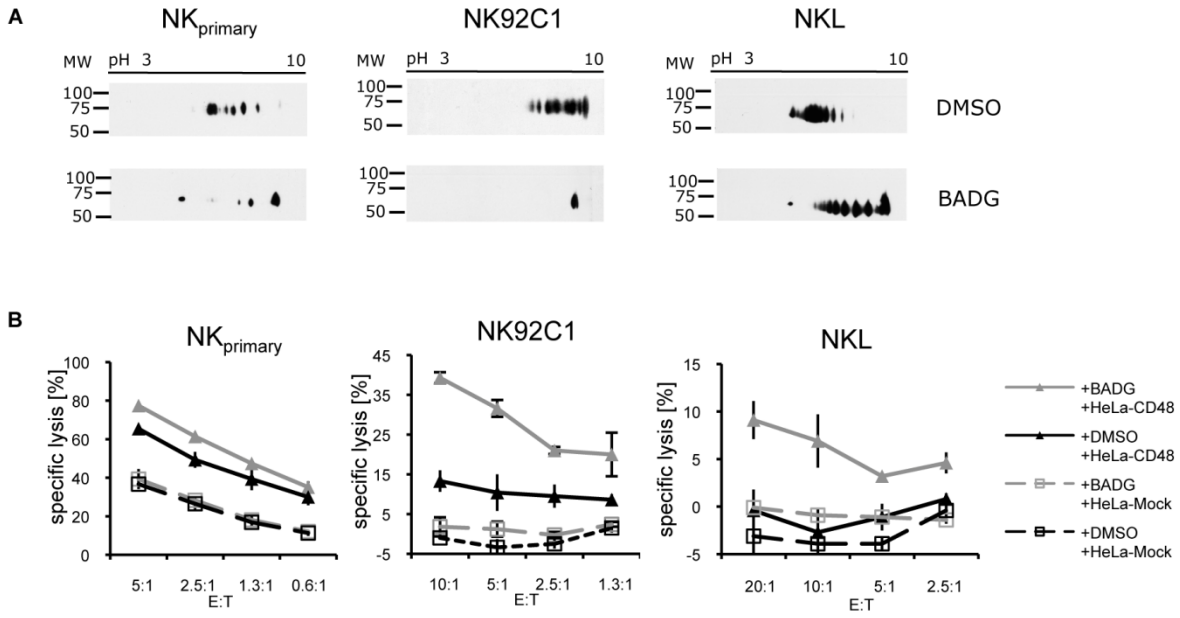

Figure 25: De-*O*-glycosylation of NK cells results in increased 2B4-mediated target cell lysis. NK cells were cultured in the presence of DMSO as control (DMSO) or the *O*-glycosylation inhibitor BADG for 48 h (BADG). (**A**) Treated NK cells were lysed and immunoprecipitated 2B4 was analyzed using 2D-gelelectrophoresis followed by anti-2B4 Western blotting. (**B**) Treated NK cells were then used as effector cells in a 4 h chromium release assay against HeLa-CD48 or HeLa-Mock cells. One representative experiment of at least four is shown.

These data demonstrate that 2B4-specific NK cell activation can be enhanced by removal of sialic acid from the surface of NK cells or the inhibition of *O*-linked glycosylation and correlates nicely with our observation that the removal of these sugars can enhance the ligand binding activity of 2B4.

5 DISCUSSION

5.1 Membrane microdomains surrounding NK cell receptors

5.1.1 Establishing of a bead-based isolation protocol to analyze the natural membrane microdomains surrounding NK cell receptors

NK cells regulate their activity by a balance of positive and negative signals upon engagement of various activating and inhibitory receptors. It has been shown that activating receptors are recruited into defined membrane microdomains termed "lipid rafts" after stimulation, whereas inhibitory receptors are excluded from these regions. This localization plays an important role in signal transduction, as disruption of lipid rafts completely blocks the target cell lysis (Watzl *et al.*, 2003). The exact mechanisms, the interplay between these receptors as well as the involved signaling molecules are not known.

Here we used a new approach to isolate membrane fragments surrounding NK cell receptors without destroying their natural composition as it has been criticized for the cold non-ionic detergent lysis. The method used here is based on the stimulation of NK cells with antibody coated magnetic beads. Cells were disrupted mechanically via nitrogen cavitation. Receptors and adjacent membrane fragments, as well as parts of the cytoplasm were immunoisolated by separation of the magnetic beads. The protein composition was analyzed using biochemical methods like Western blotting and 2D-gelelectrophoresis, as well as mass spectrometry for protein identification. Varying the setup with respect to stimulation time or engagement of different receptors enables us to gain a deeper insight into NK cell regulation.

This technique has already been established for the enrichment of activated TCR (Harder *et al.*, 2000). However, in contrast to T cells, NK cells exhibit the advantage to form separate clusters for activating and inhibitory synapses - the so called SMAC and SMIC (Orange *et al.*, 2003; Vyas *et al.*, 2002). So, two contrary operating receptor types as well as their interplay may be compared instead of an activating system in comparison to the surrounding cell membrane as it was shown for T cells (Harder *et al.*, 2001).

Nevertheless, by transferring the system established for T cells we first confirmed that it is suitable for NK cells. Thereby we could show that anti-2B4 coated beads are able to stimulate NKL cells, since receptor phosphorylation as well as IFN-γ release (Figure 11, Figure 12) could be observed. By using a bead:cell ratio of 0.5 we ensure specific binding of beads to cells, where only the engaged receptors were phosphorylated and the remaining receptors stay untouched. This finding is very essential, as it has been shown

that NK cells are able to distinguish between inhibitory and activating signals occurring at two different contact zones (Eriksson *et al.*, 1999a).

It has recently been shown, that synergistic activation of NK cells via NKG2D and 2B4 is Vav1 dependent (Kim *et al.*, 2010). Whereas these experiments were performed using antibody crosslinking, our results demonstrated that synergistic coactivation can also be performed using antibody coated beads (Figure 12B). Our results further confirm that costimulation with antibody coated magnetic beads results in proper IFN-γ release (Figure 12C,D) a characteristic feature of NK cell activation. Hence, it would be very interesting to use nitrogen cavitation to confirm the results. If the findings could be validated, analysis of membrane microdomains obtained after mechanical disruption of cells could give further insights in how NK cell receptors regulate the synergistical outcome of costimulation.

Activation of NK cells results in proceeding signaling cascades, mainly due to phosphorylation events. We were able to confirm this as stimulation for longer periods results in enhanced receptor phosphorylation (Figure 12A) as well as in the appearance of additional phosphoproteins (Figure 14). This could be a hint for the proceeding signaling cascade. As the number, as well as the appearance of molecules did not change after different stimulation time, it would be interesting to identify the proteins which were further phosphorylated after longer stimulation period. Therefore, phosphorylated proteins of immunoisolates could be post-immunoprecipitated, separated via 1D- or 2D-gelelectrophoresis and further characterized using mass spectrometry. Another possibility would be, to compare samples after stimulation using different activating receptors. As inhibition mostly results in the activation of phosphatases (Tomasello *et al.*, 2000; Vely and Vivier, 2005) instead of recruitment of kinases, as has been shown for activating receptors, one might expect that inhibitory samples do show less phosphorylated molecules. However, as this has not been investigated until now, it would be interesting, if the isolation of membrane microdomains using nitrogen cavitation would confirm this. By doing so, further insights into proceeding signaling cascades would help us to understand the very first steps occurring after NK cell receptor engagement and maybe help us to identify phosphorylated proteins involved in NK cell receptor signaling not identified up to now.

5.1.2 Inhibition versus activation – Outcome of differential NK cell receptor engagement

As we suggest that proteins occurring after costimulation differ only marginally, it would be easier to begin with a simplified experimental setup. Activating receptors are recruited into lipid rafts, whereas inhibitory receptors stay outside and are also able to block raft recruitment of activating receptors (Tomasello *et al.*, 2000; Watzl *et al.*, 2003; Watzl *et al.*, 2000). Therefore, the proteins that accumulate at the SMAC should differ highly from those at the SMIC and should easily be visualized via 2D-gelelectrophoresis. As we could confirm activation of NK cells after 2B4 stimulation and NK cell inhibition after NKG2A engagement (Figure 12) we chose these receptors to analyze membrane microdomains surrounding both receptor types. As the system has not been established for NK cells, we first concentrated on single receptor engagement. Future experiments should be performed to analyze, which consequences on the level of signaling molecules simultaneous engagement of antagonistic receptors could have.

As seen already for the silver stained samples separated via 2D-gelelectrophoresis (Figure 15), the immunoisolated proteins seemed to be to about 99 % identical. Nevertheless, by combining the method of immunoisolation with 2D-DIGE we expected to be able of getting clear differences between inhibitory and activating samples as background bound proteins would not result in significant differences. However, only few spots appear to be significantly different ($t<0.05$) whereas the average ratio between the different samples was sometimes only marginal. Furthermore, only 14 proteins were considered to be functionally relevant and were sorted according to this feature in Table 2. The complete list is attached at the end of the thesis.

One of the identified, relevant proteins is ezrin (EZRI_HUMAN). As a member of the ERM family (ezrin, radixin and moesin), it contains three domains, an N-terminal globular domain, an extended alpha-helical domain and a charged C-terminal domain (Tsukita and Yonemura, 1997). ERM proteins crosslink actin filaments with certain transmembrane proteins. Ezrin has been shown to associate with CD43, a transmembrane receptor important for ligand-receptor complexes involved in T cell activation (Bretscher *et al.*, 1997; Tsukita and Yonemura, 1999). Ezrin was either excluded from (Allenspach *et al.*, 2001) or clustered at the peripheral edges of (Roumier *et al.*, 2001) the activating T cell immunological synapse. CD43 may support adhesion as it interacts e.g. with the intercellular adhesion molecule-1 (ICAM-1).

In our case, ezrin has been found to greater extent in the 2B4 sample (average ratio 2B4 : NKG2A = 1.38). As mentioned before, it has been shown that the activating receptor 2B4 is recruited into so called DRM and that this is an actin-dependent process (Watzl *et al.*, 2003). Inhibitory receptors, in contrast, are excluded from these specialized membrane domains. Interestingly, McCann *et al.* demonstrated that ezrin and

CD43 were excluded from the NK cell inhibitory synapse (SMIC) but not from the activating synapse (SMAC) (McCann *et al.*, 2003). They proposed that the presence of CD43 in the activating NK cell synapse may be necessary to maintain effector/target contact during effector functions (Davis *et al.*, 1999). This is further supported by our finding that ezrin is probably an important molecule for 2B4 mediated signaling. Our results lead to the suggestion that ezrin is involved in SMAC formation and that it is recruited within five minutes to the NK cell activating synapse.

A second important protein identified by mass spectrometry, is RhoGDI2 (Rho GDP dissociation inhibitor beta) (ARHGDIB). Rho family proteins like Rho, Rac and Cdc42 are involved in cytoskeletal rearrangements and are essential in processes like cell motility, adhesion and phagocytosis (Hall, 1990; Ridley and Hall, 1992a; Ridley *et al.*, 1992b; Takai *et al.*, 1995; Zigmond, 1999). They are mostly found near the plasma membrane, where they directly can regulate morphological changes. The Rho family belongs to the small GTP-binding protein superfamily. Active forms (GTP-Rho) and inactive forms (GDP-Rho) are interconverted with help of guanine nucleotide exchange factors (GEFs) and GTPase-activating proteins (GAPs). RhoGDI has been identified as GEF, which catalyzes the dissociation of GTP from Rho proteins and prevents formation of the GDP-bound state, thereby keeping Rho proteins in an inactive state. First, we were surprised by the identification of RhoGDI2 as it also is primarily associated with the activating membrane microdomain. Does the finding of RhoGDI imply a termination of the signaling cascade, as soon as five minutes after stimulation? Furthermore, how would this explain the contrary finding of ezrin? Interestingly, Hirao *et al.* and Takahashi *et al.* demonstrated that the (ezrin, radixin and moesin) ERM family member moesin tightly associates in a CD44-complex with the RhoGDI in BHK (baby hamster kidney) cells (Hirao *et al.*, 1996; Takahashi *et al.*, 1997). RhoGDI has been shown to bind to the amino-terminal domain of ERM proteins. The ERM family members have been shown to appear in a closed conformation due to intramolecular association between the amino-terminal and carboxy-terminal association domain (termed N-ERMAD and C-ERMAD, respectively). This so-called "dormant" form is not able to bind e.g. F-actin or RhoGDI. Upon activation, the binding sites become unmasked and allow linkage of e.g. transmembrane receptors with the cytoskeleton. The closed "dormant" form inhibits the binding of RhoGDI to ezrin. Therefore, RhoGDI is able to bind Rho family members, inducing their inactive state. Activation of ERM proteins can cause the dissociation of RhoGDI from Rho and thus lead to an activation of the small GTP-binding proteins (Takahashi *et al.*, 1997). One target of Rho family proteins is the Rho-kinase which, in turn, can now phosphorylate ERM proteins, leading to their activation state maintenance (Mackay *et al.*, 1997; Matsui *et al.*, 1998). Hence, rather than being a negative factor for cytoskeletal rearrangement, binding of RhoGDI by ERM proteins may be a fundamental requirement for the activation of Rho signaling pathways, by promoting GTP-Rho formation. It would be very interesting

to see, if the signaling pathway of 2B4 could be linked with cytoskeletal rearrangement pathways involving ezrin and RhoGDI. A functional association between those molecules would increase our knowledge about the regulation of activating NK cell receptors.

Like ezrin, calpain is involved in cytoskeletal remodeling and signal transduction. Our mass spectrometry analysis identifies the small subunit 1 of calpain (CPNS1_HUMAN) as another signal molecule, mainly appearing in the activating sample of our experimental setup (Av. Ratio 2B4:NKG2A=1.27). As it has been reported that calpain translocates to the plasma membrane upon calcium binding (Gil-Parrado *et al.*, 2003), it would fit to our model, too. Calcium is an important mediator of adhesion and cytoplasmic processes. The ion is not only needed by cell adhesion molecules e.g. integrins in order to maintain their adhesiveness towards the extracellular matrix. Also, many intracellular signaling cascades, mainly including cytoskeletal organization, would be interrupted in the absence of Ca^{2+}. The ubiquitously expressed calpain protein family binds Ca^{2+}, too. They consist of two subunits: a large catalytic and a small regulatory subunit. Upon calcium binding, calpains are able to function as cysteine protease and thereby predominantly cleave FERM (Protein 4.1/ezrin/radixin/moesin) domains. Is the identification of the CPNS1 protein in contrast to our previously reported results or does it fit? As demonstrated previously, calpains are necessary for cell spreading and migration as they regulate actin remodeling (Potter *et al.*, 1998). ERM proteins link transmembrane proteins to the cytoskeleton and thereby stabilize a tight association of the cell membrane with the intracellular compartment. The release of this connection is important to allow the rearrangement of cell membrane molecules as well as the flattening of the cell towards the surface touched, in order to get as much contact as possible (Dewitt and Hallett, 2007). Interestingly, ezrin seems to be more sensitive to calpain mediated cleavage than e.g. moesin, another member of the ERM family (Shcherbina *et al.*, 1999). Hence, the identification of the small subunit of calpain could denote a mechanism by which the NK cell rearranges its cytoskeleton to form closer contact towards its target cell. Shenoy *et al.* suggest a negative influence of calpain-mediated proteolysis to the NK cell mediated target cell lysis (Shenoy and Brahmi, 1991). They could increase NK cell activity against K562 target cells by using two different calpain inhibitors. As protein kinase C (PKC) inhibitors circumvent this enhancement, they conclude a direct involvement of the Ca^{2+} binding protein in signaling pathways rather than in cytoskeleton rearrangement. As we analyzed partial membrane areas and adjacent cytoplasmic regions of receptor stimulated NK cells, it could be possible that calpain fulfills two different functions due to its localization and also due to its time dependent activation. Within our experimental setup, we stimulate NK cells only few minutes. Therefore, a cytoskeletal rearrangement to tighten the contact between NK cell and bead may be most likely. The functionality of

calpain in the activation of NK cells remains open and needs to be further examined. An overview of possible interactions is given in Figure 26.

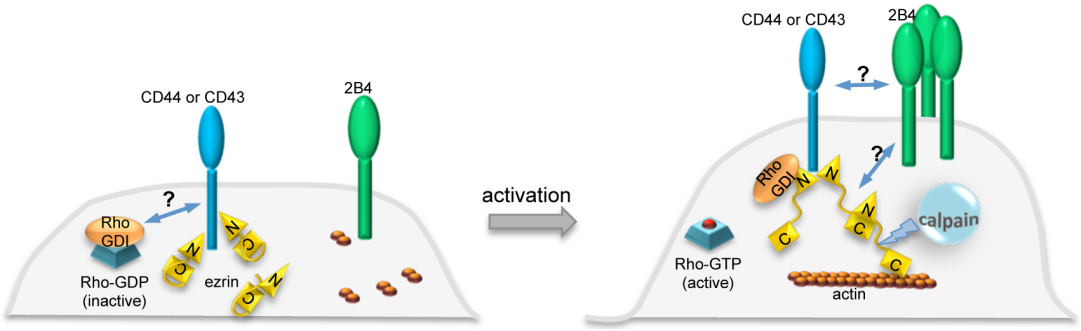

Figure 26: Model of 2B4 mediated signaling pathways due to our mass spectrometry results. Engagement of 2B4 leads to close proximity of the NK cell receptor with CD44 or CD43. Both were shown to interact with the ERM family molecule ezrin in its dormant form. Activation leads to the open conformation of ezrin and binding of RhoGDI and F-actin to ezrin. Consequently, from RhoGDI released Rho-GDP is able to exchange GDP to GTP and thus converts into its active state. This subsequently leads to activatory signaling. On the other hand, the activated form of ezrin binds F-actin as well and thereby leads to the formation or maintenance of a supramolecular activation cluster (SMAC). Calpain disrupts the tight association of ezrin and actin by cleaving the ERM molecule, thereby enabling the rearrangement of the cytoskeleton in order to form closer contacts with the target cell. Correlation between 2B4 and CD43 or CD44 as well as the interplay between receptors and cytoplasmic molecules remains to be confirmed.

Another protein identified by mass spectrometry is Grb2 (Growth factor receptor-bound protein 2 isoform 1) (GRB2_HUMAN). It consists of one Src homology 2 (SH2) and two SH3 domains. SH2 domains recognize phosphorylated tyrosines, whereas SH3 domains bind to proline-rich regions. As it functions as an adaptor molecule, it is involved in many signaling pathways e.g. MAPK, Jak-STAT or chemokine signaling pathway, but it also plays an important role in TCR or BCR mediated activation of lymphocytes. Recently, Upshaw *et al*. showed that Grb2 associated to Vav1 binds to the NKG2D-DAP10 complex, leading to the activation of downstream signaling and finally to cytotoxicity (Upshaw *et al.*, 2006). This is a quite interesting fact, as NKG2D is an activating receptor and we found Grb2 mainly in the inhibitory NKG2A sample. Interestingly, Schleinitz *et al.* found that the activating receptors 2B4 and CD2 are recruited into KIR mediated inhibitory NK cell synapses (Schleinitz *et al.*, 2008). Furthermore, they could show that CD2 is clustered at inhibitory NKIS more frequently and more rapidly than at activating synapses. They concluded that inhibitory KIRs prevent 2B4 and CD2 signaling by accumulating these activating receptors in an actin independent manner at the inhibitory NK cell synapse. Anyhow, if this is also true in our case, the appearance of Grb2 in the inhibitory sample cannot be explained as inhibitory receptors would block the recruitment of adaptor molecules. In summary, we currently cannot explain this finding.

It will be interesting to see whether the proteins identified by mass spectrometry are involved in corresponding signaling pathways. The results obtained here should thereby be confirmed by Western blotting. Thereby primary cells could be tested, too, as smaller

amounts of proteins are sufficient. If the results could be verified, knock down experiments using siRNA may give a hint for the necessity of the identified proteins in NK cell signaling.

5.1.3 Immunoisolation of transmembrane receptors - general aspects

The finding of Grb2 depicts the limitations of the mechanical disruption method. As large numbers of cells have to be used to obtain adequate protein amounts for 2D-DIGE analysis, background bound proteins cannot be avoided. As has been shown in Figure 13, we cannot get rid of the characteristic non-lipid raft marker CD45, even by reducing the size of isolated fragements. The protocol was adapted from Harder and Kuhn (Harder *et al.*, 2000) where the same amount of Jurkat T cells were stimulated with anti-CD3 coated magnetic beads and membrane fragments surrounding TCR could successfully be isolated and analyzed. It cannot be ruled out that T cells have another expression profile for the TCR than NK cells have for activating receptors. This ratio of TCR in relation to T cell surface could account for more precise isolation of membrane areas surrounding those receptors. As we monitored NKL recognition of beads by microscopy analysis (data not shown) we could not recognize any uncommon "behavior" of cells. The contacts were formed within seconds after beads recognition. On the other hand, by analyzing immunoisolates of pre-surface labeled NK cells, we recognized the occurrence of larger membrane areas in correlation with longer stimulation periods (data not shown). Those membrane areas were primarily not due to enlarged attachment of cells to beads as they occour outside the contact area. Maybe the pressure release of the nitrogen cavitation bomb causes "wrapping" of the cells around the beads which may lead to high background level of uninvolved proteins. Using a larger buffer:cell ratio could probably help to circumvent this negative side-effect. Furthermore, we plan to treat immunoisolates still bound to beads shortly with different detergents to remove uninvolved cell membrane. In fact, we wanted to avoid the use of detergents, as e.g. Triton X-100 induces the clustering of lo domains thereby leading to false positive conclusions. However, as we intend to use detergent *after* disruption of cells, the membrane surface was already shrunk to the contact area towards the beads which probably evades any raft clustering. But as weak lipid-protein interaction may also get lost by the use of detergent, the benefit of mechanical cell disruption must not be neglected. Another possibility to increase the yield of immunoisolates is the use of a non-cell-permeable crosslinker. This was already performed by Hartgroves *et al.* (Hartgroves *et al.*, 2003). The advantage would be that antibody chains would be coupled covalently to the beads. However, crosslinking also bears the disadvantage that transmembrane proteins cannot be dissolved in lysis buffer anymore. Anyhow, as 2D-gelelectrophoresis harbors the difficulty to separate highly hydrophobic proteins, the loss

of membrane proteins due to crosslinking might not be noticed, whereas a more specific isolation of intracellular proteins could be achieved. Nevertheless, the organization of lipid rafts, the interplay between receptors and the association of yet undefined receptors is highly attractive and should be investigated further. The problem of insolubility of membrane proteins could be circumvented by using new sorts of detergents. The zwitterionic detergent ASB-14 is sufficient in dissolving 2B4 and therefore may be attractive for analyzing hydrophobic proteins. To bypass the difficulty of insolubility of highly hydrophobic proteins completely, separating via 1D-gelelectrophoresis might be an alternative method. However, as this technique is unsuited to achieve a resolution as high as the combined separation via pH and molecular weight, differences between samples might not be detected. Running the samples in two different lanes followed by mass spectrometry is almost the only way to detect differences at present. The recently described SILAC (stable isotope labeling by amino acids in cell culture) technique promises the relative quantitation of differences in protein abundance. Here, one cell population is fed with growth medium containing unaltered amino acids (e.g. the later 2B4 stimulated sample), whereas the second population (e.g. the later NKG2A stimulated sample) is fed with medium containing amino acids labeled with stable heavy isotops. Samples would be prepared using nitrogen cavitation as previously described in this thesis, combined and analyzed at once by mass spectrometry, which is able to distinguish between the differentially labeled proteins. Furthermore, the peak ratio reflects the abundance of peptides. Thus, SILAC provides the huge advantage to get precise information about quantitative protein levels in two differently labeled samples. The 2D-DIGE technique requires large amounts of proteins and therefore rules out the analysis of primary cells and comparison of different donors. SILAC followed by mass spectrometry is highly sensitive and therefore could allow the analysis of primary cells, too.

In addition to proteins surrounding NK cell receptors, the analysis of lipids in proximity to transmembrane proteins could give further information about the organization of specialized membrane areas. It has been proposed that specialized membrane assemblies are stabilized by lipid-lipid and lipid-protein interactions. Therefore, even lipids seem to play an important role in maintaining the functional domains for receptor signal transduction. Simons *et al.* as well as Zech *et al.* analyzed immunoisolates of TCRs via mass spectrometry and showed that certain lipids are segregated at the receptor activation domain (Simons *et al.*, 2004; Zech *et al.*, 2009). It would be rather interesting, if immunoisolates of activating and inhibitory NK cell receptors differ in their lipid composition and if also a discrimination between the lipid composition of different activating receptors is possible.

The here established bead-based immunoisolation method is a powerful detergent-free technique to provide deeper insights into the natural composition of membrane microdomains surrounding NK cell receptors. Knowledge gained about structure and composition of membrane domains could help us to examine and understand functional consequences of the complexity of proteins and lipids in biological membranes.

5.2 Glycosylation of 2B4 and its effect in ligand binding and function

Glycosylation is an important post-translational modification of membrane proteins and crucial for proper cell function. Many cellular processes like cell adhesion, signal transduction and receptor activation involve glycosylated proteins. In recent years, it became clear that mutations in biosynthetic pathways of glycans may be lethal or lead to severe defects (Freeze *et al.*, 2001). These mutations frequently concern the formation of extracellular matrix (ECM) molecules or neuronal disorders. Thereby the organism fails to assemble essential molecular networks for trafficking and adherence. Nonetheless, receptor glycosylation also is highly regulated. Improper glycosylation affects protein folding and often results in protein retention in the ER or Golgi complexes and finally leads to its degradation. Therefore, plasma membrane proteins fail to reach the surface and ECM proteins will not be exocytosed, as well. Additionally, wrong glycosidic bonds or the attachment of incorrect carbohydrates alters the confirmation of the sugar tree resulting in masking or exposure of improper protein or glycosidic components. As sugar molecules, especially sialic acids, serve as recognition sites for receptors, improper glycosylation leads to a failure of interaction.

2B4 is an important and well-characterized activating receptor for NK cell activation. Among others its engagement results in IFN-γ production, a main characteristic of NK cell responses. Though 2B4 is characterized better than any other NK cell receptor, less is known about its extracellular part and its influence in receptor engagement. It is known that 2B4 contains several *N*-glycosylaton sites (Tangye *et al.*, 1999) but it has not been studied until now, if those influence the interaction with its ligand CD48.

Our data confirm the expression of 2B4 as a 70 kDa protein in all cell populations (Figure 17A) but also reveal a heterogeneous modification because 2B4 is distributed broadly over the pH gradient. Interestingly, the receptors of NKL, HEK-2B4 cells as well as primary NK cells exhibit mainly neutral pH, whereas the NK cell line NK92C1 represents a more basic receptor population. This could not be traced back to different phosphorylation of the cytosolic part of the SRR as dephosphorylation of 2B4 as well as analyzing the ITSM mutant and thereby phosphorylation incompetent form of 2B4 (Y1,2,3,4F) did not result in the ablation of multiple spots (Figure 17B + Figure 18).

Anyhow, a slight shift towards basic pH as well as a faint phosphotyrosine signal in untreated samples could be observed for NK cells (data not shown), which was not true for HEK-2B4 cells (Figure 18). CD48, the ligand of 2B4, is expressed on all NK cells, which led to the assumption that the SRR is slightly but constantly stimulated. This engagement may occur by interaction with other cells (*trans*) as well as on the same cell surface (*cis*). As HEK-2B4 cells did not express CD48 per se, a receptor-ligand interaction and thereby induced receptor background phosphorylation is impossible. Because of this, 2B4 on NK cells but not on transfected HEK cells receives a continuous, slight stimulus via CD48, leading to background phosphorylation of 2B4. Nevertheless, this shift seems to be of only minor importance and might as well not be responsible for the appearance of miscellaneous spots.

PNGaseF treatment of 2B4 results in a mass reduction of 30 kDa, as well as in a now comparable spot pattern between the cell populations which shifted to more basic pH after treatment. This suggests that *N*-linked carbohydrates on 2B4 differ between NK92C1 and the other examined NK cells. It further shows that *N*-linked sugars account for the 30 kDa difference between calculated and apparent molecular weight of the 2B4 receptor. Zielinska *et al.* have shown that *N*-glycosylation is not restricted to the N-!P-[S/T] sequence motif (where !P is any amino acid except proline) or the uncommon N-X-C motif but can also be found on yet unknown positions (Zielinska *et al.*, 2010). Furthermore, only 30 % of all available motifs within a protein are glycosylated with some of them showing only incomplete glycosylation (Mellquist *et al.*, 1998). This results in a heterogeneous population of differentially glycosylated proteins as we have found for the 2B4 receptor.

The 2B4 receptor still migrated as distinct spots covering a broad pH range after the removal of *N*-glycans. This suggested the presence of additional sugar moieties that are highly charged and of small size. Using Neuraminidase to desialylate immunoprecipitated 2B4 we could show, that all 2B4 molecules migrate to one distinct point and thereby verify the presence of sialic acids. These small monosaccharides exhibit a nine-carbon backbone and are always negatively charged due to their C1 carboxylate group. The common human sugar is the N-acetylneuraminic acid (Neu5Ac), containing an N-acetyl group at the 5-carbon position. But other modifications like de-N-acetylation or substitutions at the other carbons are known. This variability could further influence the charge of sialic acids and thereby influence the pI of the glycoprotein. It would be interesting if differences in pI of 2B4 from NKL and NK92C1 cells could be contributed to different numbers or different modifications of sialic acids. Therefore, various combinations of treatments with sialidases, 9-O-acetylesterases and mild periodate oxidation could be used to elucidate sialic acid moieties of 2B4 expressed by different cell populations.

The differential glycosylation of 2B4 could be attributed to sialic acid residues on both *N*- and *O*-linked sugars as removal of sialic acids created a population of 2B4 molecules migrating at one distinct pI. Considering the bioinformatic tools of the CBS prediction service databank (www.cbs.dtu.dk/services/) the sequence of 2B4 does not reveal any *O*-glycosylation site. However, there is no clear consensus sequence for *O*-glycosylation sites. As we still observed distinct spots after removal of *N*-glycosylation we suggest that 2B4 is also modified by *O*-linked sugars. The enzymatic removal of *O*-glycosidic bound carbohydrates requires first a removal of sialic acids, making a specific analysis of *O*-linked sugars difficult. As *O*-glycans are less branched and therefore less in molecular weight, a mass reduction may be difficult to visualize. We observed an increase in molecular weight of 2B4 after removal of *O*-glycosidic bound carbohydrates compared to the removal of sialic acids alone. This rather surprising result might be explained by peptide dimerisation due to diminished repulsion after removal of *O*-linked sugars.

We further analyzed the influence of the membrane proximal C2-type (IgC2) domain on the molecular weight of 2B4. Using a mutant with an ablation of IgC2 domain reveals that the distal V-type Ig domain is mainly responsible for the alterations in molecular weight of 2B4. This is highly interesting as the membrane proximal IgC2 domain contains more *N*-glycosylation sites in comparison with the distal IgV domain. As mentioned before, it has been shown (Zielinska *et al.*, 2010) that *N*-glycosylation is not restricted to the common known N-!P-[S/T] sequence. It could be possible that the membrane distal domain contains more *N*-glycosidic bound carbohydrates as shown by sequence analysis. But it is also feasible that the V-type domain contains more branched carbohydrate trees and thereby accounts more to molecular mass as the membrane proximal domain. The observation that the distal domain is mainly responsible for the molecular weight is really unexpected, as glycosidic bonds may impair the binding of 2B4 to its ligand CD48. It has been shown that the N-terminal domain is responsible for the receptor-ligand interaction (Velikovsky *et al.*, 2007). Hence, glycosylation of the distal domain may rather contribute to receptor ligand interaction than abrogating it.

The structural information available today about the interaction between 2B4 and CD48 did not implicate glycosylation to be important for this binding. Furthermore, it has been shown that binding by the 2B4 related receptor CD2 to its ligand CD58 is independent of glycosylation (Davis *et al.*, 1995). Anyhow, CD2 contains only one potential *N*-glycosylation site in its membrane distal IgV domain which lies on the opposite site of the contact area with CD58 (Davis *et al.*, 1995). Contrary to this, two of three *N*-glycosylation sites of the membrane distal IgV domain of 2B4 are in close proximity to the putative CD48 binding site (Velikovsky *et al.*, 2007) and could have major influence in ligand binding.

Based on the CD2-CD58 interaction Mathew *et al.* showed that Lys68 and Glu70 of the human 2B4 IgV domain were necessary for ligand binding (Mathew *et al.*, 2005)[29]. However, in our hands these mutations were not sufficient to abolish ligand binding. Only a 2B4 triple mutant K54A/H65A/T110A, based on the structure of the murine 2B4-CD48 complex (Velikovsky *et al.*, 2007), completely abolished binding to CD48 (Claus, Watzl, unpublished results). These results show that the human 2B4-CD48 interaction is similar to the murine receptor and that glycosylation may play an important role in ligand recognition and binding.

Our data demonstrate that *N*-glycosylation of 2B4 is essential for this interaction, as removal of these sugars from the 2B4 fusion protein almost completely prevented its binding to CD48 expressing cells (Figure 22 B,C). We are aware that de-*N*-glycosylation might also impair the structure of the isolated 2B4-ILZ fusion protein used and further controls are needed. We plan to analyze the correct folding of de-*N*-glycosylated 2B4-ILZ via correct binding of the anti-2B4 antibody (C1.7) in flow cytometry assays and also via ProteoStat Protein Aggregation Assay (Enzo, Germany), which enables the detection of aggregated proteins due to their characteristic cross-beta spine quaternary structure. Furthermore, secondary structure of 2B4 might be controlled via circular dichroism, a biophysical method able to distinguish between beta-sheet and alpha-helix conformation.

The use and modification of recombinant 2B4-ILZ fusion proteins provided first insights into the influence of different carbohydrates in receptor-ligand interaction. Furthermore, it would be interesting to modify the glycosylation structure of 2B4-ILZ proteins with respect to only minor changes in glycosidic bonds. Cell lines with different defects in glycosylation are a useful tool to alter protein glycosylation in a defined way. Chinese hamster ovary (CHO) and baby hamster kidney (BHK) lack a functional α(2,6) sialyltransferase and make exclusively α(2,3)-linked Neu5Ac (Hossler *et al.*, 2009; Jenkins, 1995). Other cell lines such as HEK cells (Durocher and Butler, 2009), human retinal cells (PERC.6) (Jones *et al.*, 2003; Petricciani and Sheets, 2008; Wurm, 2004) and mouse myeloma (NS0) (Gramer and Goochee, 1994) are also feasible to study the outcome of different glycosidic bound carbohydrates due to differences in glycosylation. Analyzing the binding of 2B4-ILZ expressed in these cells towards CD48 expressing cells could give information which carbohydrates are involved in or impair the ligand recognition. Furthermore, analysis of stepwise and combined mutations of the *N*-glycosylation sites of 2B4 would help to define the exact position of glycans which enhance or diminish receptor-ligand interaction. Use of different lectins combined with Western blotting could further help us to identify carbohydrates bound to 2B4. This technique would also be suitable to characterize the variation between 2B4 expressed by different cell lines or primary cells. Furthermore, recent advantages in mass spectrometry would be the most powerful method to evaluate glycosylation sites and

elucidate the oligosaccharide structures due to its high sensitivity and selectivity (Pan *et al.*, 2010).

The differences between the glycosylation pattern of 2B4 from NK92C1 and other NK cells or 2B4-transfected HEK cells could be attributed to *N*-linked sugars. Hence, it would be possible that this bound carbohydrates influence the binding of 2B4 to CD48, too. To investigate this, we used tunicamycin, an inhibitor of the GlcNAc phosphotransferase, which prevents the transfer of *N*-acetylglucosamine-1-phosphate from UDP-N-acetylglucosamine to dolichol phosphate, the first step of *N*-glycosylation. Tunicamycin treated NK92C1 and NKL cells showed diminished killing of CD48 expressing target cells which would confirm the essential role of *N*-glycosylation for 2B4-CD48 interactions. However, tunicamycin also had toxic side-effects on NK cells. In NKL cells the reduction of cytotoxicity could almost completely be attributed to a diminished viability of tunicamycin treated cells as seen by a shift in the forward and side scatter (FSC and SSC) population (Figure 23). Furthermore, no mass reduction due to diminished *N*-glycosylation could be observed, whereas a reduction of total 2B4 in Western blotting as well as a slight reduction of surface expression of the NK cell receptor could be observed. Interestingly, NK92C1 cells showed a clear mass reduction of 2B4 down to its calculated molecular weight of 40 kDa. Hence, it is hard to say if the reduced killing capacity of tunicamycin treated NK92C1 cells is due to successful de-*N*-glycosylation or if it is only due to toxic side effects as seen for NKL cells. Further studies, e.g. using other inhibitors, will have to address the exact role of differential *N*-glycosylation for 2B4 function.

In contrast to the use of tunicamycin, desialylation of NK cells was successful and showed that 2B4 associated sialic acids affect the binding of 2B4 to CD48. Interestingly, sialic acids seem to hinder this interaction as we observed increased binding of 2B4 to CD48 after Neuraminidase treatment. The negative charge introduced by the addition of sialic acids may lead to some repulsion within the 2B4-CD48 interaction, which would explain the positive effect on binding upon removal of sialic acids. This effect was not only seen in the binding of the recombinant 2B4 fusion protein to CD48 expressing cells, but could also be confirmed in NK cells, as Neuraminidase treatment of NK cells resulted in enhanced 2B4-mediated lysis of CD48 expressing target cells.

Our data show that 2B4 is sialylated on *N*- and *O*-linked sugars. This would explain why the inhibition of *O*-linked glycosylation in NK cells by BADG also enhanced the lysis of CD48 expressing cells and suggest that sialic acids on *O*-linked sugars are involved in the repulsion during the 2B4-CD48 interaction. Removal of sialic acids by Neuraminidase or blocking *O*-linked glycosylation by BADG treatment of NK cells does not only affect the glycosylation of 2B4, but affects many different surface molecules and can therefore have general effects on NK cell reactivity (Benson *et al.*). This explains why the treated NK cells already show some difference in lysis of Mock–transfected target cells. However,

the lysis of CD48-transfected targets was affected to a much larger extent, arguing for a specific effect on 2B4-mediated NK cell activation.

The data presented here show for the first time an influence of glycosylation on the binding and the functionality of the activating receptor 2B4. The binding of CD8 to MHC-I has also been shown to be enhanced upon removal of sialic acids (Daniels *et al.*, 2001) and desialylation increases $CD8^+$ T cell sensitivity to APC stimulation (Crespo *et al.*, 2009). Interestingly, in contrast to naïve T cells, activated T cells show a reduction in sialylation (Daniels *et al.*, 2001). Therefore, regulated surface sialylation may play a role in regulating T cell responses. No data are available to date about the regulation of sialylation in NK cells. However, it is interesting to speculate that a reduced sialylation induced by NK cell activation or during NK cell maturation would affect 2B4-mediated NK cell activation. Future studies should therefore investigate how the regulation of glycosylation could affect NK cell reactivity.

6 REFERENCES

Allenspach EJ, Cullinan P, Tong J, Tang Q, Tesciuba AG, Cannon JL, Takahashi SM, Morgan R, Burkhardt JK, Sperling AI (2001) ERM-dependent movement of CD43 defines a novel protein complex distal to the immunological synapse. *Immunity* **15:** 739-750.

Anderson DR, Grillo-Lopez A, Varns C, Chambers KS, Hanna N (1997) Targeted anti-cancer therapy using rituximab, a chimaeric anti-CD20 antibody (IDEC-C2B8) in the treatment of non-Hodgkin's B-cell lymphoma. *Biochemical Society transactions* **25:** 705-708.

Arcaro A, Gregoire C, Boucheron N, Stotz S, Palmer E, Malissen B, Luescher IF (2000) Essential role of CD8 palmitoylation in CD8 coreceptor function. *J Immunol* **165:** 2068-2076.

Arnon TI, Lev M, Katz G, Chernobrov Y, Porgador A, Mandelboim O (2001) Recognition of viral hemagglutinins by NKp44 but not by NKp30. *European journal of immunology* **31:** 2680-2689.

Belisle JA, Horibata S, Jennifer GA, Petrie S, Kapur A, Andre S, Gabius HJ, Rancourt C, Connor J, Paulson JC, Patankar MS (2010) Identification of Siglec-9 as the receptor for MUC16 on human NK cells, B cells, and monocytes. *Mol Cancer* **9:** 118.

Benson V, Grobarova V, Richter J, Fiserova A Glycosylation regulates NK cell-mediated effector function through PI3K pathway. *International immunology* **22:** 167-177.

Beyer TA, Rearick JI, Paulson JC, Prieels JP, Sadler JE, Hill RL (1979) Biosynthesis of mammalian glycoproteins. Glycosylation pathways in the synthesis of the nonreducing terminal sequences. *The Journal of biological chemistry* **254:** 12531-12534.

Bhat R, Eissmann P, Endt J, Hoffmann S, Watzl C (2006) Fine-tuning of immune responses by SLAM-related receptors. *Journal of leukocyte biology* **79:** 417-424.

Biron CA, Nguyen KB, Pien GC, Cousens LP, Salazar-Mather TP (1999) Natural killer cells in antiviral defense: function and regulation by innate cytokines. *Annual review of immunology* **17:** 189-220.

Blix G, Lindberg E, Odin L, Werner I (1956) Studies on sialic acids. *Acta Soc Med Ups* **61:** 1-25.

Bottino C, Augugliaro R, Castriconi R, Nanni M, Biassoni R, Moretta L, Moretta A (2000) Analysis of the molecular mechanism involved in 2B4-mediated NK cell activation: evidence that human 2B4 is physically and functionally associated with the linker for activation of T cells. *European journal of immunology* **30:** 3718-3722.

Bottino C, Falco M, Parolini S, Marcenaro E, Augugliaro R, Sivori S, Landi E, Biassoni R, Notarangelo LD, Moretta L, Moretta A (2001) NTB-A [correction of GNTB-A], a novel SH2D1A-associated surface molecule contributing to the inability of natural killer cells to kill Epstein-Barr virus-infected B cells in X-linked lymphoproliferative disease. *The Journal of experimental medicine* **194:** 235-246.

Bouchon A, Cella M, Grierson HL, Cohen JI, Colonna M (2001) Activation of NK cell-mediated cytotoxicity by a SAP-independent receptor of the CD2 family. *J Immunol* **167:** 5517-5521.

Brandt CS, Baratin M, Yi EC, Kennedy J, Gao Z, Fox B, Haldeman B, Ostrander CD, Kaifu T, Chabannon C, Moretta A, West R, Xu W, Vivier E, Levin SD (2009) The B7 family member B7-H6 is a tumor cell ligand for the activating natural killer cell receptor NKp30 in humans. *The Journal of experimental medicine* **206:** 1495-1503.

Bretscher A, Reczek D, Berryman M (1997) Ezrin: a protein requiring conformational activation to link microfilaments to the plasma membrane in the assembly of cell surface structures. *Journal of cell science* **110 (Pt 24):** 3011-3018.

Brown DA, London E (1997) Structure of detergent-resistant membrane domains: does phase separation occur in biological membranes? *Biochem Biophys Res Commun* **240:** 1-7.

Brown DA, London E (1998a) Functions of lipid rafts in biological membranes. *Annual review of cell and developmental biology* **14:** 111-136.

Brown MH, Boles K, van der Merwe PA, Kumar V, Mathew PA, Barclay AN (1998b) 2B4, the natural killer and T cell immunoglobulin superfamily surface protein, is a ligand for CD48. *The Journal of experimental medicine* **188:** 2083-2090.

Bryceson YT, March ME, Ljunggren HG, Long EO (2006) Synergy among receptors on resting NK cells for the activation of natural cytotoxicity and cytokine secretion. *Blood* **107:** 159-166.

Calpe S, Erdos E, Liao G, Wang N, Rietdijk S, Simarro M, Scholtz B, Mooney J, Lee CH, Shin MS, Rajnavolgyi E, Schatzle J, Morse HC, 3rd, Terhorst C, Lanyi A (2006) Identification and characterization of two related murine genes, Eat2a and Eat2b, encoding single SH2-domain adapters. *Immunogenetics* **58:** 15-25.

Cella M, Fuchs A, Vermi W, Facchetti F, Otero K, Lennerz JK, Doherty JM, Mills JC, Colonna M (2009) A human natural killer cell subset provides an innate source of IL-22 for mucosal immunity. *Nature* **457:** 722-725.

Chamberlain LH (2004) Detergents as tools for the purification and classification of lipid rafts. *FEBS Lett* **559:** 1-5.

Chavez-Galan L, Arenas-Del Angel MC, Zenteno E, Chavez R, Lascurain R (2009) Cell death mechanisms induced by cytotoxic lymphocytes. *Cell Mol Immunol* **6:** 15-25.

Chen R, Latour S, Shi X, Veillette A (2006) Association between SAP and FynT: Inducible SH3 domain-mediated interaction controlled by engagement of the SLAM receptor. *Mol Cell Biol* **26:** 5559-5568.

Chen R, Relouzat F, Roncagalli R, Aoukaty A, Tan R, Latour S, Veillette A (2004) Molecular dissection of 2B4 signaling: implications for signal transduction by SLAM-related receptors. *Mol Cell Biol* **24:** 5144-5156.

Chlewicki LK, Velikovsky CA, Balakrishnan V, Mariuzza RA, Kumar V (2008) Molecular basis of the dual functions of 2B4 (CD244). *J Immunol* **180:** 8159-8167.

Chuang SS, Kumaresan PR, Mathew PA (2001) 2B4 (CD244)-mediated activation of cytotoxicity and IFN-gamma release in human NK cells involves distinct pathways. *J Immunol* **167:** 6210-6216.

Clarkson NG, Simmonds SJ, Puklavec MJ, Brown MH (2007) Direct and indirect interactions of the cytoplasmic region of CD244 (2B4) in mice and humans with FYN kinase. *The Journal of biological chemistry* **282:** 25385-25394.

Claus M, Meinke S, Bhat R, Watzl C (2008) Regulation of NK cell activity by 2B4, NTB-A and CRACC. *Front Biosci* **13:** 956-965.

Colucci F, Caligiuri MA, Di Santo JP (2003) What does it take to make a natural killer? *Nat Rev Immunol* **3:** 413-425.

Cooper MA, Fehniger TA, Fuchs A, Colonna M, Caligiuri MA (2004) NK cell and DC interactions. *Trends in immunology* **25:** 47-52.

Crespo HJ, Cabral MG, Teixeira AV, Lau JT, Trindade H, Videira PA (2009) Effect of sialic acid loss on dendritic cell maturation. *Immunology* **128:** e621-631.

Cudkowicz G, Stimpfling JH (1964) HYBRID RESISTANCE TO PARENTAL MARROW GRAFTS: ASSOCIATION WITH THE K REGION OF H-2. *Science (New York, NY* **144:** 1339-1340.

Dall'olio F (1996) Protein glycosylation in cancer biology: an overview. *Clin Mol Pathol* **49:** M126-135.

Daniels MA, Devine L, Miller JD, Moser JM, Lukacher AE, Altman JD, Kavathas P, Hogquist KA, Jameson SC (2001) CD8 binding to MHC class I molecules is influenced by T cell maturation and glycosylation. *Immunity* **15:** 1051-1061.

Davis DM, Chiu I, Fassett M, Cohen GB, Mandelboim O, Strominger JL (1999) The human natural killer cell immune synapse. *Proc Natl Acad Sci U S A* **96:** 15062-15067.

Davis SJ, Davies EA, Barclay AN, Daenke S, Bodian DL, Jones EY, Stuart DI, Butters TD, Dwek RA, van der Merwe PA (1995) Ligand binding by the immunoglobulin superfamily recognition molecule CD2 is glycosylation-independent. *The Journal of biological chemistry* **270:** 369-375.

Degli-Esposti MA, Smyth MJ (2005) Close encounters of different kinds: dendritic cells and NK cells take centre stage. *Nat Rev Immunol* **5:** 112-124.

Dewitt S, Hallett M (2007) Leukocyte membrane "expansion": a central mechanism for leukocyte extravasation. *Journal of leukocyte biology* **81:** 1160-1164.

Durocher Y, Butler M (2009) Expression systems for therapeutic glycoprotein production. *Curr Opin Biotechnol* **20:** 700-707.

Dykstra M, Cherukuri A, Sohn HW, Tzeng SJ, Pierce SK (2003) Location is everything: lipid rafts and immune cell signaling. *Annual review of immunology* **21:** 457-481.

Eagle RA, Trowsdale J (2007) Promiscuity and the single receptor: NKG2D. *Nat Rev Immunol* **7:** 737-744.

Eggeling C, Ringemann C, Medda R, Schwarzmann G, Sandhoff K, Polyakova S, Belov VN, Hein B, von Middendorff C, Schonle A, Hell SW (2009) Direct observation of the nanoscale dynamics of membrane lipids in a living cell. *Nature* **457:** 1159-1162.

Eissmann P, Beauchamp L, Wooters J, Tilton JC, Long EO, Watzl C (2005) Molecular basis for positive and negative signaling by the natural killer cell receptor 2B4 (CD244). *Blood* **105:** 4722-4729.

Endt J, McCann FE, Almeida CR, Urlaub D, Leung R, Pende D, Davis DM, Watzl C (2007) Inhibitory receptor signals suppress ligation-induced recruitment of NKG2D to GM1-rich membrane domains at the human NK cell immune synapse. *J Immunol* **178:** 5606-5611.

Eriksson M, Leitz G, Fallman E, Axner O, Ryan JC, Nakamura MC, Sentman CL (1999a) Inhibitory receptors alter natural killer cell interactions with target cells yet allow simultaneous killing of susceptible targets. *The Journal of experimental medicine* **190:** 1005-1012.

Eriksson M, Ryan JC, Nakamura MC, Sentman CL (1999b) Ly49A inhibitory receptors redistribute on natural killer cells during target cell interaction. *Immunology* **97:** 341-347.

Fassett MS, Davis DM, Valter MM, Cohen GB, Strominger JL (2001) Signaling at the inhibitory natural killer cell immune synapse regulates lipid raft polarization but not class I MHC clustering. *Proc Natl Acad Sci U S A* **98:** 14547-14552.

Finne J, Finne U, Deagostini-Bazin H, Goridis C (1983) Occurrence of alpha 2-8 linked polysialosyl units in a neural cell adhesion molecule. *Biochem Biophys Res Commun* **112:** 482-487.

Freeze HH, Westphal V (2001) Balancing N-linked glycosylation to avoid disease. *Biochimie* **83:** 791-799.

Garni-Wagner BA, Purohit A, Mathew PA, Bennett M, Kumar V (1993) A novel function-associated molecule related to non-MHC-restricted cytotoxicity mediated by activated natural killer cells and T cells. *J Immunol* **151:** 60-70.

Gil-Parrado S, Popp O, Knoch TA, Zahler S, Bestvater F, Felgentrager M, Holloschi A, Fernandez-Montalvan A, Auerswald EA, Fritz H, Fuentes-Prior P, Machleidt W, Spiess E (2003) Subcellular localization and in vivo subunit interactions of ubiquitous mu-calpain. *The Journal of biological chemistry* **278:** 16336-16346.

Gilfillan S, Chan CJ, Cella M, Haynes NM, Rapaport AS, Boles KS, Andrews DM, Smyth MJ, Colonna M (2008) DNAM-1 promotes activation of cytotoxic lymphocytes by nonprofessional antigen-presenting cells and tumors. *The Journal of experimental medicine* **205:** 2965-2973.

Gnad F, Ren S, Cox J, Olsen JV, Macek B, Oroshi M, Mann M (2007) PHOSIDA (phosphorylation site database): management, structural and evolutionary investigation, and prediction of phosphosites. *Genome Biol* **8:** R250.

Gramer MJ, Goochee CF (1994) Glycosidase activities of the 293 and NS0 cell lines, and of an antibody-producing hybridoma cell line. *Biotechnol Bioeng* **43:** 423-428.

Hall A (1990) The cellular functions of small GTP-binding proteins. *Science (New York, NY* **249:** 635-640.

Hammond AT, Heberle FA, Baumgart T, Holowka D, Baird B, Feigenson GW (2005) Crosslinking a lipid raft component triggers liquid ordered-liquid disordered phase separation in model plasma membranes. *Proc Natl Acad Sci U S A* **102:** 6320-6325.

Harder T, Kuhn M (2000) Selective accumulation of raft-associated membrane protein LAT in T cell receptor signaling assemblies. *The Journal of cell biology* **151:** 199-208.

Harder T, Kuhn M (2001) Immunoisolation of TCR signaling complexes from Jurkat T leukemic cells. *Sci STKE* **2001:** PL1.

Harder T, Scheiffele P, Verkade P, Simons K (1998) Lipid domain structure of the plasma membrane revealed by patching of membrane components. *The Journal of cell biology* **141:** 929-942.

Hartgroves LC, Lin J, Langen H, Zech T, Weiss A, Harder T (2003) Synergistic assembly of linker for activation of T cells signaling protein complexes in T cell plasma membrane domains. *The Journal of biological chemistry* **278:** 20389-20394.

Heerklotz H (2002) Triton promotes domain formation in lipid raft mixtures. *Biophys J* **83:** 2693-2701.

Herberman RB, Nunn ME, Holden HT, Lavrin DH (1975a) Natural cytotoxic reactivity of mouse lymphoid cells against syngeneic and allogeneic tumors. II. Characterization of effector cells. *Int J Cancer* **16:** 230-239.

Herberman RB, Nunn ME, Lavrin DH (1975b) Natural cytotoxic reactivity of mouse lymphoid cells against syngeneic acid allogeneic tumors. I. Distribution of reactivity and specificity. *Int J Cancer* **16:** 216-229.

Hillyard DZ, Nutt CD, Thomson J, McDonald KJ, Wan RK, Cameron AJ, Mark PB, Jardine AG (2007) Statins inhibit NK cell cytotoxicity by membrane raft depletion rather than inhibition of isoprenylation. *Atherosclerosis* **191:** 319-325.

Hirao M, Sato N, Kondo T, Yonemura S, Monden M, Sasaki T, Takai Y, Tsukita S (1996) Regulation mechanism of ERM (ezrin/radixin/moesin) protein/plasma membrane association: possible involvement of phosphatidylinositol turnover and Rho-dependent signaling pathway. *The Journal of cell biology* **135:** 37-51.

Hoffmann SC, Schellack C, Textor S, Konold S, Schmitz D, Cerwenka A, Pflanz S, Watzl C (2007) Identification of CLEC12B, an inhibitory receptor on myeloid cells. *The Journal of biological chemistry*.

Hollingsworth MA, Swanson BJ (2004) Mucins in cancer: protection and control of the cell surface. *Nat Rev Cancer* **4:** 45-60.

Hope HR, Pike LJ (1996) Phosphoinositides and phosphoinositide-utilizing enzymes in detergent-insoluble lipid domains. *Molecular biology of the cell* **7:** 843-851.

Hossler P, Khattak SF, Li ZJ (2009) Optimal and consistent protein glycosylation in mammalian cell culture. *Glycobiology* **19:** 936-949.

Janik ME, Litynska A, Vereecken P (2010) Cell migration-the role of integrin glycosylation. *Biochimica et biophysica acta* **1800:** 545-555.

Janka GE (2007) Familial and acquired hemophagocytic lymphohistiocytosis. *Eur J Pediatr* **166:** 95-109.

Jenkins N (1995) Monitoring and control of recombinant glycoprotein heterogeneity in animal cell cultures. *Biochemical Society transactions* **23:** 171-175.

Jin L, McLean PA, Neel BG, Wortis HH (2002) Sialic acid binding domains of CD22 are required for negative regulation of B cell receptor signaling. *The Journal of experimental medicine* **195:** 1199-1205.

Jones D, Kroos N, Anema R, van Montfort B, Vooys A, van der Kraats S, van der Helm E, Smits S, Schouten J, Brouwer K, Lagerwerf F, van Berkel P, Opstelten DJ, Logtenberg T, Bout A (2003) High-level expression of recombinant IgG in the human cell line per.c6. *Biotechnol Prog* **19:** 163-168.

Jonges LE, Albertsson P, van Vlierberghe RL, Ensink NG, Johansson BR, van de Velde CJ, Fleuren GJ, Nannmark U, Kuppen PJ (2001) The phenotypic heterogeneity of human

natural killer cells: presence of at least 48 different subsets in the peripheral blood. *Scand J Immunol* **53:** 103-110.

Karlhofer FM, Ribaudo RK, Yokoyama WM (1992) MHC class I alloantigen specificity of Ly-49+ IL-2-activated natural killer cells. *Nature* **358:** 66-70.

Karre K (2008) Natural killer cell recognition of missing self. *Nat Immunol* **9:** 477-480.

Karre K, Ljunggren HG, Piontek G, Kiessling R (1986) Selective rejection of H-2-deficient lymphoma variants suggests alternative immune defence strategy. *Nature* **319:** 675-678.

Katz G, Markel G, Mizrahi S, Arnon TI, Mandelboim O (2001) Recognition of HLA-Cw4 but not HLA-Cw6 by the NK cell receptor killer cell Ig-like receptor two-domain short tail number 4. *J Immunol* **166:** 7260-7267.

Kelm S, Gerlach J, Brossmer R, Danzer CP, Nitschke L (2002) The ligand-binding domain of CD22 is needed for inhibition of the B cell receptor signal, as demonstrated by a novel human CD22-specific inhibitor compound. *The Journal of experimental medicine* **195:** 1207-1213.

Kiessling R, Hochman PS, Haller O, Shearer GM, Wigzell H, Cudkowicz G (1977) Evidence for a similar or common mechanism for natural killer cell activity and resistance to hemopoietic grafts. *European journal of immunology* **7:** 655-663.

Kiessling R, Klein E, Pross H, Wigzell H (1975a) "Natural" killer cells in the mouse. II. Cytotoxic cells with specificity for mouse Moloney leukemia cells. Characteristics of the killer cell. *European journal of immunology* **5:** 117-121.

Kiessling R, Klein E, Wigzell H (1975b) "Natural" killer cells in the mouse. I. Cytotoxic cells with specificity for mouse Moloney leukemia cells. Specificity and distribution according to genotype. *European journal of immunology* **5:** 112-117.

Kim HS, Das A, Gross CC, Bryceson YT, Long EO (2010) Synergistic signals for natural cytotoxicity are required to overcome inhibition by c-Cbl ubiquitin ligase. *Immunity* **32:** 175-186.

Kiss E, Nagy P, Balogh A, Szollosi J, Matko J (2008) Cytometry of raft and caveola membrane microdomains: from flow and imaging techniques to high throughput screening assays. *Cytometry A* **73:** 599-614.

Kleene R, Schachner M (2004) Glycans and neural cell interactions. *Nat Rev Neurosci* **5:** 195-208.

Kornfeld R, Kornfeld S (1985) Assembly of asparagine-linked oligosaccharides. *Annu Rev Biochem* **54:** 631-664.

Kottgen E, Reutter W, Tauber R (2003) [Human lectins and their correspondent glycans in cell biology and clinical medicine]. *Med Klin (Munich)* **98:** 717-738.

Kuan SF, Byrd JC, Basbaum C, Kim YS (1989) Inhibition of mucin glycosylation by aryl-N-acetyl-alpha-galactosaminides in human colon cancer cells. *The Journal of biological chemistry* **264:** 19271-19277.

Kubin MZ, Parshley DL, Din W, Waugh JY, Davis-Smith T, Smith CA, Macduff BM, Armitage RJ, Chin W, Cassiano L, Borges L, Petersen M, Trinchieri G, Goodwin RG (1999) Molecular cloning and biological characterization of NK cell activation-inducing ligand, a counterstructure for CD48. *European journal of immunology* **29:** 3466-3477.

Lanier LL (2005) NK cell recognition. *Annual review of immunology* **23:** 225-274.

Lanier LL (2008) Up on the tightrope: natural killer cell activation and inhibition. *Nat Immunol* **9:** 495-502.

Lanoue A, Batista FD, Stewart M, Neuberger MS (2002) Interaction of CD22 with alpha2,6-linked sialoglycoconjugates: innate recognition of self to dampen B cell autoreactivity? *European journal of immunology* **32:** 348-355.

Latchman Y, McKay PF, Reiser H (1998) Identification of the 2B4 molecule as a counter-receptor for CD48. *J Immunol* **161:** 5809-5812.

Latour S, Roncagalli R, Chen R, Bakinowski M, Shi X, Schwartzberg PL, Davidson D, Veillette A (2003) Binding of SAP SH2 domain to FynT SH3 domain reveals a novel mechanism of receptor signalling in immune regulation. *Nature cell biology* **5:** 149-154.

Latour S, Veillette A (2004) The SAP family of adaptors in immune regulation. *Semin Immunol* **16:** 409-419.

Lee KM, McNerney ME, Stepp SE, Mathew PA, Schatzle JD, Bennett M, Kumar V (2004) 2B4 acts as a non-major histocompatibility complex binding inhibitory receptor on mouse natural killer cells. *The Journal of experimental medicine* **199:** 1245-1254.

Lichtenberg D, Goni FM, Heerklotz H (2005) Detergent-resistant membranes should not be identified with membrane rafts. *Trends Biochem Sci* **30:** 430-436.

Lingwood D, Simons K (2010) Lipid rafts as a membrane-organizing principle. *Science (New York, NY* **327:** 46-50.

Ljunggren HG, Karre K (1990) In search of the 'missing self': MHC molecules and NK cell recognition. *Immunol Today* **11:** 237-244.

Lou Z, Jevremovic D, Billadeau DD, Leibson PJ (2000) A balance between positive and negative signals in cytotoxic lymphocytes regulates the polarization of lipid rafts during the development of cell-mediated killing. *The Journal of experimental medicine* **191:** 347-354.

Ma CS, Nichols KE, Tangye SG (2007) Regulation of cellular and humoral immune responses by the SLAM and SAP families of molecules. *Annual review of immunology* **25:** 337-379.

Mackay DJ, Esch F, Furthmayr H, Hall A (1997) Rho- and rac-dependent assembly of focal adhesion complexes and actin filaments in permeabilized fibroblasts: an essential role for ezrin/radixin/moesin proteins. *The Journal of cell biology* **138:** 927-938.

Malmberg KJ, Ljunggren HG (2009) Spotlight on IL-22-producing NK cell receptor-expressing mucosal lymphocytes. *Nat Immunol* **10:** 11-12.

Mandelboim O, Porgador A (2001) NKp46. *Int J Biochem Cell Biol* **33:** 1147-1150.

Masilamani M, Nguyen C, Kabat J, Borrego F, Coligan JE (2006) CD94/NKG2A inhibits NK cell activation by disrupting the actin network at the immunological synapse. *J Immunol* **177:** 3590-3596.

Mathew PA, Garni-Wagner BA, Land K, Takashima A, Stoneman E, Bennett M, Kumar V (1993) Cloning and characterization of the 2B4 gene encoding a molecule associated with

non-MHC-restricted killing mediated by activated natural killer cells and T cells. *J Immunol* **151:** 5328-5337.

Mathew SO, Kumaresan PR, Lee JK, Huynh VT, Mathew PA (2005) Mutational analysis of the human 2B4 (CD244)/CD48 interaction: Lys68 and Glu70 in the V domain of 2B4 are critical for CD48 binding and functional activation of NK cells. *J Immunol* **175:** 1005-1013.

Mathew SO, Rao KK, Kim JR, Bambard ND, Mathew PA (2009) Functional role of human NK cell receptor 2B4 (CD244) isoforms. *European journal of immunology* **39:** 1632-1641.

Matsui T, Maeda M, Doi Y, Yonemura S, Amano M, Kaibuchi K, Tsukita S (1998) Rho-kinase phosphorylates COOH-terminal threonines of ezrin/radixin/moesin (ERM) proteins and regulates their head-to-tail association. *The Journal of cell biology* **140:** 647-657.

McCann FE, Vanherberghen B, Eleme K, Carlin LM, Newsam RJ, Goulding D, Davis DM (2003) The size of the synaptic cleft and distinct distributions of filamentous actin, ezrin, CD43, and CD45 at activating and inhibitory human NK cell immune synapses. *J Immunol* **170:** 2862-2870.

Meinke S (2010) Regulation of human lymphocytes by SLAM-related receptors. Dissertation, Universitätsbibliothek der Universität Heidelberg, Heidelberg.

Mellquist JL, Kasturi L, Spitalnik SL, Shakin-Eshleman SH (1998) The amino acid following an asn-X-Ser/Thr sequon is an important determinant of N-linked core glycosylation efficiency. *Biochemistry* **37:** 6833-6837.

Michaelsson J, Teixeira de Matos C, Achour A, Lanier LL, Karre K, Soderstrom K (2002) A signal peptide derived from hsp60 binds HLA-E and interferes with CD94/NKG2A recognition. *The Journal of experimental medicine* **196:** 1403-1414.

Mooney JM, Klem J, Wulfing C, Mijares LA, Schwartzberg PL, Bennett M, Schatzle JD (2004) The murine NK receptor 2B4 (CD244) exhibits inhibitory function independent of signaling lymphocytic activation molecule-associated protein expression. *J Immunol* **173:** 3953-3961.

Moremen KW, Trimble RB, Herscovics A (1994) Glycosidases of the asparagine-linked oligosaccharide processing pathway. *Glycobiology* **4:** 113-125.

Moretta A (2002) Natural killer cells and dendritic cells: rendezvous in abused tissues. *Nat Rev Immunol* **2:** 957-964.

Moretta A, Bottino C, Vitale M, Pende D, Cantoni C, Mingari MC, Biassoni R, Moretta L (2001) Activating receptors and coreceptors involved in human natural killer cell-mediated cytolysis. *Annual review of immunology* **19:** 197-223.

Moretta A, Vitale M, Bottino C, Orengo AM, Morelli L, Augugliaro R, Barbaresi M, Ciccone E, Moretta L (1993) P58 molecules as putative receptors for major histocompatibility complex (MHC) class I molecules in human natural killer (NK) cells. Anti-p58 antibodies reconstitute lysis of MHC class I-protected cells in NK clones displaying different specificities. *The Journal of experimental medicine* **178:** 597-604.

Nakajima H, Cella M, Langen H, Friedlein A, Colonna M (1999) Activating interactions in human NK cell recognition: the role of 2B4-CD48. *European journal of immunology* **29:** 1676-1683.

Nichols KE, Ma CS, Cannons JL, Schwartzberg PL, Tangye SG (2005) Molecular and cellular pathogenesis of X-linked lymphoproliferative disease. *Immunological reviews* **203:** 180-199.

Ogata S, Maimonis PJ, Itzkowitz SH (1992) Mucins bearing the cancer-associated sialosyl-Tn antigen mediate inhibition of natural killer cell cytotoxicity. *Cancer Res* **52:** 4741-4746.

Ohtsubo K, Marth JD (2006) Glycosylation in cellular mechanisms of health and disease. *Cell* **126:** 855-867.

Orange JS (2008) Formation and function of the lytic NK-cell immunological synapse. *Nat Rev Immunol* **8:** 713-725.

Orange JS, Fassett MS, Koopman LA, Boyson JE, Strominger JL (2002) Viral evasion of natural killer cells. *Nat Immunol* **3:** 1006-1012.

Orange JS, Harris KE, Andzelm MM, Valter MM, Geha RS, Strominger JL (2003) The mature activating natural killer cell immunologic synapse is formed in distinct stages. *Proc Natl Acad Sci U S A* **100:** 14151-14156.

Pan S, Chen R, Aebersold R, Brentnall TA (2010) Mass spectrometry based glycoproteomics - from a proteomics perspective. *Mol Cell Proteomics*.

Parolini I, Topa S, Sorice M, Pace A, Ceddia P, Montesoro E, Pavan A, Lisanti MP, Peschle C, Sargiacomo M (1999) Phorbol ester-induced disruption of the CD4-Lck complex occurs within a detergent-resistant microdomain of the plasma membrane. Involvement of the translocation of activated protein kinase C isoforms. *The Journal of biological chemistry* **274:** 14176-14187.

Petricciani J, Sheets R (2008) An overview of animal cell substrates for biological products. *Biologicals* **36:** 359-362.

Pogge von Strandmann E, Simhadri VR, von Tresckow B, Sasse S, Reiners KS, Hansen HP, Rothe A, Boll B, Simhadri VL, Borchmann P, McKinnon PJ, Hallek M, Engert A (2007) Human Leukocyte Antigen-B-Associated Transcript 3 Is Released from Tumor Cells and Engages the NKp30 Receptor on Natural Killer Cells. *Immunity* **27:** 965-974.

Potter DA, Tirnauer JS, Janssen R, Croall DE, Hughes CN, Fiacco KA, Mier JW, Maki M, Herman IM (1998) Calpain regulates actin remodeling during cell spreading. *The Journal of cell biology* **141:** 647-662.

Pralle A, Keller P, Florin EL, Simons K, Horber JK (2000) Sphingolipid-cholesterol rafts diffuse as small entities in the plasma membrane of mammalian cells. *The Journal of cell biology* **148:** 997-1008.

Rajagopalan S, Long EO (1997) The direct binding of a p58 killer cell inhibitory receptor to human histocompatibility leukocyte antigen (HLA)-Cw4 exhibits peptide selectivity. *The Journal of experimental medicine* **185:** 1523-1528.

Rajagopalan S, Long EO (2010) Antagonizing inhibition gets NK cells going. *Proc Natl Acad Sci U S A* **107:** 10333-10334.

Rao M, Mayor S (2005) Use of Forster's resonance energy transfer microscopy to study lipid rafts. *Biochimica et biophysica acta* **1746:** 221-233.

Reff ME, Carner K, Chambers KS, Chinn PC, Leonard JE, Raab R, Newman RA, Hanna N, Anderson DR (1994) Depletion of B cells in vivo by a chimeric mouse human monoclonal antibody to CD20. *Blood* **83:** 435-445.

Ridley AJ, Hall A (1992a) The small GTP-binding protein rho regulates the assembly of focal adhesions and actin stress fibers in response to growth factors. *Cell* **70:** 389-399.

Ridley AJ, Paterson HF, Johnston CL, Diekmann D, Hall A (1992b) The small GTP-binding protein rac regulates growth factor-induced membrane ruffling. *Cell* **70:** 401-410.

Roncagalli R, Taylor JE, Zhang S, Shi X, Chen R, Cruz-Munoz ME, Yin L, Latour S, Veillette A (2005) Negative regulation of natural killer cell function by EAT-2, a SAP-related adaptor. *Nat Immunol* **6:** 1002-1010.

Roumier A, Olivo-Marin JC, Arpin M, Michel F, Martin M, Mangeat P, Acuto O, Dautry-Varsat A, Alcover A (2001) The membrane-microfilament linker ezrin is involved in the formation of the immunological synapse and in T cell activation. *Immunity* **15:** 715-728.

Sanni TB, Masilamani M, Kabat J, Coligan JE, Borrego F (2004) Exclusion of lipid rafts and decreased mobility of CD94/NKG2A receptors at the inhibitory NK cell synapse. *Molecular biology of the cell* **15:** 3210-3223.

Schatzle JD, Sheu S, Stepp SE, Mathew PA, Bennett M, Kumar V (1999) Characterization of inhibitory and stimulatory forms of the murine natural killer cell receptor 2B4. *Proc Natl Acad Sci U S A* **96:** 3870-3875.

Schauer R (2009) Sialic acids as regulators of molecular and cellular interactions. *Curr Opin Struct Biol* **19:** 507-514.

Schleinitz N, March ME, Long EO (2008) Recruitment of activation receptors at inhibitory NK cell immune synapses. *PLoS ONE* **3:** e3278.

Schuck S, Honsho M, Ekroos K, Shevchenko A, Simons K (2003) Resistance of cell membranes to different detergents. *Proc Natl Acad Sci U S A* **100:** 5795-5800.

Sharma P, Varma R, Sarasij RC, Ira, Gousset K, Krishnamoorthy G, Rao M, Mayor S (2004) Nanoscale organization of multiple GPI-anchored proteins in living cell membranes. *Cell* **116:** 577-589.

Shcherbina A, Bretscher A, Kenney DM, Remold-O'Donnell E (1999) Moesin, the major ERM protein of lymphocytes and platelets, differs from ezrin in its insensitivity to calpain. *FEBS Lett* **443:** 31-36.

Shenoy AM, Brahmi Z (1991) Inhibition of the calpain-mediated proteolysis of protein kinase C enhances lytic activity in human NK cells. *Cell Immunol* **138:** 24-34.

Simons K, Ikonen E (1997) Functional rafts in cell membranes. *Nature* **387:** 569-572.

Simons K, Toomre D (2000) Lipid rafts and signal transduction. *Nat Rev Mol Cell Biol* **1:** 31-39.

Simons K, Vaz WL (2004) Model systems, lipid rafts, and cell membranes. *Annu Rev Biophys Biomol Struct* **33:** 269-295.

Sivori S, Falco M, Marcenaro E, Parolini S, Biassoni R, Bottino C, Moretta L, Moretta A (2002) Early expression of triggering receptors and regulatory role of 2B4 in human natural killer cell precursors undergoing in vitro differentiation. *Proc Natl Acad Sci U S A* **99:** 4526-4531.

Sivori S, Parolini S, Falco M, Marcenaro E, Biassoni R, Bottino C, Moretta L, Moretta A (2000) 2B4 functions as a co-receptor in human NK cell activation. *European journal of immunology* **30:** 787-793.

Sperandio M, Gleissner CA, Ley K (2009) Glycosylation in immune cell trafficking. *Immunological reviews* **230:** 97-113.

Spiro RG (2002) Protein glycosylation: nature, distribution, enzymatic formation, and disease implications of glycopeptide bonds. *Glycobiology* **12:** 43R-56R.

Stark S, Flaig RM, Sandusky M, Watzl C (2005) The use of trimeric isoleucine-zipper fusion proteins to study surface-receptor-ligand interactions in natural killer cells. *J Immunol Methods* **296:** 149-158.

Stebbins CC, Watzl C, Billadeau DD, Leibson PJ, Burshtyn DN, Long EO (2003) Vav1 dephosphorylation by the tyrosine phosphatase SHP-1 as a mechanism for inhibition of cellular cytotoxicity. *Mol Cell Biol* **23:** 6291-6299.

Tabiasco J, Rabot M, Aguerre-Girr M, El Costa H, Berrebi A, Parant O, Laskarin G, Juretic K, Bensussan A, Rukavina D, Le Bouteiller P (2006) Human decidual NK cells: unique phenotype and functional properties -- a review. *Placenta* **27 Suppl A:** S34-39.

Takahashi K, Sasaki T, Mammoto A, Takaishi K, Kameyama T, Tsukita S, Takai Y (1997) Direct interaction of the Rho GDP dissociation inhibitor with ezrin/radixin/moesin initiates the activation of the Rho small G protein. *The Journal of biological chemistry* **272:** 23371-23375.

Takai Y, Sasaki T, Tanaka K, Nakanishi H (1995) Rho as a regulator of the cytoskeleton. *Trends Biochem Sci* **20:** 227-231.

Tangye SG, Lazetic S, Woollatt E, Sutherland GR, Lanier LL, Phillips JH (1999) Cutting edge: human 2B4, an activating NK cell receptor, recruits the protein tyrosine phosphatase SHP-2 and the adaptor signaling protein SAP. *J Immunol* **162:** 6981-6985.

Tarp MA, Clausen H (2008) Mucin-type O-glycosylation and its potential use in drug and vaccine development. *Biochimica et biophysica acta* **1780:** 546-563.

Tomasello E, Blery M, Vely F, Vivier E (2000) Signaling pathways engaged by NK cell receptors: double concerto for activating receptors, inhibitory receptors and NK cells. *Semin Immunol* **12:** 139-147.

Tsukita S, Yonemura S (1997) ERM proteins: head-to-tail regulation of actin-plasma membrane interaction. *Trends Biochem Sci* **22:** 53-58.

Tsukita S, Yonemura S (1999) Cortical actin organization: lessons from ERM (ezrin/radixin/moesin) proteins. *The Journal of biological chemistry* **274:** 34507-34510.

Ungar D (2009) Golgi linked protein glycosylation and associated diseases. *Semin Cell Dev Biol* **20:** 762-769.

Upshaw JL, Arneson LN, Schoon RA, Dick CJ, Billadeau DD, Leibson PJ (2006) NKG2D-mediated signaling requires a DAP10-bound Grb2-Vav1 intermediate and phosphatidylinositol-3-kinase in human natural killer cells. *Nat Immunol* **7:** 524-532.

Urlaub D (2009) Molecular analysis of the decision making process in NK cells. Dissertation, Universitätsbibliothek der Universität Heidelberg, Heidelberg.

Vales-Gomez M, Reyburn HT, Erskine RA, Lopez-Botet M, Strominger JL (1999) Kinetics and peptide dependency of the binding of the inhibitory NK receptor CD94/NKG2-A and the activating receptor CD94/NKG2-C to HLA-E. *The EMBO journal* **18:** 4250-4260.

Vales-Gomez M, Reyburn HT, Erskine RA, Strominger J (1998) Differential binding to HLA-C of p50-activating and p58-inhibitory natural killer cell receptors. *Proc Natl Acad Sci U S A* **95:** 14326-14331.

Valiante NM, Trinchieri G (1993) Identification of a novel signal transduction surface molecule on human cytotoxic lymphocytes. *The Journal of experimental medicine* **178:** 1397-1406.

van de Wiel-van Kemenade E, Ligtenberg MJ, de Boer AJ, Buijs F, Vos HL, Melief CJ, Hilkens J, Figdor CG (1993) Episialin (MUC1) inhibits cytotoxic lymphocyte-target cell interaction. *J Immunol* **151:** 767-776.

van der Goot FG, Harder T (2001) Raft membrane domains: from a liquid-ordered membrane phase to a site of pathogen attack. *Semin Immunol* **13:** 89-97.

Varki A, Schauer R (2009) Sialic Acids.

Veillette A (2006) Immune regulation by SLAM family receptors and SAP-related adaptors. *Nat Rev Immunol* **6:** 56-66.

Veillette A, Dong Z, Latour S (2007) Consequence of the SLAM-SAP signaling pathway in innate-like and conventional lymphocytes. *Immunity* **27:** 698-710.

Velikovsky CA, Deng L, Chlewicki LK, Fernandez MM, Kumar V, Mariuzza RA (2007) Structure of natural killer receptor 2B4 bound to CD48 reveals basis for heterophilic recognition in signaling lymphocyte activation molecule family. *Immunity* **27:** 572-584.

Vely F, Vivier E (2005) Natural killer cell receptor signaling pathway. *Sci STKE* **2005:** cm6.

Vyas YM, Maniar H, Dupont B (2002) Cutting edge: differential segregation of the SRC homology 2-containing protein tyrosine phosphatase-1 within the early NK cell immune synapse distinguishes noncytolytic from cytolytic interactions. *J Immunol* **168:** 3150-3154.

Vyas YM, Maniar H, Lyddane CE, Sadelain M, Dupont B (2004) Ligand binding to inhibitory killer cell Ig-like receptors induce colocalization with Src homology domain 2-containing protein tyrosine phosphatase 1 and interruption of ongoing activation signals. *J Immunol* **173:** 1571-1578.

Walzer T, Blery M, Chaix J, Fuseri N, Chasson L, Robbins SH, Jaeger S, Andre P, Gauthier L, Daniel L, Chemin K, Morel Y, Dalod M, Imbert J, Pierres M, Moretta A, Romagne F, Vivier E (2007a) Identification, activation, and selective in vivo ablation of mouse NK cells via NKp46. *Proc Natl Acad Sci U S A* **104:** 3384-3389.

Walzer T, Jaeger S, Chaix J, Vivier E (2007b) Natural killer cells: from CD3(-)NKp46(+) to post-genomics meta-analyses. *Current opinion in immunology* **19:** 365-372.

Watzl C (2003) The NKG2D receptor and its ligands-recognition beyond the "missing self"? *Microbes Infect* **5:** 31-37.

Watzl C (2006) Production and use of trimeric isoleucine zipper fusion proteins to study surface receptor ligand interactions. *Curr Protoc Protein Sci* **Chapter 19:** Unit 19 11.

Watzl C, Long EO (2003) Natural killer cell inhibitory receptors block actin cytoskeleton-dependent recruitment of 2B4 (CD244) to lipid rafts. *The Journal of experimental medicine* **197:** 77-85.

Watzl C, Stebbins CC, Long EO (2000) NK cell inhibitory receptors prevent tyrosine phosphorylation of the activation receptor 2B4 (CD244). *J Immunol* **165:** 3545-3548.

Welte S, Kuttruff S, Waldhauer I, Steinle A (2006) Mutual activation of natural killer cells and monocytes mediated by NKp80-AICL interaction. *Nat Immunol* **7:** 1334-1342.

Wurm FM (2004) Production of recombinant protein therapeutics in cultivated mammalian cells. *Nature biotechnology* **22:** 1393-1398.

Xu X, Bittman R, Duportail G, Heissler D, Vilcheze C, London E (2001) Effect of the structure of natural sterols and sphingolipids on the formation of ordered sphingolipid/sterol domains (rafts). Comparison of cholesterol to plant, fungal, and disease-associated sterols and comparison of sphingomyelin, cerebrosides, and ceramide. *The Journal of biological chemistry* **276:** 33540-33546.

Yamaji T, Mitsuki M, Teranishi T, Hashimoto Y (2005) Characterization of inhibitory signaling motifs of the natural killer cell receptor Siglec-7: attenuated recruitment of phosphatases by the receptor is attributed to two amino acids in the motifs. *Glycobiology* **15:** 667-676.

Zech T, Ejsing CS, Gaus K, de Wet B, Shevchenko A, Simons K, Harder T (2009) Accumulation of raft lipids in T-cell plasma membrane domains engaged in TCR signalling. *The EMBO journal* **28:** 466-476.

Zhang W, Trible RP, Samelson LE (1998) LAT palmitoylation: its essential role in membrane microdomain targeting and tyrosine phosphorylation during T cell activation. *Immunity* **9:** 239-246.

Zhao Y, Sato Y, Isaji T, Fukuda T, Matsumoto A, Miyoshi E, Gu J, Taniguchi N (2008) Branched N-glycans regulate the biological functions of integrins and cadherins. *FEBS J* **275:** 1939-1948.

Zielinska DF, Gnad F, Wisniewski JR, Mann M (2010) Precision Mapping of an In Vivo N-Glycoproteome Reveals Rigid Topological and Sequence Constraints. *Cell* **141:** 897-907.

Zigmond SH (1999) A method for movement. *Nature cell biology* **1:** E12.

7 ABBREVIATIONS

#	number
`	minute
α	anti (in connection with antibodies)
ADCC	antibody-dependent cellular cytotoxicity
AICL (CLEC2B)	activation-induced C-type lectin
ANOVA	analysis of variance
APC	antigen presenting cells
BADG	Benzyl-2-acetoamido-2-deoxy-α-D-galactopyranoside
Bat3	human leukocyte antigen-B-associated transcript 3
BCR	B cell receptor
BVA	Biological Variation Analysis
CD	cluster of differentiation
CEA	carcinoembryonic antigen
CEACAM1	carcinoembryogenic antigen-related cellular adhesion molecule 1
CIP	calf intestine phosphatase
CRACC	CD2-like receptor-activating cytotoxic cells
CTXB	subunit B of cholera toxin
DAP	DNAX activation protein
DC	dendritic cell
DIGE	difference in gelelectrophoresis
DNAM-1	DNAX accessory molecule 1
Dol-P	dolichol phosphate
DRM	detergent resistant membrane
EAT2	Ewing's sarcoma-associated transcript 2
EBV	Epstein-Barr virus
ELISA	Enzyme-linked immunosorbent assay
ERM	ezrin, radixin and moesin
ERT	EAT-2 related transcript
ESI	electrospray ionization
FACS	fluorescence-activated cell sorting
FRET	Förster resonance energy transfer
Fuc	L-fucose
Gal	D-galactose
GalNAc	*N*-acetylgalactosamin
GDI	GDP dissociation inhibitor

GEF	guanine exchange factor
Glc	D-glucose
GlcNAc	*N*-acetylglucosamin
GPI	glycosylphosphatidylinositol
GPT	GlcNAc phosphotransferase
GRB	growth factor receptor-bound protein
GRB2	growth factor receptor-bound protein2
h	hour
HLA	human leukocyte antigen
IFN	interferon
Ig	immunoglobulin
IL	interleukin
ILZ	isoleucin zipper
IS	immunological synapse
ITAM	immunoreceptor tyrosine-based activation motif
ITIM	immunoreceptor tyrosine-based inhibition motif
ITSM	immunoreceptor tyrosine-based switch motif
IU	international unit
kDa	kilo dalton
KIR	killer cell immunoglobulin-like receptors
LAT	linker for activation of T cells
lo	liquid-ordered
mAb	monoclonal antibody
MALDI	matrix-assisted laser desorption/ionization
Man	D-mannose
MFI	mean fluorescence intensity
MHC	major histocompatibility complex
MIC	MHC class I related chain
min	minute
MS	mass spectrometry
NCR	natural cytotoxicity receptor
Neu5Ac	sialic acid
NK cell	natural killer cell
NKIS	NK cell immunological synapse
NTB-A	NK, T, B cell antigen
PAGE	polyacrylamide gel electrophoresis
PLC	phospholipase C
PNGase	Peptide: N-Glycosidase
POI	protein of interest

PVR	poliovirus receptor
rER	rough endoplasmic reticulum
Rho GDI	Rho GDP dissociation inhibitor beta
SA	sialic acid
SAP	SLAM-associated protein
SDS	sodium dodecyl sulfate
SH2	Src homology 2
SHIP	SH2-domain containing inositol-phosphatase
SHP-1/2	SH2-domain containing phosphatase 1/2
Siglec	sialic-acid-binding immunoglobulin-like lectins
SLAM	signaling lymphocyte activation molecule
SMAC	supramolecular activating cluster
SMIC	supramolecular inhibition cluster
SRR	SLAM-related receptor
STED	stimulated emission depletion
TAP	transporter associated with antigen processing
TCR	T cell receptor
TM	tunicamycin
TNF	tumor necrosis factor
TRAIL	TNF-related apoptosis inducing ligand
U	unit
ULBP	UL-16 binding protein
WB	Western blot
XLP	X-linked lymphoproliferative disease
Xyl	D-xylose

The single amino acid code was used to describe amino acid residues.

8 APPENDIX

8.1 Table of identified proteins by mass spectrometry

Sample ID	T-test[a]	Av. Ratio[b]	Protein score[c]	Protein Mass[d] [Da]	pI[d]	No. of hits[e]		Acc. Nr.[g]	Protein Name[k]
1	0.012	-1,15	438	262237	6.58	11		gi|58530842	desmoplakin isoform II [Hs]
			384	114670	4.9	8		gi|119703744	desmoglein 1 [Hs]
			90	82434	5.75	2		gi|4504811	junction plakoglobin [Hs]
			84	79830	5.71	2		gi|516764	motor protein [Hs]
			67	22014	6.84	3	[f]	gi|438069	thiol-specific antioxidant protein [Hs]
			60	67172	8.72	2	[f]	gi|68563515	keratinocyte proline-rich protein [Hs]
			27	22324	8.27	1		gi|4505591	peroxiredoxin 1 [Hs]
			32	93668	5.26	1		gi|457464	Dsc1a precursor [Hs]
2	0.021	1,38	236	74118	6.46	5		gi|21614499	ezrin [Hs]
			39	78166	5.88	1		gi|600727	glycyl tRNA synthetase [Hs]
			35	28476	6.82	1		gi|110077	immunoglobulin gamma-chain [Mm]
3	$7.1x10^{-4}$	2,44	39	58262	5.90	1		gi|4584820	protein phosphatase 3, catalytic subunit, alpha isoform isoform 1 [Hs]
			34	57044	6.38	2	[f]	gi|303618	phospholipase C-alpha [Hs]
4	$1.8x10^{-3}$	1,54	460	57794	6.01	14		gi|5453603	chaperonin containing TCP1, subunit 2 [Hs]
			281	33345	5.45	7		gi|8439415	tryptophanyl-tRNA synthetase [Hs]
			261	56578	7.14	7		gi|4557817	3-oxoacid CoA transferase 1 precursor [Hs]
			240	57421	5.96	7		gi|3273316	UDP-N-acetylglucosamine pyrophosphorylase [Hs]
			117	28476	6.82	3		gi|51653	immunoglobulin gamma-chain [Mm]
			54	58000	5.83	1		gi|5453980	DnaJ (Hsp40) homolog, subfamily C, member 3 [Hs]
			48	12394	8.88	1		gi|110301	immunoglobulin heavy chain variable region [Mm]
			47	57624	6.37	2	[f]	gi|11559925	X-prolyl aminopeptidase (aminopeptidase P) 3, putative [Hs]
5	$4.9x10^{-3}$	7,66	63	28476	6.82	2	[f]	gi|51653	immunoglobulin gamma-chain [Mm]
			49	12394	8.88	1		gi|110301	immunoglobulin heavy chain variable region [Mm]
			41	50055	4.81	1		gi|35959	tubulin 5-beta [Hs]
			39	49484	5.89	1		gi|5031753	heterogeneous nuclear ribonucleoprotein H1 [Hs]
			39	71316	6.05	1		gi|28592	serum albumin [Hs]
			35	44534	6,43	1		gi|239552	squamous cell carcinoma antigen 1 [Hs]
6	$9.6x10^{-3}$	-1,29	581	56226	6.44	19		gi|66933016	inosine monophosphate dehydrogenase 2 [Hs]
			57	11006	9.34	2	[f]	gi|61608473	immunoglobuliln heavy chain variable region [Hs]
			53	54886	7,21	1		gi|118674	dihydrolipoamide dehydrogenase [Hs]
			31	52143	9.25	1		gi|487420	Semenogelin I [Hs]
7	0.035	1,50	514	51693	5.70	14		gi|4758384	FK506 binding protein 5 [Hs]
			396	53088	5.58	13		gi|8922699	CNDP dipeptidase 2 [Hs]
			309	49484	5.89	9		gi|5031753	heterogeneous nuclear ribonucleoprotein H1 [Hs]
			108	57753	5.97	3		gi|5453603	chaperonin containing TCP1, subunit 2 [Hs]
			63	56066	5.44	1		gi|149589008	peptidase D [Hs]
			57	28476	6.82	1		gi|51653	immunoglobulin gamma-chain [Mm]
8	0.043	-1,17	MS: 91	55574	9,4	19%		gi|119617402	serine hydroxymethyltransferase 2 (mitochondrial), isoform
9	0.027	1,14	MS: 101	18259		53%		gi|119591666	septin 2, isoform CRA_c [Hs]
10	$7.2x10^{-3}$	-1,16	63	36297	6.49	2	[f]	gi|3377279	heterogeneous nuclear ribonucleoprotein A/B isoform a [Hs]
11	0.045	1,16		23031	4,9	52%		gi|56676393	Rho GDP dissociation inhibitor (GDI) beta [Hs]
12	$7.9x10^{-3}$	1,27		28469	4,9	25%		gi|4502565	calpain, small subunit 1 [Hs]
13	$1.8x10^{-4}$	-2,06	393	25133	6.00	11		gi|4758638	peroxiredoxin 6 [Hs]
			142	24361	8.29	5		gi|11139093	GrpE-like protein cochaperone [Hs]
			78	27811	6.34	2		gi|123997751	proteasome (prosome, macropain) subunit, alpha type, 6 [Hs]
			66	27021	6.90	2	[f]	gi|17389815	Triosephosphate isomerase 1 [Hs]
			64	12098	5.60	1		gi|52120	immunoglobulin kappa light chain [Mm]
			38	114702	4,9	1		gi|416917	desmoglein 1 [Hs]
			188	25133	6.00	6		gi|4758638	peroxiredoxin 6 [Hs]
14	$5.3x10^{-5}$	-5,60	102	23583	5.43	2		gi|726098	glutathione S-transferase-P1c [Hs]
			42	26180	8.14	1		gi|7706497	cytidine monophosphate (UMP-CMP) kinase 1, cytosolic isoform a [Hs]

15	1.0x10^{-4}	7,29	134	23596	6.18	3		gi|7657033	5',3'-nucleotidase, cytosolic [Hs]
			71	12098	5.60	1		gi|52120	immunoglobulin kappa light chain [Mm]
16	3.5x10^{-4}	4,44	147	27134	7.66	4		gi|4758504	hydroxysteroid (17-beta) dehydrogenase 10 isoform 1 [Hs]
			146	57578	5.82	5		gi|169170768	keratin 8 [Hs]
			112	12098	5.60	10		gi|52120	immunoglobulin kappa light chain [Mm]
			117	61187	5.60	2		gi|31542947	chaperonin [Hs]
			98	27134	5.70	3		gi|4758504	hydroxysteroid (17-beta) dehydrogenase 10 isoform 1 [Hs]
			92	14847	7.66	1		gi|37848	vimentin [Hs]
			73	15256	10.14	1		gi|90831	Ig kappa chain precursor V region (4C11) - mouse (fragment)
			70	50437	9.00	5	f	gi|31092	eukaryotic translation elongation factor 1 alpha 1 [Hs]
			36	71316	10.87	1		gi|28592	serum albumin [Hs]
17	6.6x10^{-5}	4,77	105	24835	6.05	2		gi|180637	protein-L-isoaspartate (D-aspartate) O-methyltransferase [Hs]
			77	12098	5.60	4	f	gi|52120	immunoglobulin kappa light chain [Mm]
			94	57753	5.97	1		gi|468546	chaperonin containing TCP1, subunit 2 [Hs]
			93	28467	8.50	4	f	gi|1545813	KNP-Ia [Hs]
			60	50437	9.10	1		gi|31092	eukaryotic translation elongation factor 1 alpha 1 [Hs]
			59	12098	5.60	1		gi|52120	immunoglobulin kappa light chain [Mm]
			40	39193	5.26	1		gi|27806751	alpha-2-HS-glycoprotein [Bos taurus]
			40	59004	5.48	1		gi|51452	chaperonin [Hs]
			33	25188	5.37	1		gi|162805	beta-casein [Bos taurus]
18	0.019	1,16	255	26023	8,39	4		gi|1709759	Proteasome subunit alpha type-2 [Hs]
			238	24835	6.05	4		gi|180637	L-isoaspartyl/D-aspartyl protein carboxyl methyltransferase [Hs]
			93	50437	9.10	2	f	gi|31092	eukaryotic translation elongation factor 1 alpha 1 [Hs]
			42	59004	5.48	1		gi|51452	chaperonin [Hs]
			34	57753	5.97	1		gi|468546	chaperonin containing TCP1, subunit 2 [Hs]
19	0.023	1,27	MS: 106	23555	5,3	48%		gi|2554831	Chain A, Crystal Structure Of Human Glutathione S-Transf
20	0.032	1,13	MS: 95	17401	9,4	51%		gi|4505409	non-metastatic cells 2, protein (NM23B) expressed in
21	6.2x10^{-6}	-4,51	244	29298	7.86	9		gi|2623274	MHC class II antigen [Hs]
			175	23655	6.31	9		gi|4504111	growth factor receptor-bound protein 2 isoform 1 [Hs]
			163	24361	8.29	8		gi|11139093	GrpE-like protein cochaperone [Hs]
			123	11433	8.65	4		gi|50540932	MHC class II antigen [Hs]
			109	12098	5.60	9		gi|52120	immunoglobulin kappa light chain [Mm]
			244	29298	7,86	9		gi|22538467	proteasome beta 4 subunit [Hs]
			95	27134	7.66	2		gi|4758504	hydroxysteroid (17-beta) dehydrogenase 10 isoform 1 [Hs]
			72	24835	6.05	2	f	gi|180637	protein-L-isoaspartate (D-aspartate) O-methyltransferase [Hs]
			70	35807	8.57	2	f	gi|4929649	CGI-90 protein [Hs]
			66	27329	5.95	1		gi|37460	unnamed protein product [Hs]
			49	9031	8.12	1		gi|110230	immunoglobulin light chain variable region [Mm]
22	1.6x10^{-3}	3,95	MS: 116	62255				gi|55956899	keratin 9 [Hs]
23	1.8x10^{-3}	2,72	MS: 91	53474	5,8	27%		gi|47419914	tryptophanyl-tRNA synthetase isoform a [Hs]
			318	53088	5.58	11		gi|15620780	glutamate carboxypeptidase [Hs]
			131	49484	5.89	2		gi|5031753	heterogeneous nuclear ribonucleoprotein H1 [Hs]
			109	51693	5.70	4		gi|4758384	FK506 binding protein 5 [Hs]
			108	28476	6.82	5		gi|121040	immunoglobulin gamma-chain [Mm]
			65	12098	5.60	2	f	gi|52140	immunoglobulin kappa light chain [Mm]
			48	12394	8.88	1		gi|110301	Ig heavy chain V-D-J region (106-10E) - mouse (fragment)
			39	24318	5.30	1		gi|30794348	casein alpha s1 [Bos taurus]
			37	36202	8.26	1		gi|31645	glyceraldehyde-3-phosphate dehydrogenase [Hs]

[a] *p* value calculated using the Student's T-test.
[b] Average ratio between 2B4 and NKG2A (>1 greater extend in the 2B4 samples; <-1 greater extend in the NKG2A samples.
[c] Probability-based Mascot scores
[d] Theoretical molecular mass (Da) and pI from the ExPASy database.
[e] Number of hits resulting from ESI analysis. Percent values indicates sequence coverage of MALDI analysis.
[f] Single peptidscore non-significant, sum of singlescores significant.
[g] Accession number derived from PubMed.
[k] Protein name derived from PubMed. [Hs] means *homo sapiens* [Mm] means *mus musculus*.

9 PUBLICATIONS & AWARDS

9.1 Papers

S. Margraf-Schönfeld, C. Böhm, C. Watzl, 2010, Glycosylation affects ligand binding and function of the activating Natural Killer cell receptor 2B4 (CD244), *submitted*

9.2 Oral presentations

S. Margraf-Schönfeld, C. Böhm, C. Watzl, 2009, Glycosylation pattern of the activating human NK cell receptor 2B4 (CD244), Signal Transduction Disease, Trinational Fall Meeting of the Societies for Biochemistry and Molecular Biology of Belgium, Germany and The Netherlands, Aachen, Germany

S. Margraf-Schönfeld, C. Watzl, 2009, Investigation of Membrane Microdomains surrounding Natural Killer Cell Receptors, Signal Transduction Disease, Trinational Fall Meeting of the Societies for Biochemistry and Molecular Biology of Belgium, Germany and The Netherlands, Aachen, Germany

9.3 Posters

S. Margraf, Carsten Watzl, 2007, Investigation of membrane microdomains surrounding Natural Killer cell receptors, 37th Annual Meeting of the German Society for Immunology, Heidelberg, Germany

R. Bhat, D. Urlaub, **S. Margraf**, C. Watzl, 2008, Enhancement of NK cell cytotoxicity throug co-stimulation of activating receptors, EFIS-EJI NK Cell Symposium 2008, Bad Herrenalb, Germany

S. Margraf, C. Watzl, 2008, Investigation of Membrane Microdomains surrounding Natural Killer Cell Receptors, Joint Annual Meeting of Immunology of the Austrian and German Societies (ÖGAI, DGfI), Vienna, Austria

S. Margraf-Schönfeld, C. Böhm, C. Watzl, 2009, Glycosylation pattern of the activating human NK cell receptor 2B4 (CD244), EFIS-EJI NK Cell Symposium 2009, Freiburg, Germany

S. Margraf-Schönfeld, C. Böhm, C. Watzl, 2010, Glycosylation functionally impacts the activity of the human NK cell receptor 2B4 (CD244), 12th Meeting of the Society for Natural Immunity (NK2010), Dubrovnik - Cavtat, Croatia

9.4 Awards

Travel Bursary, sponsored by the European Federation of the Immunological Societies & European Journal of Immunology, 2010, 12th Meeting of the Society for Natural Immunity (NK2010), Dubrovnik - Cavtat, Croatia

10 ERKLÄRUNG

Hiermit erkläre ich, dass ich die vorgelegte Dissertation selbst verfasst und mich dabei keiner anderen als der von mir ausdrücklich bezeichneten Quellen und Hilfen bedient habe. Weiterhin erkläre ich hiermit, dass ich an keiner anderen Stelle ein Prüfungsverfahren beantragt bzw. die Dissertation in dieser oder anderer Form bereits anderweitig als Prüfungsarbeit verwendet oder einer anderen Fakultät als Dissertation vorgelegt habe.

_____ _____

(Datum) (Unterschrift)